PARAMETRIC STUDY ON SELECTED MATHEMATICAL MODELS FOR DYNAMIC CREEP BEHAVIOR OF ASPHALT CONCRETE

A THESIS SUBMITTED TO
THE GRADUATE SCHOOL OF NATURAL AND APPLIED SCIENCES
OF
MIDDLE EAST TECHNICAL UNIVERSITY

BY

HANDE IŞIK ÖZTÜRK

IN PARTIAL FULFILLMENT OF THE REQUIREMENTS
FOR
THE DEGREE OF MASTER OF SCIENCE
IN
CIVIL ENGINEERING

NOVEMBER 2007

Approval of the thesis:

PARAMETRIC STUDY ON SELECTED MATHEMATICAL MODELS FOR DYNAMIC CREEP BEHAVIOR OF ASPHALT CONCRETE

Submitted by **HANDE IŞIK ÖZTÜRK** in partial fulfillment of the requirements for the degree of Master of Science in **Civil Engineering Department, Middle East Technical University** by,

Prof. Dr. Canan Özgen
Dean, Graduate School of **Natural and Applied Sciences** _____

Prof. Dr. Güney Özcebe
Head of Department, **Civil Engineering** _____

Instr. Dr. Soner Osman Acar
Supervisor, **Civil Engineering Dept., METU** _____

Examining Committee Members:

Prof. Dr. Ayhan İnal
Civil Engineering Dept., METU _____

Instr. Dr. Soner Osman Acar
Civil Engineering Dept., METU _____

Asst. Prof. Dr. Murat Güler
Civil Engineering Dept., METU _____

Asst. Prof. Dr. İsmail Özgür Yaman
Civil Engineering Dept., METU _____

Asst. Prof. Dr. Hikmet Bayırtepe
Civil Engineering Dept., Gazi University _____

Date: _____

I hearby declare that all information in this document has been obtained and presented in accordance with academic rules and ethical conduct. I also declare that, as required by these rules and conduct, I have fully cited and referenced all material and results that are not original to this work.

Name, Last name: Hande Işık Öztürk

Signature :

ABSTRACT

PARAMETRIC STUDY ON SELECTED MATHEMATICAL MODELS FOR DYNAMIC CREEP BEHAVIOR OF ASPHALT CONCRETE

Öztürk, Hande Işık

MS., Department of Civil Engineering

Supervisor : Instr. Dr. Soner Osman Acar

November 2007,126 pages

Rut formation has long been recognized as a distress mechanism in flexible pavements. One of the causes of rut formation in flexible pavements is permanent deformation of uppermost asphalt concrete layers due to repeatedly applied traffic loading. The long term permanent deformation of asphalt concrete under repeated load is commonly called as dynamic creep. The primary objective of this thesis is to examine dynamic creep behavior of asphalt concrete specimens tested in laboratory and also study some suitable mathematical models for representing dynamic creep behavior.

In this study, a set of uniaxial repeated load creep tests were performed on standard Marshall specimens prepared at three different bitumen contents. The effects of bitumen content and test condition parameters on dynamic creep behavior are examined. Among several mathematical creep models suggested by researchers, two well known models and a model proposed by the author are selected for representing the laboratory creep behavior. For each of these models, the interactions of the model parameters with varying bitumen content and test conditions are studied to detect probable definite

trends, and to evaluate whether some relations for the model parameters as functions of bitumen content and test conditions can be developed or not.

The results of analyses showed that all three mathematical models used in this study are successful in representing the laboratory dynamic creep behavior of asphalt concrete. The Power Model which has only two parameters is found to be the most stable and suitable model for parametric study among the three selected models. More consistent and definite interactions are observed between the parameters of this model and test conditions. However, within the scope of this study, no relations could be developed for the parameters of selected models as functions of bitumen content and test conditions because of limited test data.

Keywords: Permanent Deformation, Flexible Pavements, Asphalt Concrete, Dynamic Creep Behavior, Mathematical Creep Model

ÖZ

ASFALT BETONUNUN DİNAMİK SÜNME DAVRANIŞI İÇİN SEÇİLEN MATAMATİKSEL MODELLER ÜZERİNDE PARAMETRİK ÇALIŞMA

Öztürk, Hande Işık
Yüksek Lisans, İnşaat Mühendisliği Bölümü
Tez Yöneticisi: Öğr. Gör. Dr. Soner Osman Acar

Kasım 2007,126 Sayfa

Tekerlek izi oluşumu esnek üstyapıların bozulmasında etken bir mekanizma olarak uzun zamandır kabul görmektedir. Tekerlek izi oluşumunun sebeplerinden bir tanesi trafik yüklerinin etkisiyle esnek üstyapının en üstteki asfalt betonu tabakalarının kalıcı deformasyonudur. Tekrarlı yük altında uzun sürede oluşan kalıcı deformasyon genellikle dinamik sünme olarak adlandırılır. Bu tezin öncelikli amacı, laboratuarda test edilen asfalt betonu numunelerinin dinamik sünme davranışının incelenmesi ve aynı zamanda dinamik sünme davranışının temsili için uygun bazı matematiksel modeller üzerinde çalışılmasıdır.

Bu çalışmada, üç farklı bitüm oranı içeren Marshall numuneleri üzerinde tek eksenli yükleme altında sünme deneyleri uygulanmıştır. Bitüm oranının ve deney ortamı şartlarının dinamik sünme testi üzerindeki etkileri incelenmiştir. Asfalt betonunun laboratuardaki sünme davranışını temsil etmek üzere araştırmacılar tarafından önerilmiş bir çok matematiksel model arasından iki iyi bilinen model ve yazar tarafından önerilen diğer bir model seçilmiştir. Bu modellerin her biri için, model parametreleri ile değişken bitüm oranı ve deney şartları arasındaki etkileşimler incelenerek olası belirgin eğilimler

bulunmaya ve model parametreleri için bitüm oranı ve test şartlarına bağlı muhtemel ilişkiler kurulup kurulamayacağı değerlendirilmeye çalışılmıştır.

Analizlerin sonucunda, çalışmada kullanılan üç matematiksel modelin de asfalt betonunun laboratuar sünme davranışını temsil etmekte başarılı olduğu gözlenmiştir. Seçilen üç model arasında, sadece iki parametresi olan üstlü modelin (Power Model), parametrik çalışma için en stabil ve uygun model olduğu belirlenmiştir. Bu modelin parametreleri ile bitüm oranı ve deney şartları arasında daha tutarlı ve belirgin etkileşimler gözlenmiştir. Bununla birlikte, test verilerinin sınırlı olması nedeniyle bu test çalışması kapsamında seçilen modellerin parametreleri ile bitüm oranı ve deney şartları arasında ilişkiler kurulamamıştır.

Anahtar Kelimeler: Kalıcı Deformasyon, Esnek Üstyapı, Asfalt Betonu, Dinamik Sünme Davranışı, Matematiksel Sünme Modeli

To

My Parents

ACKNOWLEDGEMENTS

I would like to express my sincere thanks to my supervisor Inst. Dr. Soner Osman Acar for his guidance, advice, constructive criticism, and encouragements throughout the study.

I would like to express my gratitude to Asst. Prof. Dr. Murat Güler, who answered my questions patiently, shared his valuable experiences and opinions with me, and encouraged me throughout the study.

I am grateful to transportation laboratory technician Ahmet Sağlam for his friendship, and technical assistance throughout the laboratory work.

I deeply thank my parents for their love, support and understanding throughout my life. I wish to express my gratitude to my father who encouraged me to spend many hours in the laboratory.

TABLE OF CONTENTS

LIST OF TABLES

LIST OF FIGURES

LIST OF SYMBOLS

AASHTO	: American association of state Highway and Transportation Officials
ASTM	: American Society of Testing and Materials
CDAS	: Control and Data Acquisition System
GDH	: General Directorate of Highways
HMA	: Hot Mix Asphalt
LVDT	: Linear Variable Displacement Transducers
METU	: Middle East Technical University
NCHRP	: National Cooperative Highway Research Program
P. Strain	: Permanent Strain
SHRP	: The Strategic Highway Research Program
UMATTA	: Universal Materials Testing Apparatus
V.M.A	: Voids in the Mineral Aggregate

CHAPTER 1

INTRODUCTION

1.1 Objective of the Study

Rut formation along mean wheel paths due to repeated traffic loading is one of the most prominent distress mechanisms observed in flexible pavements. Thus, one of the design criteria considered for flexible pavements is to limit the rut formation during its service life. Permanent deformation of uppermost an asphalt concrete layer is one of the major causes of rut formation observed on the surface of flexible pavements, especially where heavy and slow vehicular traffic exists. This phenomenon is called instability rut formation due to creep deformation of asphalt concrete.

This study focuses on dynamic creep behavior, or in other words, permanent deformation characteristics of asphalt concrete under repeated loading. The main objective of this study is to assess the influence of bitumen content of asphalt concrete mixture and loading condition parameters on the dynamic creep behavior by laboratory dynamic creep tests. In order to quantify such an assessment, it is necessary to prepare laboratory specimens and conduct dynamic creep tests. Furthermore, it is also necessary to use mathematical models to represent creep data recorded as relations of deformation versus number of load pulses.

Uniaxial repeated loading tests are conducted to study the creep behavior of unconfined asphalt concrete specimens. The time dependent deformation of a cylindrical specimen is measured and recorded while repeated axial loading is applied on the specimen during such tests. Standard Marshall

specimens are prepared and tested by using a universal testing machine called UMATTA, for the repeated load test program established for this study.

The optimum bitumen content of the asphalt mix is determined to be 4.75%. The specimens of three different bitumen contents, namely 4.75%, 5.25% and 5.75%, are prepared for the testing program.

The main test temperature is selected as 40°C regarding the softening point of the asphalt used. The tests are conducted under 300Kpa (43.5 psi), 400Kpa (58psi) and 500Kpa (72.5 psi) stress levels. These stress levels are chosen randomly to represent recreational vehicles and some small trucks. For today's heavy vehicles, tire pressure of commonly used radial tires ranges from 120 psi (827.5 Kpa) and 150 psi (1034.5 Kpa). Since the maximum pressure can be applied to the specimens by UMATTA testing machine is 700KPa, higher stress levels are not applied in laboratory tests. In general, the loading time of 0.1 sec and the rest time 0.9 sec are usually chosen for repeated loading laboratory tests to represent the moving traffic. Two different load pulses with loading time of 0.2 sec and loading time 0.8 sec are selected for the test program to represent fast and slow traffic regarding the applicable ranges of the UMATTA testing machine. The rest time of 0.6 sec and 1.0 sec are applied, respectively, for loading time of 0.2 sec and loading time 0.8 sec.

Once creep data are generated and recorded for a tested specimen, it can be modeled by using suitable mathematical models. In the literature, there exist several suggested mathematical creep models. The most well known models are Power Law model derived by Monismith et al. (1975), VESYS model derived by Moavenzedeh et al (1974), AASHTO2002 model derived by Witczak and Kaloush (1998) and model proposed by Beckedahl et al. (1992). Nearly, all of these models are successful in representing the laboratory creep test data.

During this study, three mathematical models are used. Two of these are the Power law model of Monismith et al. (1975) and the model proposed by Beckedahl et al. (1992). The third model suggested by the author within the scope of this thesis is the modified form of the model proposed by Beckedahl et al. (2007)

Once the creep data are generated and recorded for a single test, it can be modeled by using the selected mathematical models by regression analysis. The capability of the selected model to represent the individual creep test data can be assessed by studying goodness of fit between test data and the model equation both graphically and statistically.

For test series with different bitumen contents, the mathematical model parameters versus test conditions are also statistically analyzed in order to seek for any correlations, and if possible develop relations, between the model parameters and different test condition parameters. Graphical analyses are used to support the statistical results. However, no constitutive relations could be developed for the parameters of all three mathematical models because no definite trends indicating any possible relation are observed. This may be due to the limited data and the limited number of test condition parameters used within the varied ranges.

A short list of specific research objectives are as follows:

- Investigation of the influence of test conditions on dynamic creep behavior.
- Investigation of the parameters of selected models among the test conditions both statistically and graphically.
- Development of relationships to define the response between the selected model parameters and test conditions.

1.2 Outline of the Study

This study includes chapters describing the background of the creep phenomenon, test results, data analyses, conclusions, and recommendations. Chapter 2 provides a literature review on the fundamentals of engineering rutting and creep phenomenon. Material selection, properties, and mix design is explained in detail, in Chapter 3. The test equipment, experiment procedure, and experiment design are described in Chapter 4. In Chapter 5, test data is presented. Creep models are explained in a detailed way and their parameters are tabulated. Statistical and graphical analyses of parameter versus test conditions are also presented. Chapter 6 is the conclusion part. Outcomes of the research are summarized and recommendations for further studies are given.

CHAPTER 2

LITERATURE REVIEW

2.1 Rut Formation

“Rutting is defined as the formation of twin longitudinal depression along the wheel paths mainly caused by progressive movement of materials due to repeated loading.” (Tarefder, Zaman, Hobson 2003) Rutting has long been recognized as a problem in flexible pavements, with the increase in the tire pressures, permanent deformation potential in hot mix asphalt layers has also increased. This type of deformation does not generally cause surface cracks but provides some riding discomfort, creates a traffic hazard, permits water to accumulate and create steering difficulty.

2.2 Types of Rut

There are three basic causes of ruts which can develop on flexible pavements. These are wearing, structural and instability rutting.

1. **Wear Rutting:** Wear Rutting occurs due to progressive loss of coated aggregate particles from the asphalt pavement surface. This aggregate loss is generally combined effect of environment and traffic. The rate of wearing rutting may be accelerated when winter ice control such as abrasive sand accumulates. It may also be accelerated when the pavement surface becomes disintegrable and aggregate particles move from their places as the bitumen becomes fragile by the environmental effect and traffic loading. An exaggerated plot of wearing rutting is given in Figure 2.1. (Foo 1994)

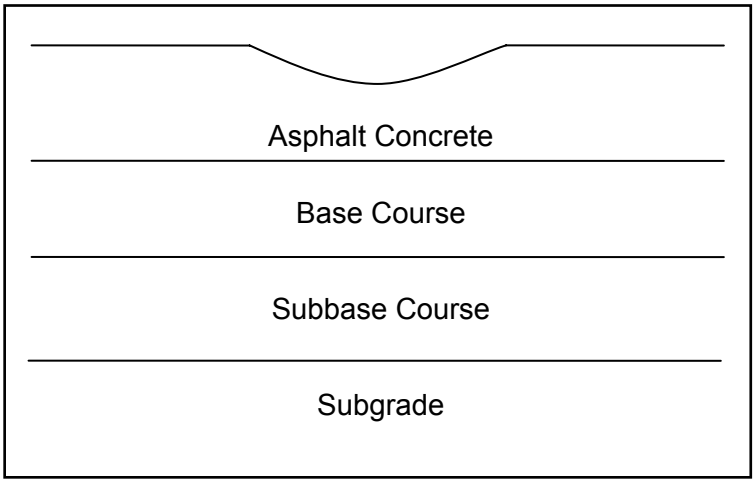

Figure 2.1: Wear rutting

2. **Structural Rutting:** Structural rutting occurs due to vertical deformation of the pavement structure under repeated traffic loads. Permanent deformation can occur in one or more layers of pavement structure. Surface cracks may occur in this type of rutting. A schematic plot of structural rutting is given in Figure 2.2. (Foo 1994)

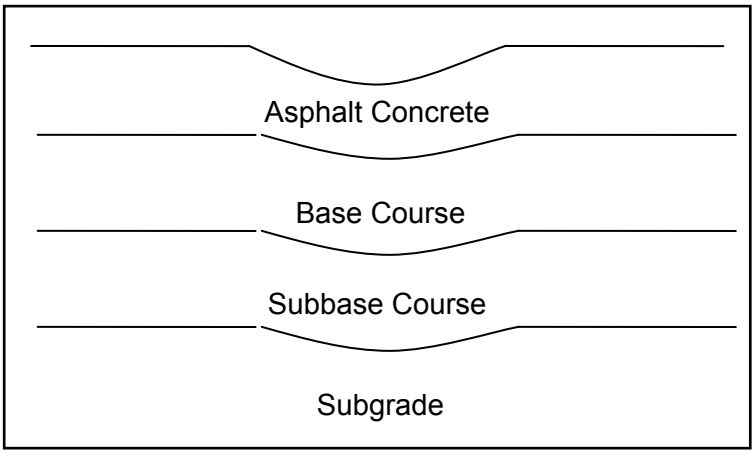

Figure 2.2: Structural Rutting

3. **Instability Rutting:** Instability rutting occurs due to lateral displacement of materials within the asphalt concrete layer. When the structural properties of the compacted asphalt concrete are inadequate to resist the required number of repetitive loads exerted on asphalt concrete layer, instability rutting can be formed. Instability rutting becomes significant under heavy and frequent traffic. A schematic plot of instability rutting is given in Figure 2.3. (Foo 1994)

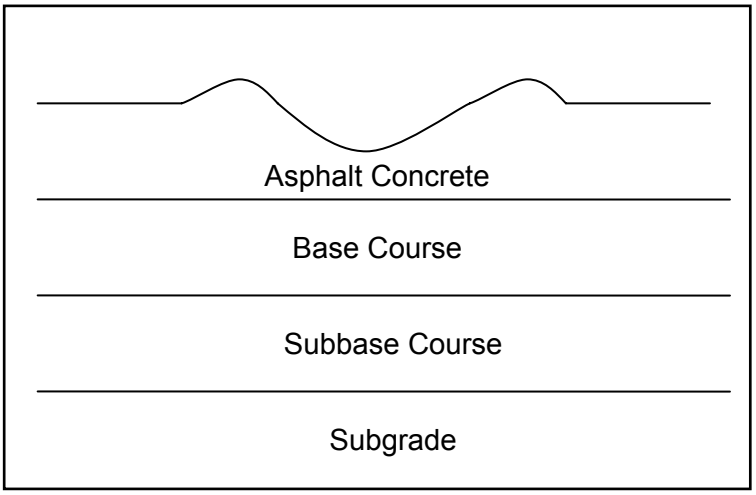

Figure 2.3: Instability Rutting

Dawley, Hogewiede, and Anderson (1990) state that the majority of flexible pavement rutting is primarily due to instability rutting. (Foo 1994)

2.3 Creep

As indicated in Part 2.2, the general cause of rutting is instability. One of the reasons of instability rutting is the creep formation. Creep is the continuous time-dependent deformation under constant or repeated stress or load. The creep phenomenon was first reported in 1834 by Vicat.

2.4 Creep Behavior

Lai and Huffered (1976), Abdulshafi (1983), Perl et al. (1983), Sides et al. (1985), and Uzan et al. (1985) have shown that asphalt concrete creep strain can be divided into four components.(Eqn 2.1) The component strains consist of recoverable and irrecoverable elements, some of which are time dependent and some are time independent. (Uzan J. 2005)

$$\varepsilon_t = \varepsilon_e + \varepsilon_p + \varepsilon_{ve} + \varepsilon_{vp} \qquad \text{(Eqn. 2.1)}$$

ε_t = creep strain
ε_e = elastic strain (recoverable and time-independent)
ε_p = plastic strain (irrecoverable and time-independent)
ε_{ve} = viscoelastic strain (recoverable and time-dependent)
ε_{vp} = viscoplastic strain (irrecoverable and time-dependent)
t_1 = load duration
t_2-t_1 = rebound time

Figure 2.4 shows a typical asphalt concrete creep behavior. A strain ε_o containing the elastic and plastic components occurs instantaneously, when load is applied at t= t_o. Viscoelastic and viscoplastic strains appear during the load duration (t_o< t< t_1). As soon as the load is removed at t=t_1, the elastic strain is recovered instantaneously. During the rebound period, the viscoelastic strain is recovered. At the end of the rebound period, the permanent creep strain is the sum of the viscoplastic and plastic strains.

.

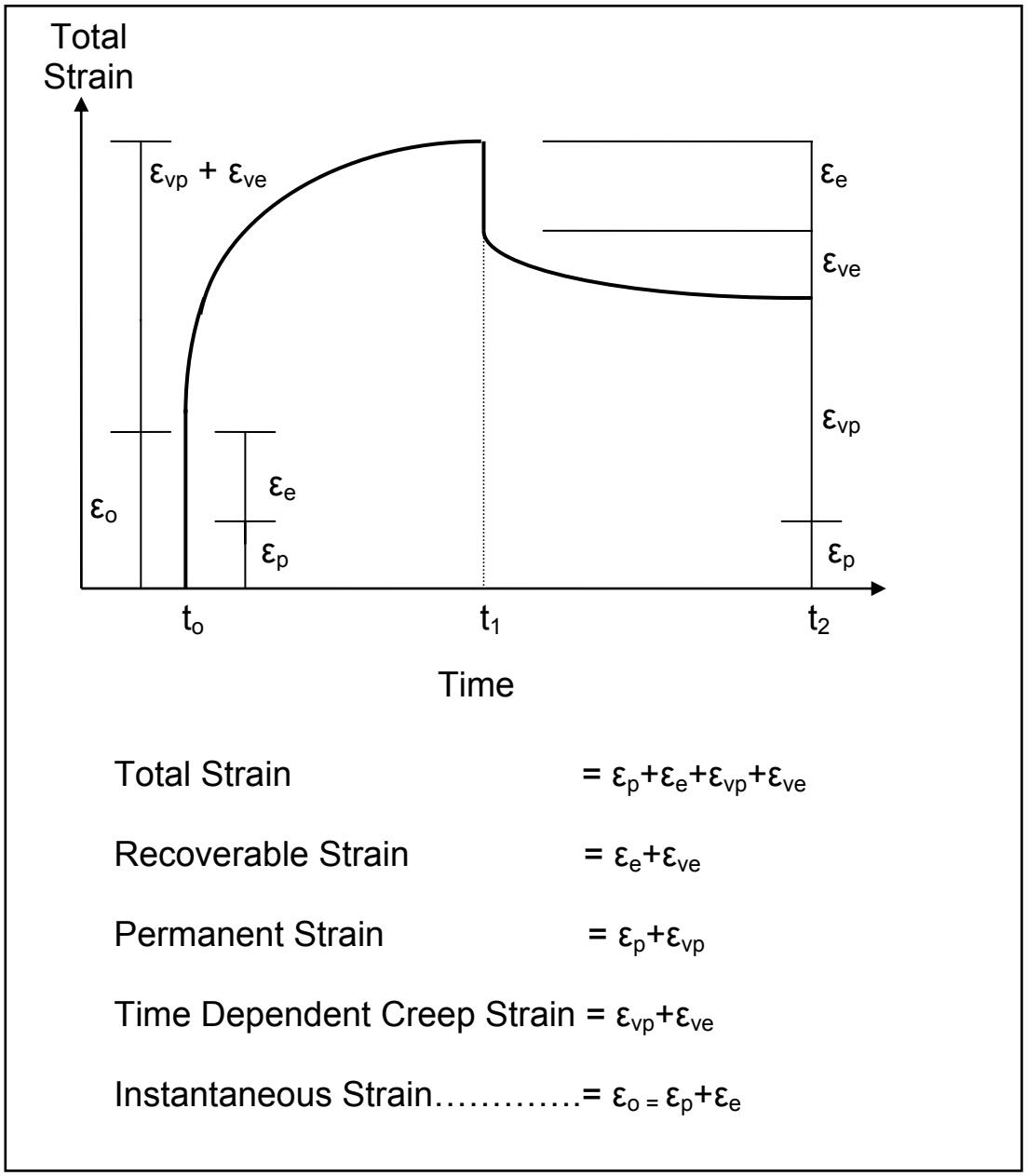

Figure 2.4: Asphalt concrete creep behavior [Perl et al. 1983] (Brown E. R. Foo K.Y. 1994)

Elastic Behavior: Asphalt concrete behaves elastically under small stresses. An instantaneous elastic strain response is observed upon loading. The elastic strain stays constant as long as stress is fixed and disappears immediately upon removal of stress.

Plastic Behavior: The behavior becomes plastic when the stress is too high. The limiting stress, above which the behavior is plastic, is called Elastic Limit. The strain, that does not disappear after the stress is removed, is called inelastic strain or plastic strain.

Viscoelastic Behavior: A material shows elastic action upon loading followed by a slow continuous increase of strain at a decreasing rate. When the material is unloaded, a continuously decreasing strain follows an initial elastic recovery. These materials are called viscoelastic.

Asphalt concrete mixes are viscoelastic materials. Several models are developed to describe the viscoelastic nature of asphalt cement. Classical Hookean springs and Newtonian dashpots are generally used to model the creep behavior.

The spring element shows instantaneous elasticity due to loading and recovery due to unloading. The spring model (Eqn 2.2) can well fit to purely elastic material.

$$\sigma = E * \varepsilon \qquad \text{(Eqn. 2.2)}$$

σ =stress

E = Young's Modulus (or linear spring constant)

ε = Strain

The spring element can not be used for describing viscoelastic models like asphalt concrete. The time dependency of viscoelastic materials are generally modeled with a linear viscous dashpot. The dashpot continuously deforms at a constant rate when constant stress is exerted.

$$\sigma = \eta \frac{\partial \varepsilon}{\partial t} = \eta \dot{\varepsilon} \qquad \text{(Eqn.2.3)}$$

η =coefficient of viscosity

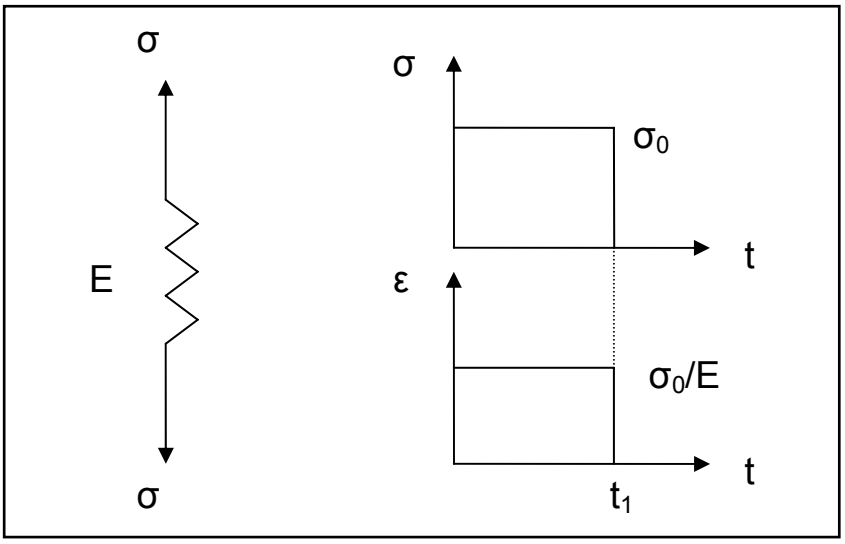

Figure 2.5: Linear elastic spring model

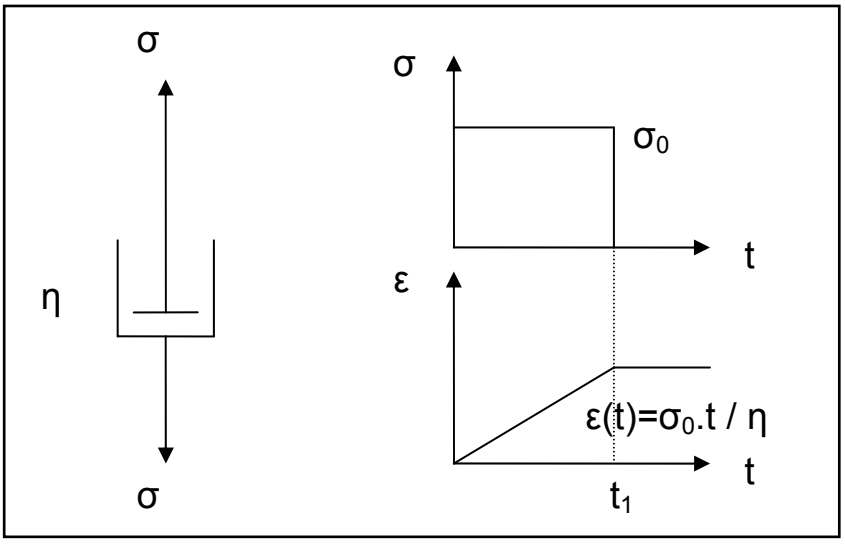

Figure 2.6: Linear dashpot model

Several mathematical models are developed to describe the nature of viscoelastic materials using springs and dashpots. Maxwell, Kelvin, Van der Poel and Burgers models are the well-known models.

Maxwell Model:

The simple combination of Hookean springs and Newtonian dashpots are connected in series in the Maxwell Model. The total strain is the sum of elastic strain and viscous strain given in Eqn. 2.4. Figure 2.7 illustrates the Maxwell Model. (Gabrielson 1992)

$$\varepsilon(t) = \frac{\sigma_0}{E} + \frac{\sigma_0}{\mu} t \qquad \text{(Eqn.2.4)}$$

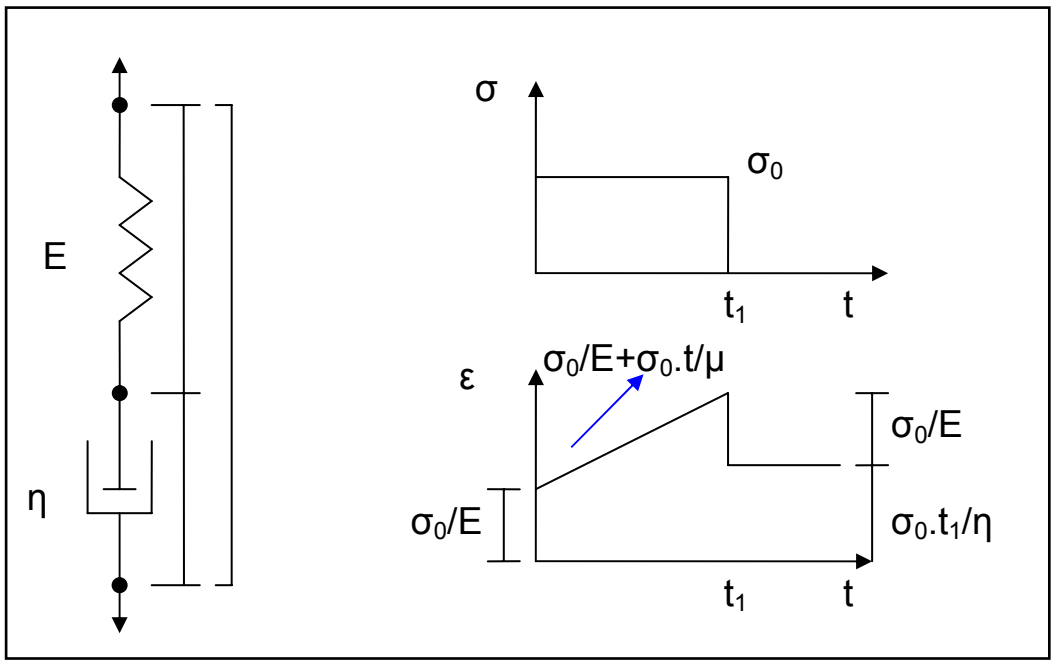

Figure 2.7 :Maxwell Model

Kelvin Model:

A Kelvin or Voigt Model introduces the characteristic of delayed elasticity and is achieved by combining Hookean springs and Newtonian dashpots in parallel. When the load is applied, an immediate deformation occurs as the dashpot takes the entire load. As the time passes, the piston starts to move

and the spring also deforms correspondingly. Spring continuously take the load till no load is left on the dashpot. No deformation occurs when the system is unloaded. Equation 2.5 and Figure 2.8 illustrate the Kevin Model. (Gabrielson 1992)

$$\sigma = \sigma_1 + \sigma_2$$

$$\sigma = E\varepsilon + \eta\dot{\varepsilon}$$

$$\frac{\sigma}{\eta} = \frac{E\varepsilon}{\eta} + \dot{\varepsilon}$$

$$\varepsilon = \frac{\sigma_0}{E}(1 - e^{\frac{-Et}{\eta}}) \qquad \text{(Eqn. 2.5)}$$

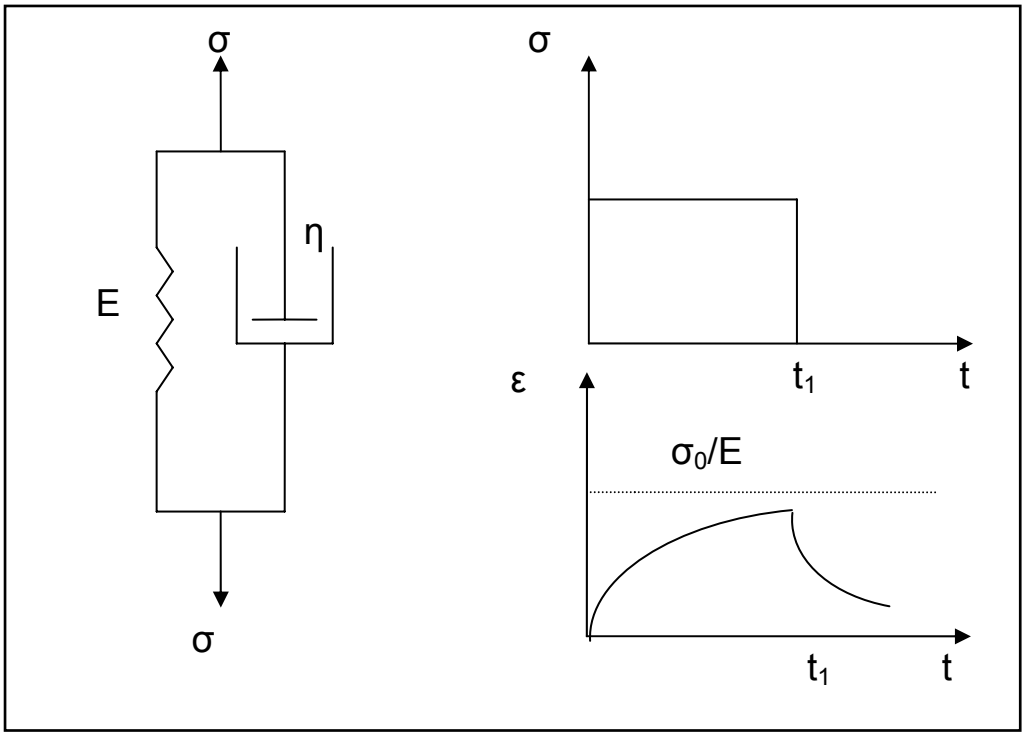

Figure 2.8: Kelvin Model

Neither the Kelvin nor the Maxwell model can fully describe the behavior of viscoelastic materials. The Kelvin model does not show both the time independent strain during loading and the unloading and permanent strain after unloading.

Van der Poel Model:

Van der Poel model is the combination of Hooken spring in series with the Kelvin model. Equation 2.6 and Figure 2.9 illustrate the Van der Poel Model. (Gabrielson 1992)

$$\varepsilon = \varepsilon_1 + \varepsilon_2$$

$$\varepsilon = \frac{\sigma}{E_1} + \frac{\sigma}{E_2}(1 - e^{-E_2 \frac{t}{\eta}}) \qquad \text{(Eqn.2.6)}$$

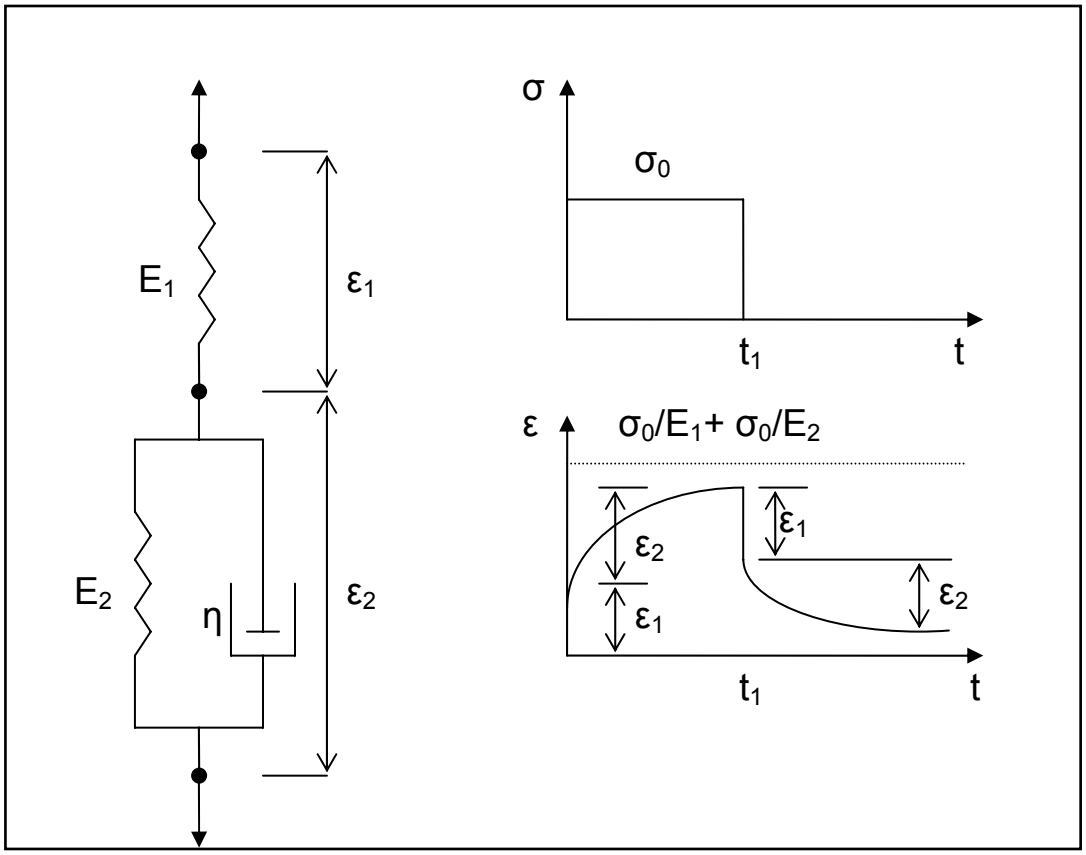

Figure 2.9 Van der Poel Model

Burgers Model:

The shortcoming of the Van der Poel model can be overcome by combining an additional Newtonian dashpot. The Burgers Model and its constitutive equation are given in Figure 2.10 and Equation 2.7. (Szydlo, Mackiewicz 2005)

$$\varepsilon = \varepsilon_1 + \varepsilon_2 + \varepsilon_3$$

$$\varepsilon(t) = \frac{\sigma_0}{E_1} + \frac{\sigma_0}{\eta_1} t + \frac{\sigma_0}{E_2}\left(1 - e^{\frac{-E_2 t}{\eta_2}}\right) \qquad \text{(Eqn. 2.7)}$$

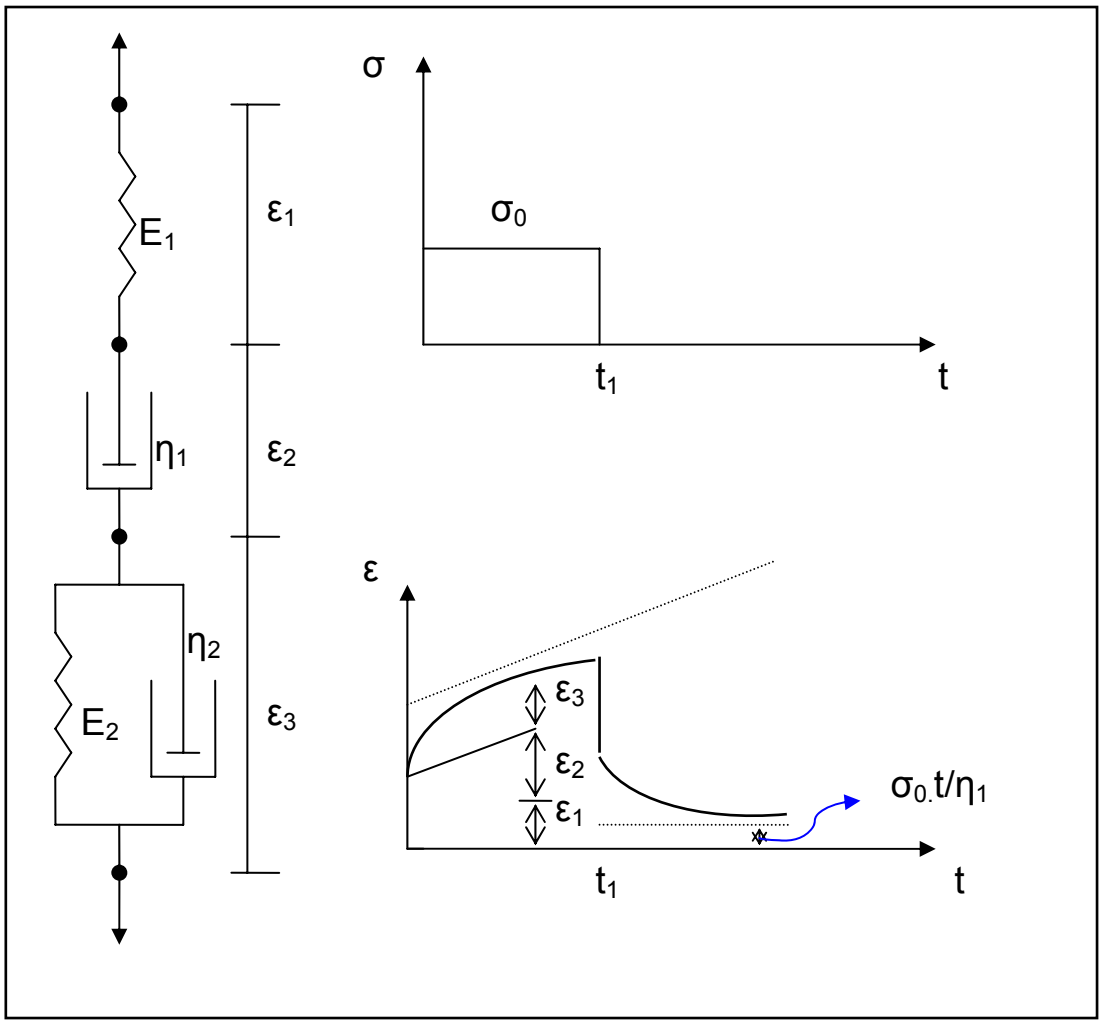

Figure 2.10: Burgers Model

2.5 Mathematical Creep Models

In this part, a short list of well known mathematical creep models for asphalt concrete is given.

2.5.1 Power Model

The relationship between the permanent strain and the number of load applications can successfully be expressed by the classical power model developed by Monismith et al. (1975). Detailed information on the Power Model (Eqn. 2.8) is given in Part 5.2.4. (NCHRP 9-19 2000)

$$\varepsilon_p = an^b \qquad \text{(Eqn. 2.8)}$$

ε_p = permanent strain

a, b = constants of power model

n = # of load applications

2.5.2 VESYS Model

The VESYS program was initially developed by Moavenzedeh et al.(1974) using the multilayer viscoelastic theory at the Massachusetts Institute of Technology in 1974. The VESYS model is improved over the years. The latest version of the model (VESYS-5) is developed by Brademeyer (1988). In the model, it is basically assumed that the permanent strain is proportional to the resilient strain in the following form (Eqn.2.9). (NCHRP 1-37A 2005)

$$\varepsilon_{pn} = \mu\varepsilon_r n^{-\alpha} \qquad \text{(Eqn. 2.9)}$$

ε_{pn} = the permanent or plastic strain due to a single load application

μ = a permanent deformation parameter representing the constant of proportionality between permanent strain and elastic strain

ε_r = resilient strain

n = load applications

α = 1-b is a permanent deformation parameter indicating the rate of decrease in the incremental permanent deformation as the number of load repetitions increases. Normally, the α value is greater than 0.

2.5.3 Ohio State Model

Majidzadeh et al. (1981) developed a permanent strain accumulation model at the Ohio State University. The model is valid for describing the rut formation in all pavement layers. The model is given in Eqn. 2.10 (NIH 1993).

$$\frac{\varepsilon_p}{N} = A(N)^{-m} \quad \text{(Eqn. 2.10)}$$

ε_p = permanent strain

N = number of allowable load applications

A = experimental constant dependent on material type and stress state

m = experimental constant dependent on material type. M is equal to (b-1). b is equal to the slope of the log permanent strain versus log pulse count.

2.5.4 Allen and Deen Model

Allen and Deen (1986) developed permanent deformation models from laboratory tests in order to predict rutting in asphalt concrete layers, dense graded aggregate layers, and subbases. The model is given in Eqn.2.11 and the regression coefficients for the Allen and Deen rutting prediction models are illustrated in Table 2.1 (NCHRP 1-37A 2005).

$$\log \varepsilon_p = C_0 + C_1(\log N) + C_2(\log N)^2 + C_3(\log N)^3 \quad \text{(Eqn.2.11)}$$

ε_p = permanent Strain (axial), in/in

N = number of stress repetitions

C0, C1, C2, C3 = regression coefficients that are factors of temperature and the deviator stress.

Table 2.1: Regression coefficients for the Allen and Deen rutting prediction models

Coefficient	HMA	Dense-Graded Aggregate Base	Subgrade
C_o	- 0.000663 T^2 + 0.1521 T - 13.304 + (1.46 - 0.00572 T) * log Φ_1	- 4.41 + (0.173 + 0.003 w) * Φ_1 - (0.00075 + 0.0029 w) * Φ_3	- 6.5 + 0.38w - 1.1 (log Φ_3) + 1.86 (log Φ_1)
C_1	0.63974	0.72	$10^{(-1.1 + 0.1\ w)}$
C_2	- 0.10392	- 0.142 + 0.092 (log w)	0.018 w
C_3	0.00938	0.0066 - 0.004 (log w).	0.007 - 0.001 w

where,

T = Temperature, °F.
σ_1 = Deviator stress, lbf/in2.
w = Moisture content, percent.
σ_1 = Deviator stress, lbf/in2.
σ_3 = Confining pressure, lbf/in2

2.5.5 AASHTO2002 Model

The AASHTO 2002 Model was developed by Witczak and Kaloush at the University of Maryland in 1998. The AASHTO 2002 model is given in Eqn. 2.12 (NCHRP 1-37A 2005).

$$\log \frac{\varepsilon_p}{\varepsilon_r} = \log C + 0.4262 \log n \qquad \text{(Eqn.2.12)}$$

ε_p = accumulated permanent strain

C = $T^{2.02755}$/5615.391 is a function of temperature (Temperature (T) in °F).

ε_r = resilient strain

n = load applications

2.5.6 Model proposed by Beckedahl et al

A closed mathematical formula is derived by Beckedahl et al.(1992), which well fits with the experimental data of the creep tests. Detailed information on the model is given in Part 5.2.2.

$$\varepsilon(n) = E0 + An^{k} + B(e^{nC} + 1) \qquad \text{(Eqn.2.13)}$$

ε(n) = permanent strain

E0, A, B, C, k = constants of model proposed by Beckedahl et al.

n = number of load applications

2.6 Creep Stages

A typical creep curve, exhibiting three stages, was first observed and described by Thurston. These stages are primary, secondary and tertiary creeps. However, there exists one more component of creep observed just prior to the primary stage and called as instantaneous deformation. A typical creep curve is represented in Figure 2.10.

Instantaneous deformation: Under the application of an initial and relatively small load, material behaves as elastic. There occurs a sudden deformation as soon as the initial load is applied. The strains are fully recoverable, which can be explained by the behavior of a Hooken *spring.* In other words, no permanent strain is generated during a loading and unloading cycle. Additionally, this phenomenon is independent of the rate of loading. (Uluğtekin 1999)

Primary Stage: If the load is continuously applied, the material continues to deform with a decreasing rate. In other words, the permanent strain rate slows down with time. The deformation characteristic can be simply explained by the *Kelvin model.* The behavior is that after unloading the material, a part of deformation is recoverable.

The physical damage process during the primary stage is called strain hardening. This damage occurs due to the movement of dislocations in asphalt concrete under repeated traffic loading. This results in increase in the plastic strain. On the contrary, the dislocation intersections decrease the movement in the body, which causes a permanent strain rate reduction. (Zhou F. and Scullion T. 2002)

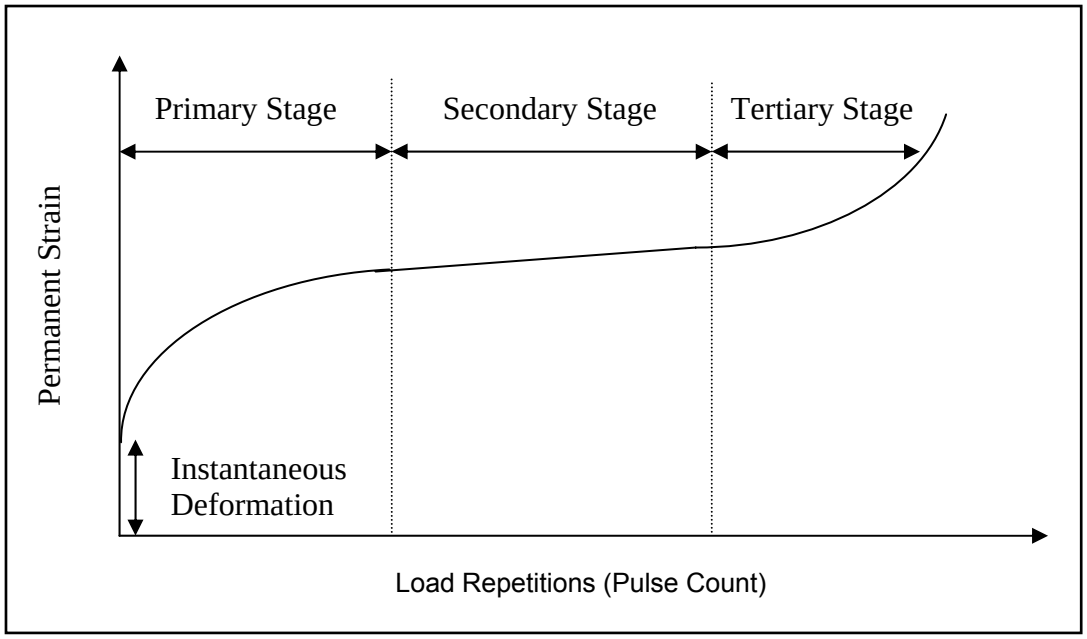

Figure 2.11: Typical Creep Curve

Secondary Stage: Secondary creep, also known as steady- state creep, is the part when the microcracks are initialized. Microcracing is the damage process during the secondary stage. At the point where microcracking initiates, the decrease in the permanent stain ends. (Zhou, Scullin 2002) During this stage, the slope of deformation is nearly linear. At this stage, the strain rate eventually reaches a minimum and becomes nearly constant. The "creep strain rate" is typically the rate in this secondary stage. The stress dependence of this rate is related to the creep mechanism. The deformation characteristic in this stage can be represented by the dashpot of a *Maxwell*

element in the model. The deformation that accumulates at this stage is unrecoverable. (Uluğtekin 1999)

Tertiary Stage: The permanent deformation rate starts to increase, and rapidly accumulates in this stage. The damage process is called macrocraking during tertiary stage. Macrocracks are formed with the combinations of microcracks under continuous loading. With the initiation of the macrocracking, the deformation rate is accelerated. This stage represents the plastic failure of the material. (Uluğtekin 1999)

2.7 Factors Affecting Creep

Researchers identified many factors affecting the pavement performance. These factors are classified into asphalt related and non- asphalt related factors. Non asphalt related factors can be listed as environmental conditions such as temperature, moisture, traffic loading, and load frequency. Asphalt related factors are the aggregate, bitumen and mixture properties. The large number of variations in these factors prevent to design common experiment conditions. (Marks, Monroe, Adams 1991)

Effect of Frequency of Load:

Shorter pulse periods cause higher cumulative permanent strain in the repeated load asphalt creep tests.(Zwu, Fwa, Liu 2002) In other words, higher loading rates increase the permanent strain. Loading frequency is illustrated in Figure 2.12

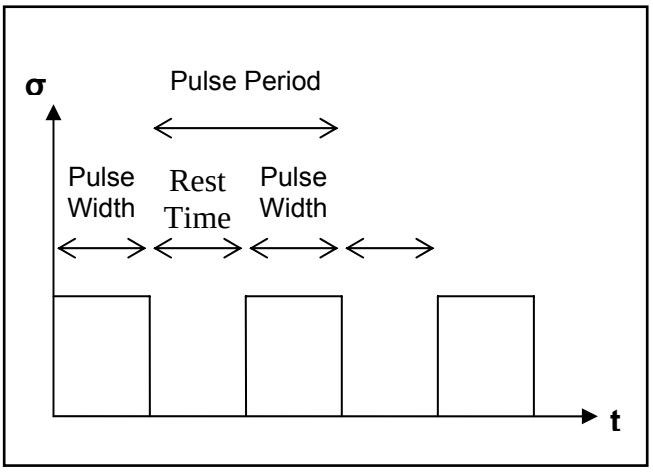

Figure 2.12: Repeated loading/unloading history

Effect of Applied Load:

Tire pressure and wheel load are the major factor affecting the creep behavior under repeated traffic load. “An increase in tire pressure decreases the contact area between tire and pavement surface, therefore, increases the stress in hot mix asphalt.”(Tarefder et al. 2003) In Figure 2.13, the effect of increase in stress at the constant temperature is illustrated. Permanent strain increases due to the increase in the stress and the failure duration under high stresses becomes shorter than low stress levels.

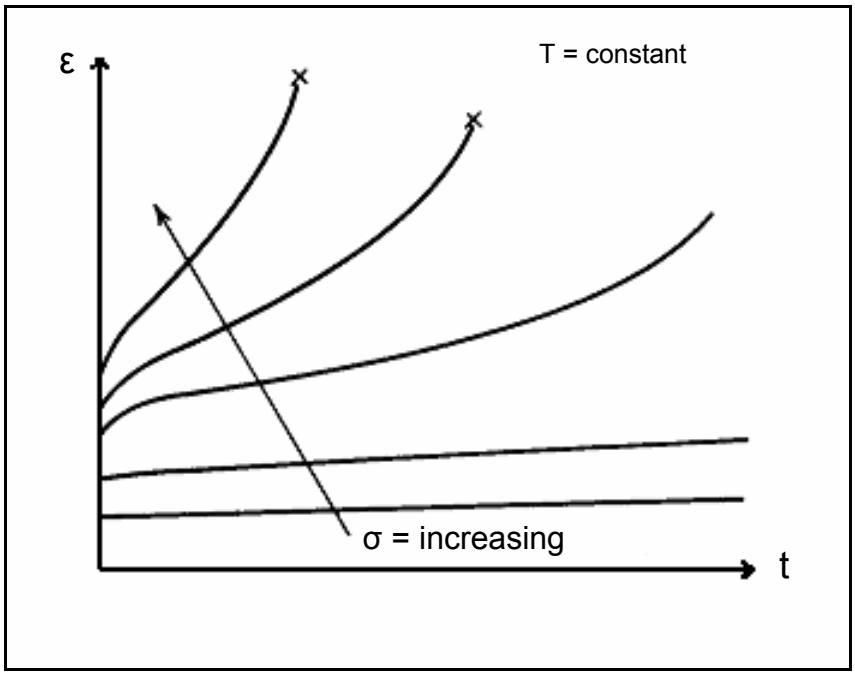

Figure 2.13: Effect of stress on the creep curve at constant temperature.

Effect of Temperature:

Temperature is a factor affecting the stiffness of asphalt concrete. The bitumen behavior is seriously influenced by the temperature change. The stiffness of asphalt concrete decreases with the increase in the temperature. As it is plotted in Figure 2.14, the increase of temperature under constant stress (traffic load) causes a dramatic increase in the permanent strain. The failure duration at high temperatures become comparably shorter than at low temperatures.

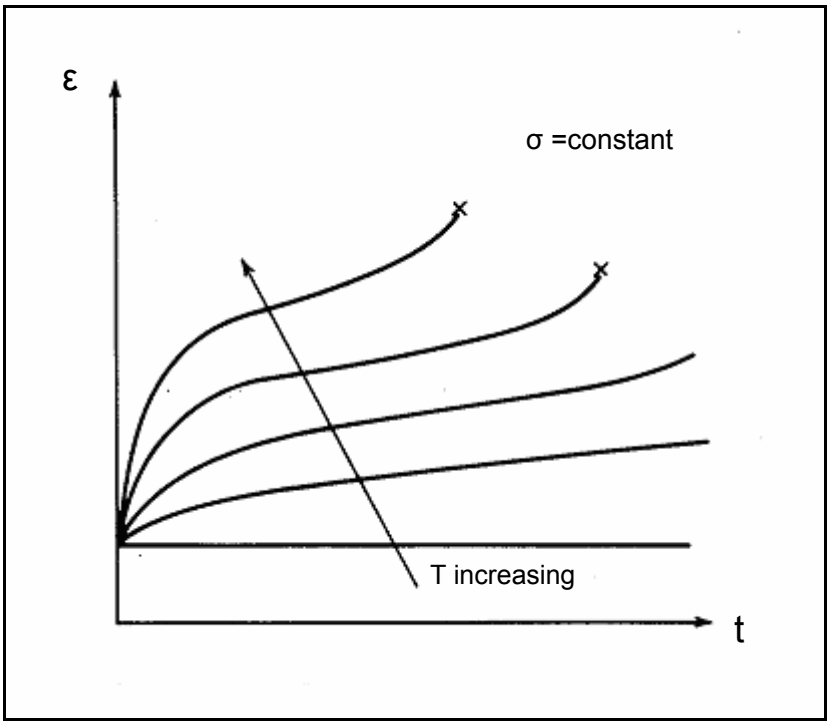

Figure 2.14: Effect of temperature on the creep curve at constant stress (Krauss H. 1980)

Effect of Mixture Properties:

Aggregate type, porosity, gradation and hardness are the essential factors affecting the mixture properties. Bitumen grade, content and quality also influence the behavior of asphalt concrete. In addition to these, the mixing temperature, compaction type and aggregate and bitumen contents in the mix all influence the asphalt concrete behavior under loading.

Barksdale (1993) states that the permanent deformation in dense-graded asphalt concrete is directly related to the asphalt content. The bonding force of asphalt in asphalt film and the frictional force acting on contacts between aggregates resists shear forces; which appear due to repeated traffic loading. A loss of internal friction at aggregate contacts is analyzed if the bitumen content exceeds the optimum bitumen content. The aggregate blend having a maximum density with the same gradation has low air void content. The

contact between aggregate particles is considerably high. The stiffness of the mixture increases upon repeated traffic loading.

Air void content in asphalt concrete plays an important role upon loading. Abdullah, Obaidat, and Abu-Sa'da (1998) concluded that a low void content, which is caused by overfilling the voids with bitumen, decreases the stiffness under loading. On the other hand, low bitumen content causes pavements to reveal under the traffic. The optimum content and the gradation of aggregate blend must be carefully determined in order to prevent early failures.

CHAPTER 3

MATERIAL AND MIXTURE PROPERTIES

The general physical characteristics of the materials and mixtures are represented in this chapter. The bitumen and aggregate used in the study are supplied by the General Directorate of Highways (GDH)

All material tests are performed according to the relevant ASTM standards at the METU Rüştü Yüce Transportation Laboratory. The bitumen used is 50/70 Pen produced by the Kırıkkale Refinery. The aggregate is from the Alaçatı Quarry.

3.1 Physical Properties of Aggregate

Aggregate used in the study is calcareous based. ASTM C 128-79 specification is used to determine the bulk and apparent specific gravity and absorption of fine aggregate. The properties of fine aggregate are given in Table 3.1. ASTM C 127-80 specification is used to determine the bulk and apparent specific gravity and absorption of coarse aggregate. The properties of coarse aggregate are given in Table 3.2.

Table: 3.1: Specific Gravity and Absorption of Fine Aggregate

Specific Gravity and Absorption of Fine Aggregate ASTM C 128-79		
Bulk Specific Gravity	2.667	gr/cm^3
Apparent Specific Gravity	2.682	gr/cm^3
Absorption	0.341	%

Table 3.2: Specific Gravity and Absorption of Coarse Aggregate

Specific Gravity and Absorption of Coarse Aggregate ASTM C 127-80		
Bulk Specific Gravity	2.668	gr/cm^3
Bulk Specific Gravity (Saturated Surface Dry Basis)	2.685	gr/cm^3
Apparent Specific Gravity	2.713	gr/cm^3
Absorption	0.623	%

3.2 Physical Properties of Bitumen

Three important physical properties of bitumen are studied. Specific gravity, penetration and softening point of bitumen are determined in the laboratory according to the relevant ASTM specification. These results are given in Table 3.3. Penetration Index (PI) of the bitumen is calculated to be -1.50 being within normal range (-2<PI<2) and validates the use of the bitumen in hot-mix asphaltic mixtures.

Table 3.3: Physical Properties of Bitumen

ASTM Specification	**Test**		**Unit**
ASTM D70-76	Specific Gravity of Bituminous Material	1.024	gr/cm^3
ASTM D5-73	Penetration of Bituminous Materials	52.20	
ASTM D36-76	Softening Point Test	48.40	°C

3.3 Physical Properties of HMA

3.3.1 Gradation of Aggregate and Sieve Analysis

A dense graded aggregate blend is chosen for HMA. “General Directorate of Highways’ Wearing Course Type 3” gradation limits are determined to be used. The gradation limits are given in Table 3.4 and plotted in Figure 3.1

Table 3.4: Mixture Gradation (GDH Wearing Course Type 3)

Sieve Size	Gradation Limits	% Passing	%Retained on
½"	100	100	0
3/8"	87-100	93.5	6.5
No. 4	66-82	74	19.5
No. 10	47-64	55.5	18.5
No. 40	24-36	30	25.5
No. 80	13-22	17.5	12.5
No. 200	04-10	7	10.5
Pan			7

For typical Marshall Specimen fabrication, 1/2”, #4, #10, #40, #80, #200 and pan materials are needed. The crushed aggregate size larger than #80 is not used for specimens in order to prevent the intrusion of flaky materials in the prepared mixtures.

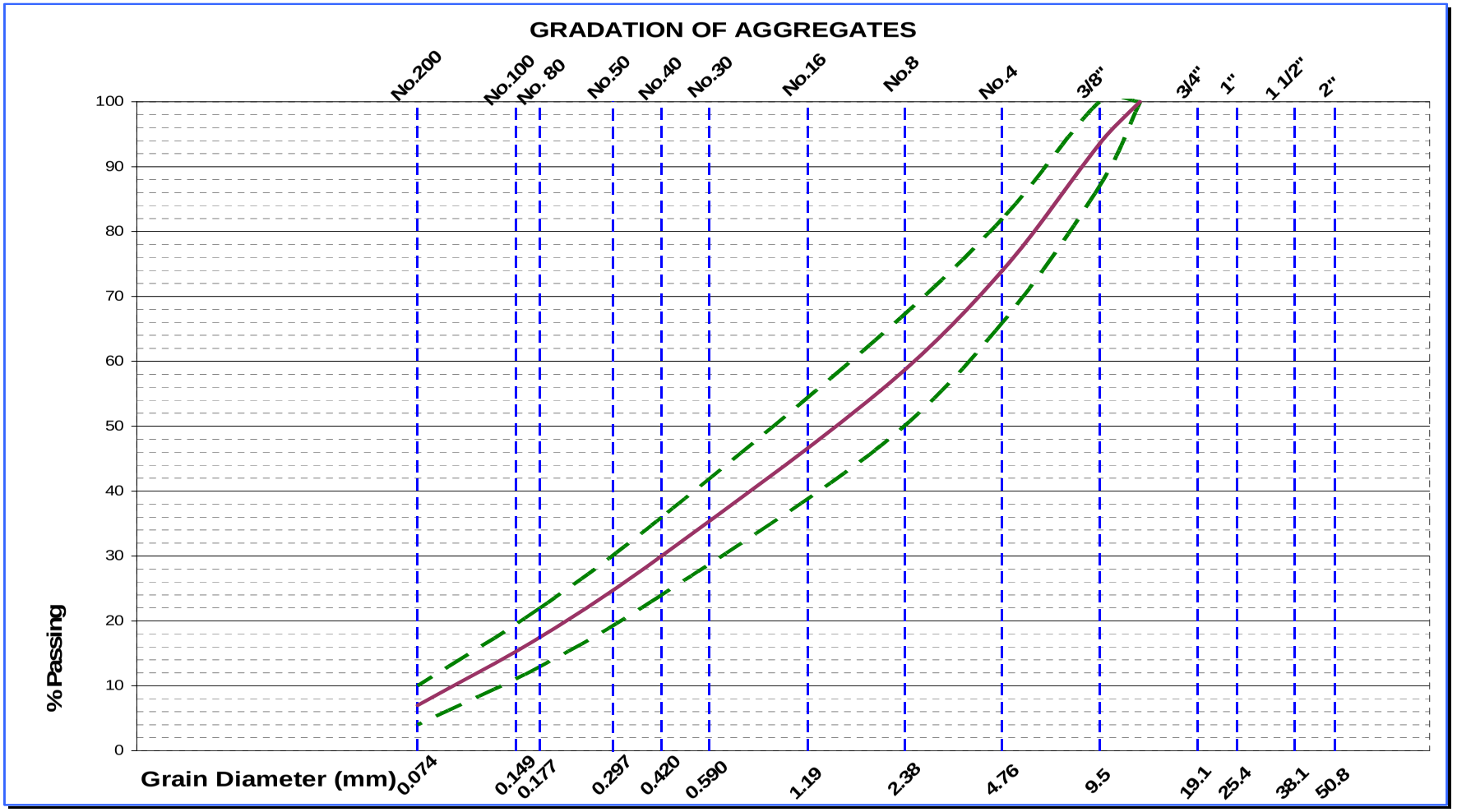

Figure 3.1 Gradation of Aggregates

3.3.2 Preparation of Marshall Specimens

The grading of an aggregate denotes the distribution of sizes. The grading is determined by running the sample through a series of sieves with progressively smaller openings. Following sieve sizes are u sed for this purpose1/2", #4, #10, #40, #80, #200 and pan. Aggregates with known gradation are blended in a mixing bowl by weighing accurately for the calculated gradation. Each test specimen requires 1100 g of aggregate.

The aggregate-blend, mold and collar are heated in the oven to 200 ^{0}C for 24 hours. 1 hour before the sample preparation, bitumen is started to be heated to 170 ^{0}C. Mixing bowl is taken out of the oven and placed on a digital scale. Bitumen is poured on to the aggregates in accordance with the accumulative batch weights. Aggregate and bitumen are quickly mixed with a mechanical mixer and yield a mixture having a uniform disruption of asphalt. A portable heater is kept under the mechanical mixer since the temperature of the mixture should not be less than 110 ^{0}C.

The mold, collar and base are taken out of the oven near to the compactor. A filter paper is placed on the base in order to prevent the mixture to stick to the base and not to loose any material. The mixture is laid into the mold in three layers and each layer is spaded with a heated spatula to provide a homogeneous air void distribution. Another filter layer is placed on top of the specimen. 50 blows are applied to each side. After compaction the specimen is left to cool with its mold about half an hour. The specimen and mold are separated by a hydraulic jack with a slow loading speed to avoid disturbance to the specimens and cooled on a flat plane at room temperature overnight. The height of specimens is measured at equal distant three points and the average height is accepted as sample height. The specimen is carefully weighted in air and water and recorded for further calculation of physical properties.

3.3.3 Optimum Bitumen Content

The Marshall Test method for determining the resistance to plastic flow of bituminous mixtures using Marshall Apparatus (ASTMD 155-76) is performed to determine the optimum bitumen content for the standard Marshall specimens of 2 ½ inches height x 4 inches diameter. Bitumen content is varied within the range of 4% to 7%.The Marshall test results are given in Table A1 in Appendix A. The test property curves plotted from Marshall Test data are also presented in Figure A1 in Appendix A.

According to ASTMD 155-76, the optimum bitumen content is determined by averaging the bitumen contents corresponding to maximum density, maximum stability and optimum air void content given by the standard. The bitumen content corresponding to the maximum specific gravity is found out to be 5.10% from the Figure A1a in Appendix A. The maximum Marshall stability corresponds to 4.60% bitumen content from the Figure A1c in Appendix A. The bitumen content corresponding to 4% air void suggested by the standard for dense asphalt concrete mixtures is determined as 4.55% from the Figure A1b in Appendix A. The optimum bitumen content is calculated as 4.75% by averaging three bitumen contents determined as explained above.

CHAPTER 4

LABORATORY WORK AND EQUIPMENT

The permanent deformation behavior of asphalt concrete is investigated through various experimental studies performed by the researchers over the last 50 years. Some of the important conclusions in the literature regarding the deformation properties of bitumen mixes are listed below (Cheung 1995, Deshpande 1997):

- At small strains, bituminous mixes show linear viscoelastic behavior. However, at large strains, nonlinear behavior become dominant.
- The deformation mechanism of bituminous mixes is dependent on loading rate and temperature same as pure bitumen.
- The deformation behavior is a function of the hydrostatic and deviatoric stress states.
- The mixes dilate even under compressive stresses.

There are four types of tests used to characterize the permanent deformation of asphalt concrete in the literature. These are Uniaxial Stress Tests, Triaxial Stress Tests, Diametral Tests and Wheel Track Tests. Uniaxial Stress Tests include the tests of unconfined cylindrical specimens in creep, repeated, or dynamic loading. Triaxial Stress Tests include the tests of confined cylindrical specimens in creep, repeated, or dynamic loading. Diametral Tests include the tests of cylindrical specimens in creep or repeated loading. Wheel Track Tests include the tests of slab specimens or actual pavement cross section. (SHRP-A-415 1994)

However, no single experiment method and equipment have been developed during the studies. The universal testing machine (UTM) was developed to measure the permanent deformation characteristics of asphalt concrete by uniaxial and triaxial stress tests.

In this study, Universal Materials Testing Apparatus (UMATTA) is used to test the Marshall Test Samples under uniaxial repeated loading. However, restricted test temperatures and load levels of the equipments do not simulate field conditions. (Brown, Kandhal, Zhang 2001)

4.1 Test Equipment

Universal Materials Testing Apparatus (UMATTA) is developed by Industrial Process Controls Limited (IPC) in Australia for performing computer controlled pneumatic loading tests on both bound and unbound materials. The system is capable of recording and displaying stress, strain and stiffness data of tested specimens. UMATTA is composed of three elements; a Control and Data Acquisition System (CDAS), a personnel computer and software (Figure 4.1).

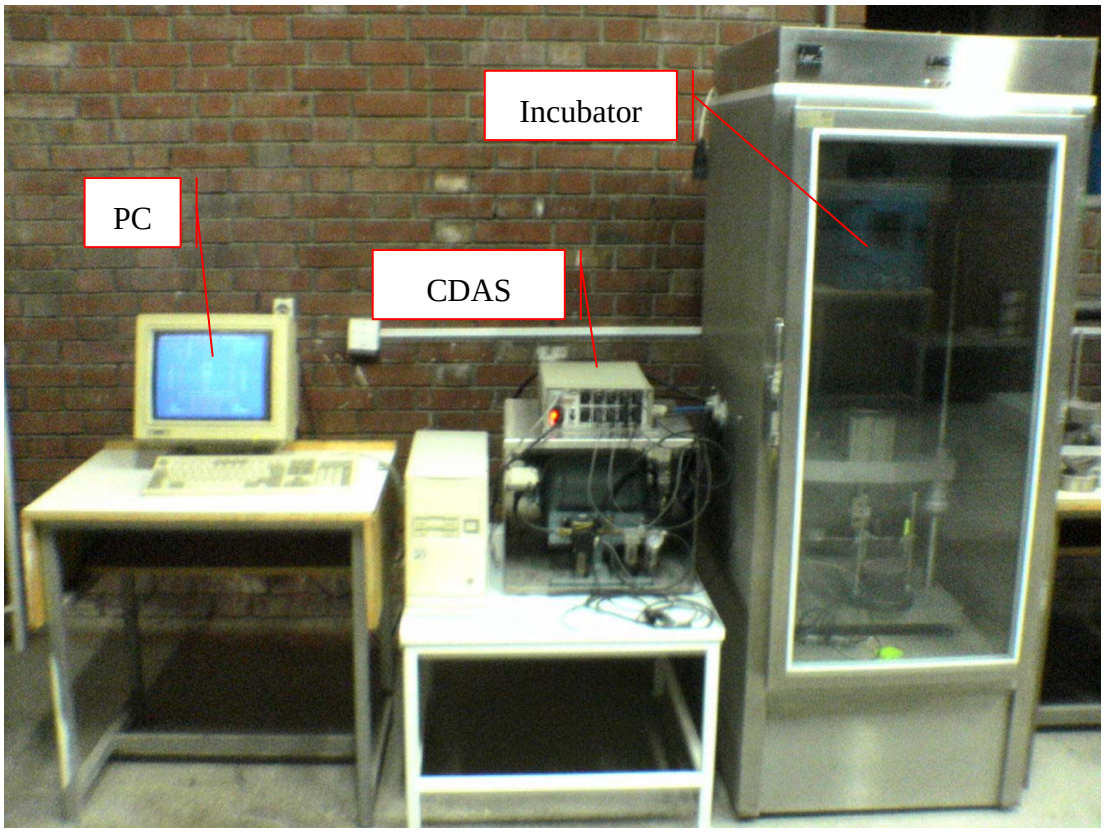

Figure 4.1: UMMATA Test Setup

4.1.1 Control Data Acquisition System (CDAS)

CDAS is a complex system managing all critical control, timing and data acquisition functions for testing frame and transducers. Its responsibility is to capture and digitize analogue signals from the transducers then to transfer the data to a PC for further processing.

4.1.2 UMATTA Software

The UMATTA Software is written in Turbo Pascal (version 5.5). The software package is recommended to be used in 386SX PC. It is activated by typing “UMAT” to DOS prompt.

During the test, the software controls and adjusts all test condition parameters. Continuous data flow from the transducers attached to the specimen is processed by the software. Software also performs calculations and displays plots of accumulated and instantaneous dynamic data on the computer screen. These plots show strain components, and modulus versus pulse count. Waveforms of current pulse can also be monitored on the computer screen during the test. The software automatically saves the test data in binary files.

4.1.3 Loading Frame

Loading frame is capable of testing specimens in the range of 100 mm to 150 mm diameter. It is made of high quality heavy stainless steel in order to minimize deflections and vibrations, so that the accuracy of the uniaxial repeated load test is not influenced.

4.1.4 Load Cell

Load cell fixed in line with the loading shaft is a strain gauge force transducer. It measures the force applied on the specimen. Loading forces are exerted through the shaft of a pneumatic actuator fixed in the center of crosshead.

4.1.5 Pneumatic System

For uniaxial asphalt tests, only vertical force pneumatics are required. The system is activated with an air pressure of 8 atm, generated by an 10 atm air compressor. The air is passed through a filter, mist separator and regulator assembly for adjustment to provide the required pressure. CDAS is capable of controlling air pressure over the range 0 to 700 kpa.

4.1.6 Transducers

Deflection measurement system is composed of two Linear Variable Differential Transformers (LVDT) displacement transducers. LVDT's are capable of measuring the deflections with 0.001 mm accuracy. CDAS controls the operation of the loading frame and captures data from the transducers. The data are transferred to a personnel computer for processing, displaying and storage.

It is important to set transducers within their displacement range in order to have correct displacement records. The LVDTs are located 180° apart to increase the accuracy of the data.

4.1.7 Asphalt Creep Jig

Asphalt creep jig is composed of stainless steel base plate, top plate and two rods mounted to the base plate as support for two transducer clamps.

4.1.8 Temperature Chamber

The loading frame is mounted in a temperature controlled incubator unit. The test temperature can be kept in between room temperature to 60 ^{0}C with an accuracy of 0.1 ^{0}C.

CDAS does not control the test temperature but displays the assigned temperature and instantaneous temperature. The temperature is to be adjusted manually through the control panel of the incubator.

4.2 The Repeated Load Uniaxial Asphalt Creep Test

The creep test is composed of four stages. First stage is the conditioning stage. For all specimens, the duration of conditioning is chosen as 1 min and 100 kpa stress is applied during this stage. Second stage is the rest period.

The rest period is selected as 2 minutes and no load is applied on the specimen. Third stage is the duration within which dynamic loading is applied on the specimen during that stage. The maximum number of pulses is chosen to be 10.000 pulses as it is recommended in the literature. (NCHRP 9-19 1990) Final stage is the 15 minutes recovery part.

During the first stage, approximately 100 Kpa of maximum conditioning stress is applied. On the computer screen, conditioning strain and conditioning time change is displayed continuously. At the end of the stage, peak conditioning stress, accumulated conditioning strain and duration is displayed permanently on the screen.

In the second stage of two minutes, no force is applied on the specimen. On the computer screen, preload rest strain versus condition time variation can be monitored. At the end of this stage, accumulated preload rest strain and duration is displayed permanently on the screen.

During the third stage, the plot of permanent strain versus total loading pulse counts and resilient strain versus total loading pulse counts are displayed on the screen. Besides, this change can be followed from the tabulated data on the screen. On the other hand, the loading time, resilient modulus, and the peak loading stress is only given on the tabulated data section of the screen. CDAS is also capable of displaying the waveforms in another screen, selectable from the screen menu.

In the final stage, no load is applied on the specimen. The unloading stage continues for 15 minutes. During this stage, the change of recovery strain versus time is displayed on the tabulated data.

From the start of the first stage to the end of the fourth stage, the core and the skin temperature of specimen are continuously displayed.

4.3 Test Setup Parameters

Under edit command, test setup parameters are loaded prior to the start of each test. Specimen Name is recorded to identify the specimen. Comments comprises from three text fields. Users are free to write anything such as the specimen origin etc. Specimen length and diameter should be carefully assigned for each specimen since these parameters affects the stiffness calculations. Conditioning and test loading stresses are the stresses applied during the test. Pulse width is the loading duration of one pulse. Repetition period is the time, the sum of pulse width and the rest time. Set temperature is the test temperature.

4.4 Calculation Procedure of UMMATA Software

The following equations are used by the software for uniaxially loaded cylindrical specimen for the calculation of test outputs at any load pulse count.

$$\varepsilon_p = (L3_n)/h$$

$$\varepsilon_r = (L2_n - L3_n)/(h - (L3_n - L1))$$

$$E_r = \sigma/\varepsilon_r$$

$$\sigma = F/A$$

Parameters:

n = the pulse count that the calculation is performed.

ε_p = the permanent axial strain

ε_r = the resilient axial strain

E_r = the resilient modulus

h = the specimen height at the beginning of test

L1 = the initial zero reference displacement of the transducers without vertical stress applied

$L2_n$ = the maximum displacement of the transducers with stress applied for pulse n

$L3_n$ = the final displacement levels of the transducers for pulse ‘n’ just prior to the application of stress for pulse n+1

ó = the peak vertical stress

F = the peak vertical force

A = the cross-sectional area

4.5 Uniaxial Asphalt Creep Test Procedure

Before the test is started in the UMMATA, the specimen is left at room temperature for 48 hours after compaction due to NCHRP 9-19 Report. The irregularities on the specimen surfaces are rubbed with emery paper. These irregularities may have adverse effects on the test results if not removed. They can cause sudden and early deformations. Additionally, they increase the friction between the plates and specimen. In order to minimize interfacial friction between specimen and the plates, an additional treatment rather than rubbing with emery paper is needed. Therefore, glycerin is spread on both sides of latex membranes and these membranes are carefully placed on top and bottom of the specimen avoiding air void formation between the plates and membrane.

The vertical LVDTs are mounted to the support rods. They are adjusted in the range due to the accumulation of permanent deformation. The adjustment is done by using “LEVELS” command in UMATTA Software.

Before running the test, the specimens are left for 2-3 hours in the incubator to stabilize the temperature. In order to control the skin and core temperatures, a dummy specimen is placed into the incubator with the test specimen.

Test parameters are assigned by the user under “EDIT” command. The test is started by pressing “RUN” command. During the test, two graphic screen options are available. The first option is for permanent strain versus pulse count and resilient strain versus pulse counts on the screen. The second option is for waveform display of the repeated load uniaxial creep test.

The test can be terminated manually or by the software when one of the test termination conditions (maximum pulse count or strain threshold) is reached. An ASCII file is created by the software to monitor and process the test results. A typical sample test result is presented in Appendix C.

4.6 Experiment Design

The primary factors affecting dynamic creep behavior are found to be temperature, number of load applications (time of loading), mixture properties, and the repeatedly applied load. In this study, all four factors are varied and their affects on creep behavior models are investigated. Furthermore, the effects of these factors on the mathematical creep model parameters are studied.

During this study, aggregate type, gradation of the aggregate and bitumen type in the blend are not changed. On the other hand, in specimen preparation, three different bitumen contents of 4.75%, 5.25% and 5.75% are used. Namely, these are optimum bitumen content, 0.5% and 1.0% higher bitumen contents than the optimum bitumen content.

At first, two test temperature levels are chosen to be 40°C and 50°C. Though, initial test results show that 50°C is too high for testing specimens containing more bitumen than optimum bitumen content. The reason is that the softening point of the bitumen is to 48°C and the loading time before failure is too short to be modeled. 40°C is chosen as the pivot test temperature for the study. In the literature, the testing temperature is also suggested as 40±1°C for creep tests by the Shell Laboratory and Swiss

Federal Institute of Technology (Tapkın H. 1980). In order the see the temperature affect on the creep curves, a set of tests is run at 35°C for specimens having 5.75% bitumen content and a set of tests is run at 50°C for specimens having 4.75% (optimum) bitumen content.

Two different frequencies are used for load application. One is that pulse width is equal to 0.2 sec and pulse period is equal to 0.8 sec. The other is that pulse width is equal to 0.8 sec and pulse period is equal to 1.8 sec. The first one refers to faster and the second one refers to the slower traffic.

Three different load levels are chosen. These are 300kpa, 400kpa, and 500kpa.

The test terminated after the application of 10.000 load cycles if the sample doesn't fail before 10.000 load cycles.

In Figure 4.2, the experimental design is given in detail.

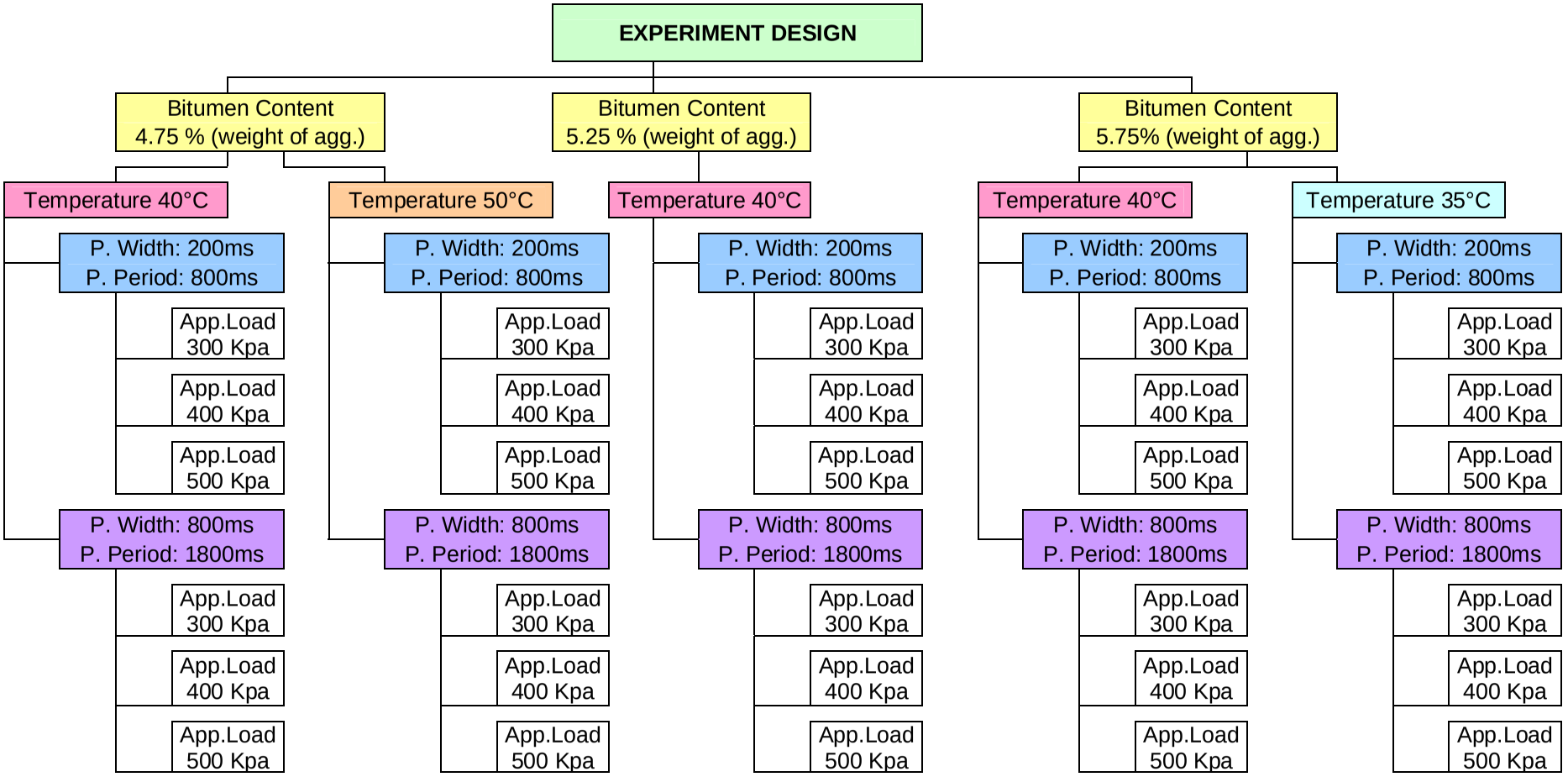

Figure 4.2: Experiment Design

4.7 Naming Convention of Specimens Due To Test Conditions

The name of a tested specimen points out the test conditions and the number of replicate. The letter in the first place expresses the bitumen content of the specimen. The letters A, B and C refer to respectively 4.75%, 5.25% and 5.75% bitumen contents on aggregate basis. The second and third digits express the test temperature in Celsius. The fourth and fifth digits express the pulse width in seconds. The sixth and seventh digits express the pulse period in seconds. The next three digits refer the applied axial stress on the specimen. And finally, the last digit is the replicate number. If the last digit (repeat no) is missing, this refers to the average of the replicates. Naming convention is presented in Figure 4.3.

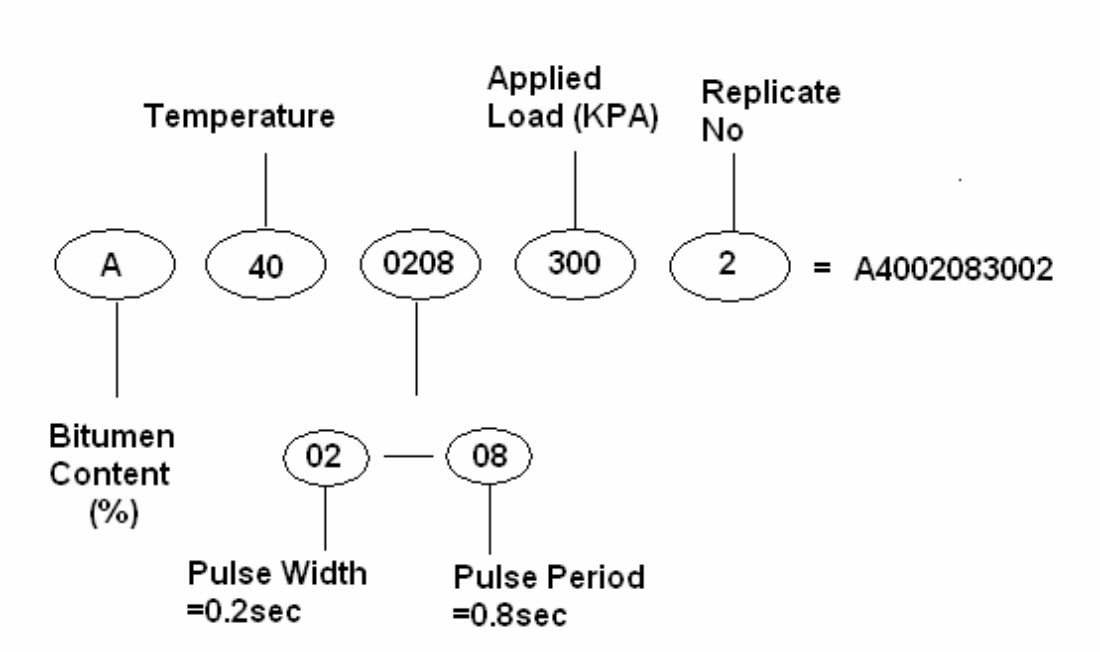

Figure 4.3: A sample of specimen name

4.8 Specimen Properties

As stated in the previous sections, the physical properties of specimens are recorded with great care since the length and diameter of each specimen significantly affects the calculations of the UMMATA software. The specimens without surface and shape irregularities are used for the tests.

Not only the specimen's dimensions, but also the air voids content of specimens has tremendous affects on the analysis as stated in the previous researches.

Physical properties of the test specimens of which the test results are examined, are given in Table A.2 in Appendix A.

CHAPTER 5

EVALUATION OF TEST RESULTS

In this study, a total of 144 standard asphalt concrete Marshall specimens were prepared and subsequently used for both calibration of the test instrument and establishing experimental design program. Among these, only the test results of 54 specimens were used in the analyses. At least two replicate tests were performed for each different combination of material and test condition parameters.

As discussed in chapter 4, the pivot temperature was chosen to be 40°C and two other test temperatures are set as 35°C and 50°C. From the initial test results of the tests conducted on specimens with the optimum bitumen content, it is observed that the test results at 35°C slightly differs from the test results at 40°C, indicating 5°C temperature decrease at this temperature level has no considerable effect on the creep behavior. On the other hand, the specimens tested at 50°C failed rapidly. Especially for the specimens with bitumen contents of 4.75% and 5.75, it was hardly possible to save permanent strain data because the specimens failed after the application of a few load pulses. Because of these and additionally the time constraint faced with due to the scheduled research program in the Laboratory, the remaining tests to be conducted at 35°C and 50°C were cancelled.

A limited number of test results were obtained at 35°C and 50°C because of the above reasons. Although, initially these tests were planned to be analyzed statistically, the number of test results was too few to carry out such analysis. The available test results at 35°C and 50°C were used for studying the effect of temperature on the dynamic creep behavior only graphically.

The results of all tests are presented as groups of creep curves in Figures B1 to B10 in Appendix B. Although the recorded creep curves conform to the expected trends of asphalt concrete creep behavior, the test results of identical specimens tested under identical test conditions show considerable deviations from each other indicating that the repeatability is too low to be studied analytically. For this reason, it is decided to use average creep curves in order to have a single mean creep curve to represent the creep behavior of identical specimens tested under identical test conditions. Thus, a reduced creep test database is established to simplify the analysis.

5.1 Factors Affecting Creep Behavior

The creep behavior of asphalt concrete can be analyzed with respect to both mix parameters and test condition parameters. The groups of mean creep curves obtained for each replicate can be presented in such a way that the graphical evaluation of creep behavior can readily be performed with respect to bitumen content, applied load, load frequency and temperature. The plots prepared in this manner are evaluated in the following sections.

5.1.1 Bitumen Content

The mean creep curves for analysis with respect to bitumen content are presented in Figure 5.1 and Figure 5.2. In Figure 5.1, permanent strain versus pulse count for specimens tested under 0.2 sec pulse width and 0.8 sec pulse period at 40°C are plotted with respect to applied stress. In Figure 5.2, permanent strain versus pulse count for specimens tested under 0.8 sec pulse width and 1.8 sec pulse period at 40°C are plotted with respect to applied stress. In both figures, mean creep curves for 4.75%, 5.25% and 5.75% bitumen contents are shown. As expected, the increase in the bitumen content causes increases in permanent strain and shortens failure duration. In addition to that, slope of creep curves in the second stage increase with the increase in the bitumen content.

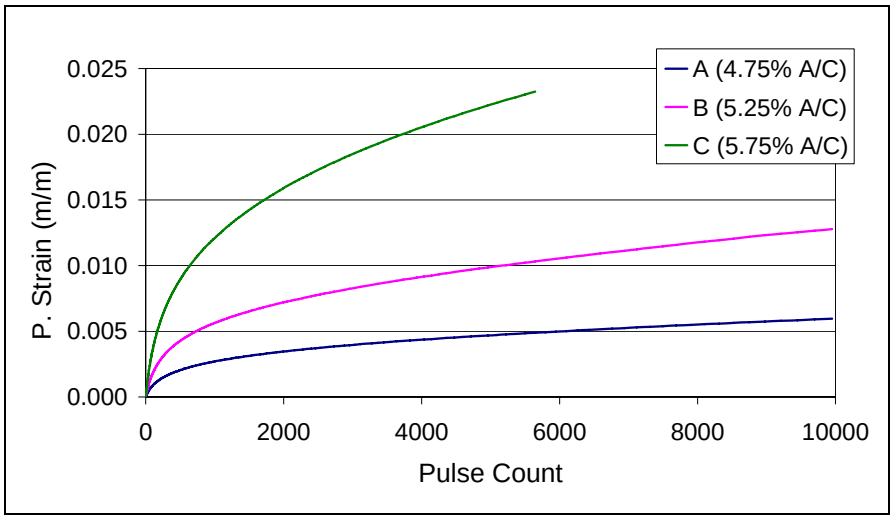

a) For 300 KPa Stress

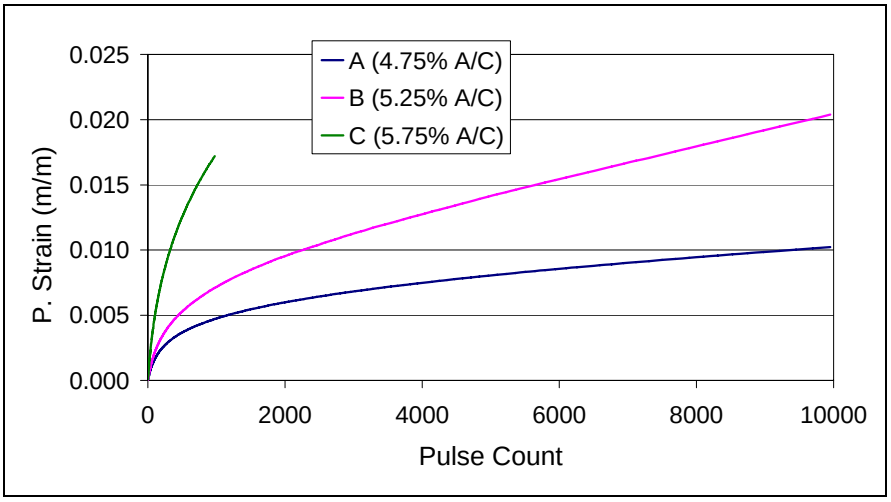

b) For 400 KPa Stress

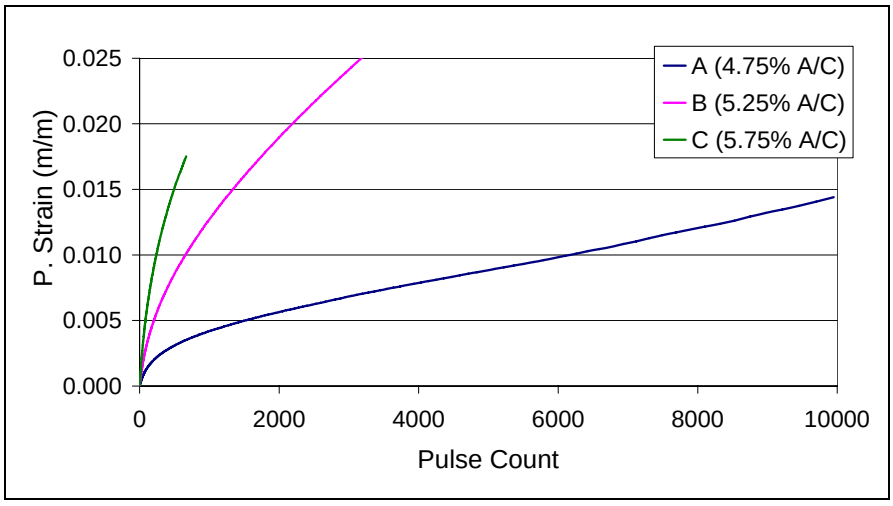

c) For 500 KPa Stress

Figure 5.1: Creep curves for specimens tested under 0.2 sec pulse width and 0.8 sec pulse period at 40°C

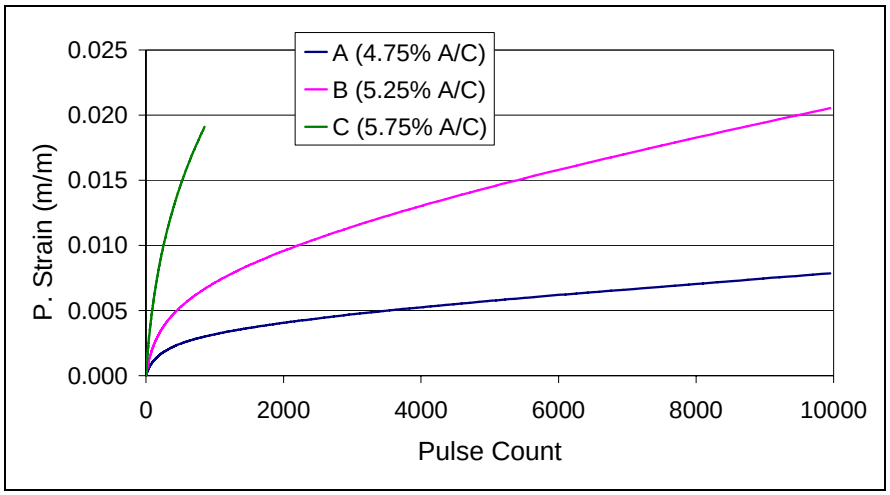

a) For 300 KPa Stress

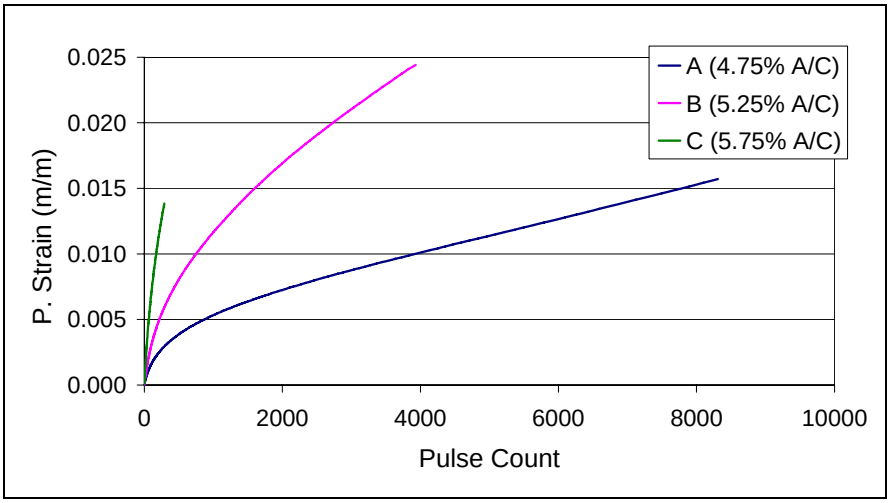

b) For 400 KPa Stress

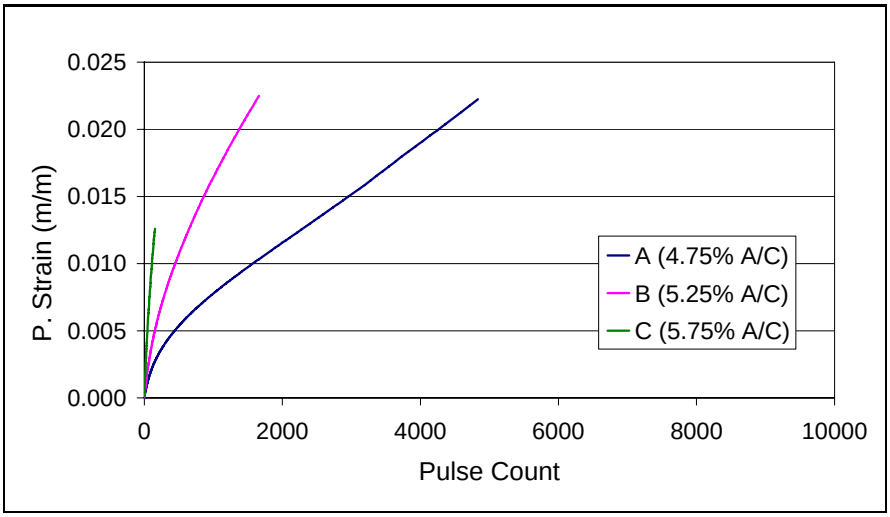

c) For 500 KPa Stress

Figure 5.2: Creep curves for specimens tested under 0.8 sec pulse width and 1.8 sec pulse period at 40°C

5.1.2 Load Frequency

The mean creep curves presented in previous section can be rearranged to observe and analyze the effect of pulse width on the creep behavior. Figure 5.3, Figure 5.4 and Figure 5.5 show the effect of two pulse widths of 0.2 sec and 0.8 sec used in this study on the creep behavior.

As expected, the permanent strain accumulations for the tests conducted with 0.2 sec pulse width are considerably low with respect to ones conducted with 0.8 sec pulse width. This observation approves that the permanent strain of asphalt concrete under fast traffic should be less than the permanent strain under slow traffic.

5.1.3 Applied Load

The mean creep curves presented in Figure 5.6, Figure 5.7 and Figure 5.8 are prepared to examine the variation of creep behavior under three stress levels, 300 Kpa, 400 Kpa, and 500 KPa applied in this study.

As expected, the increase in applied load increases permanent strain and thus shortens failure duration. The change in the slope of the curve in the second stage of creep due to load variation clearly observed from the creep curves. The creep curves presented in this manner reflect the expected asphalt concrete creep behavior under different levels of repeated load.

5.1.4 Temperature

The mean creep curves obtained from the limited number of tests conducted at 35°C and 50°C are presented together with the mean creep curves obtained from the tests conducted at pivot temperature of 40°C are presented in Figures 5.9 thorough 5.12. As expected, the increase in the test temperature increases the accumulated permanent strain at any instant of the test which ends up with a decrease in failure duration.

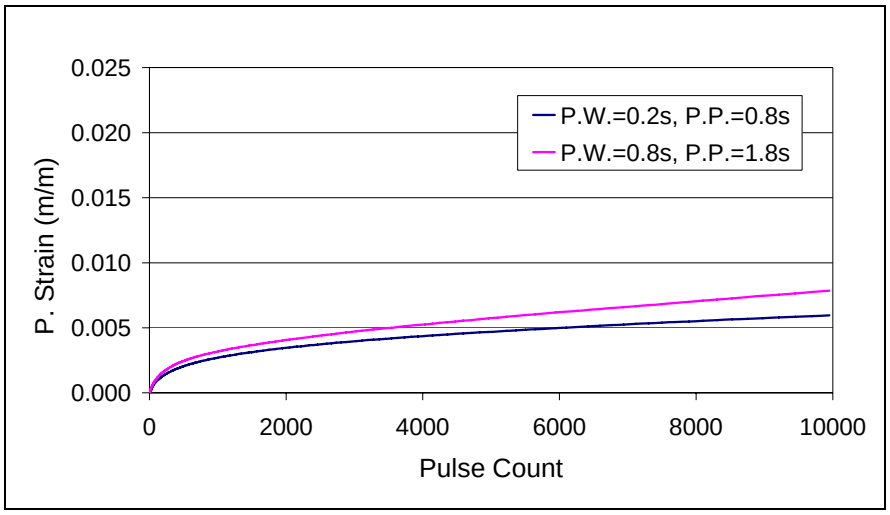

a) For 300 KPa Stress

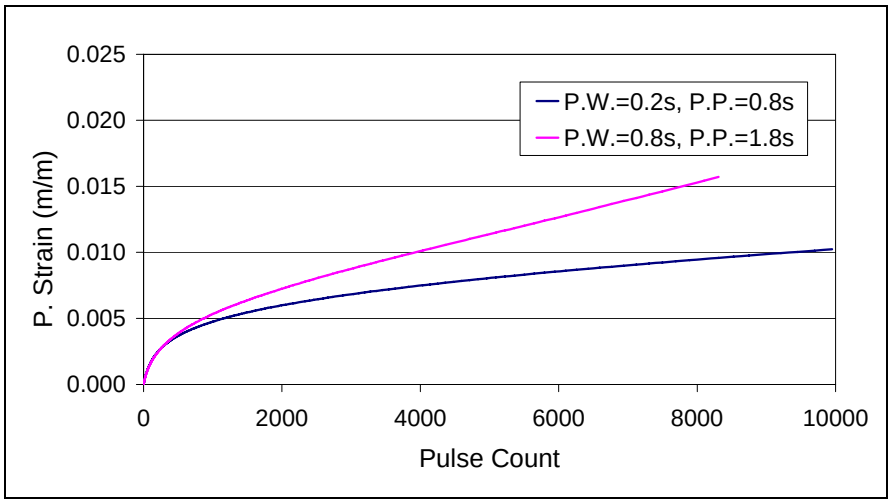

b) For 400 KPa Stress

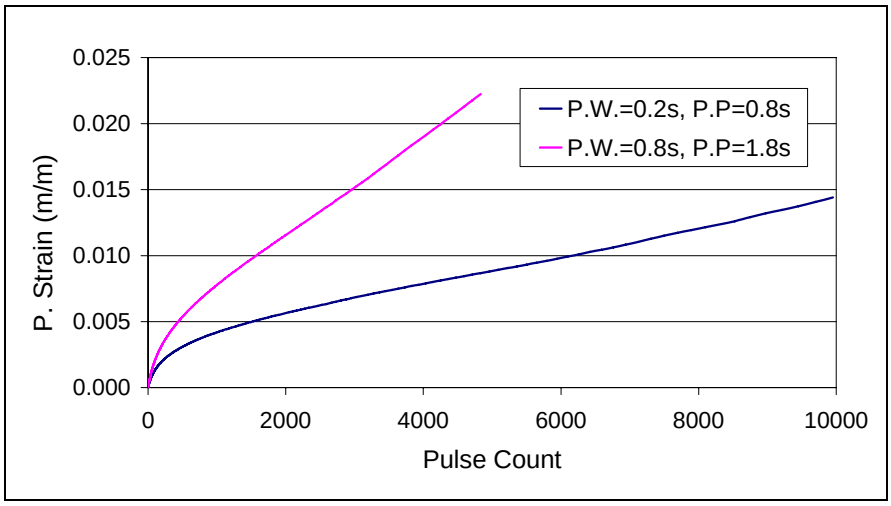

c) For 500 KPa Stress

Figure 5.3: Creep curves for specimens with 4.75% bitumen content tested at 40°C

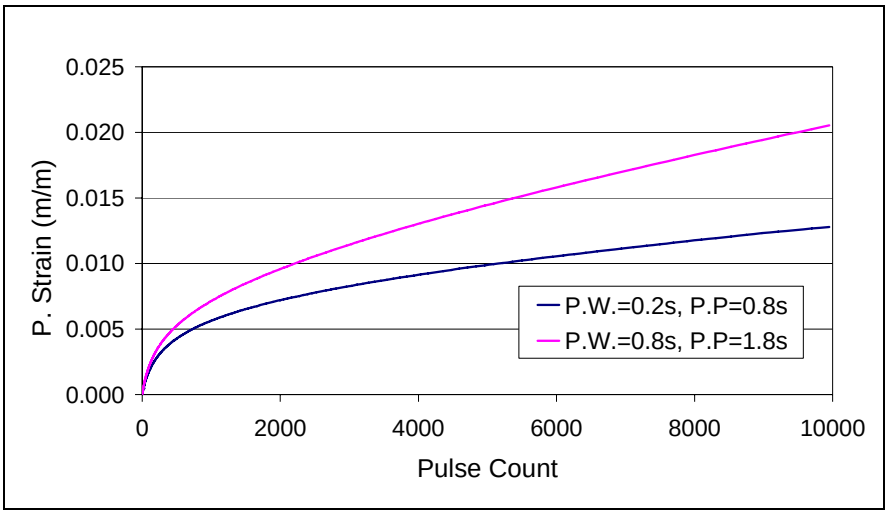

a) For 300 KPa Stress

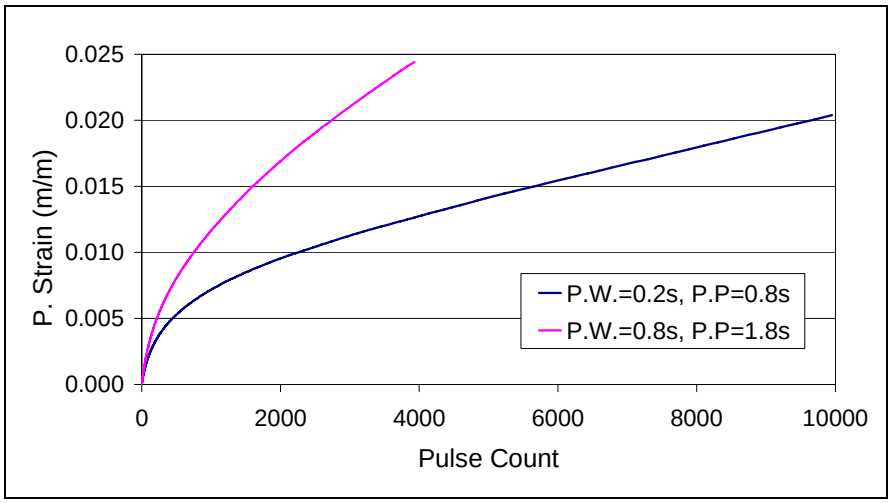

b) For 400 KPa Stress

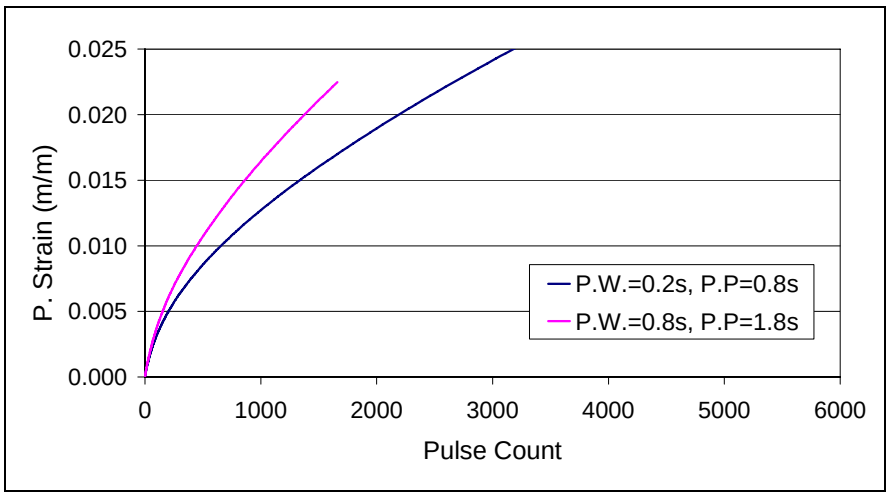

c) For 500 KPa Stress

Figure 5.4: Creep curves for specimens with 5.25% bitumen content tested at 40°C

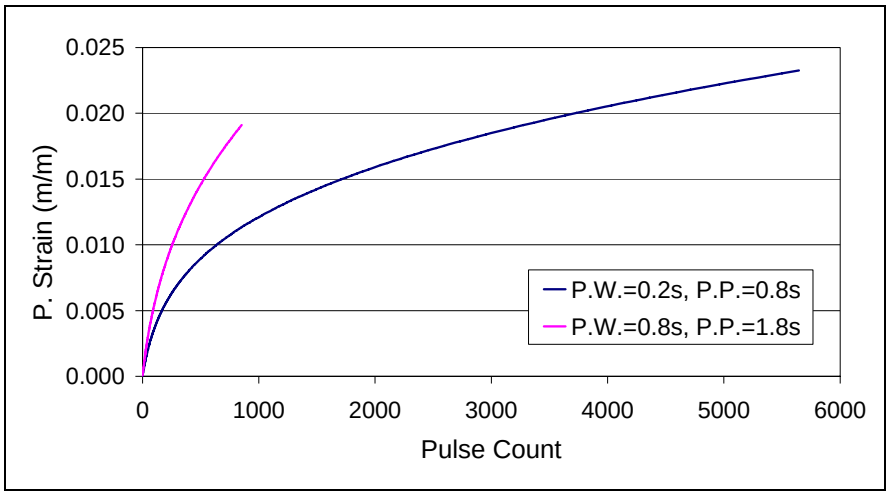

a) For 300 KPa Stress

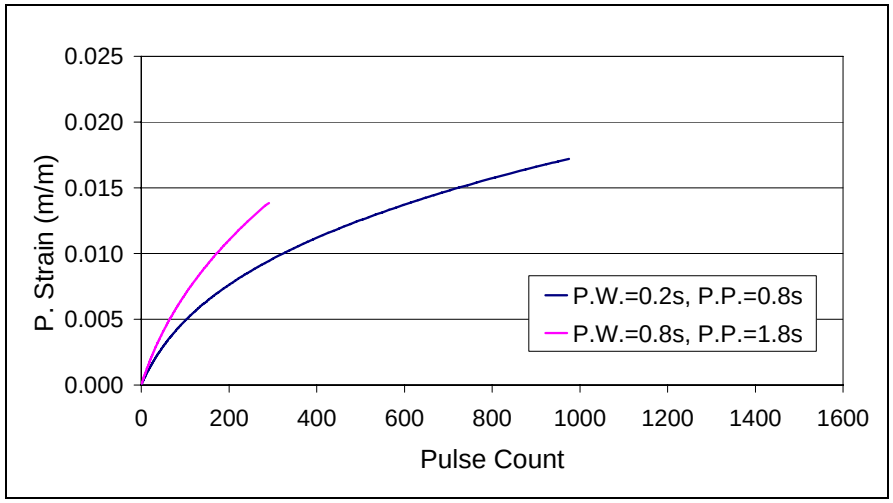

b) For 400 KPa Stress

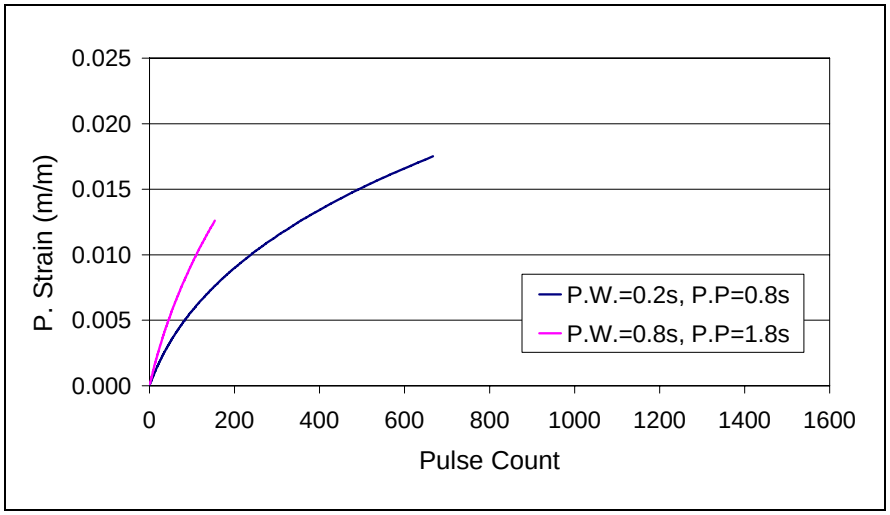

c) For 500 KPa Stress

Figure 5.5: Creep curves for specimens with 5.75% bitumen content tested at 40°C

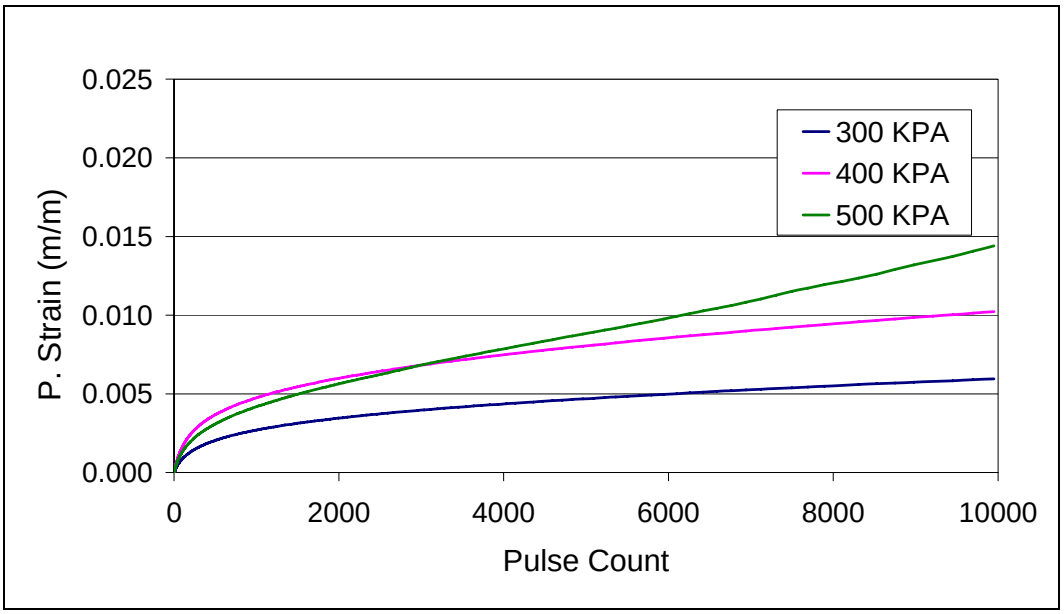

a) Under 0.2 sec pulse width and 0.8 sec pulse period

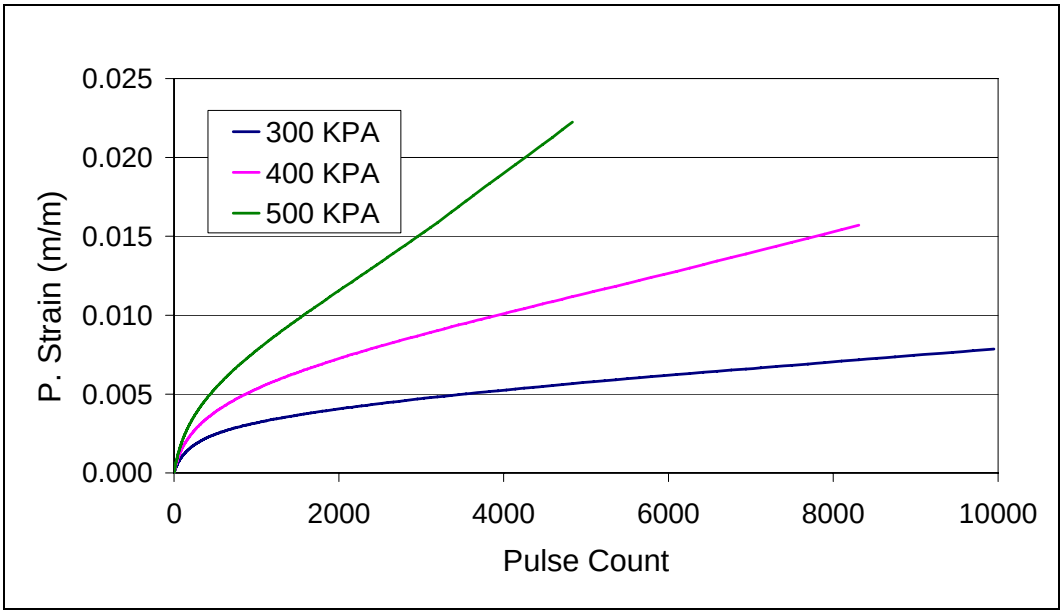

b) Under 0.8 sec pulse width and 1.8 sec pulse period

Figure 5.6: Creep curves for specimens with 4.75% bitumen content tested at 40°C

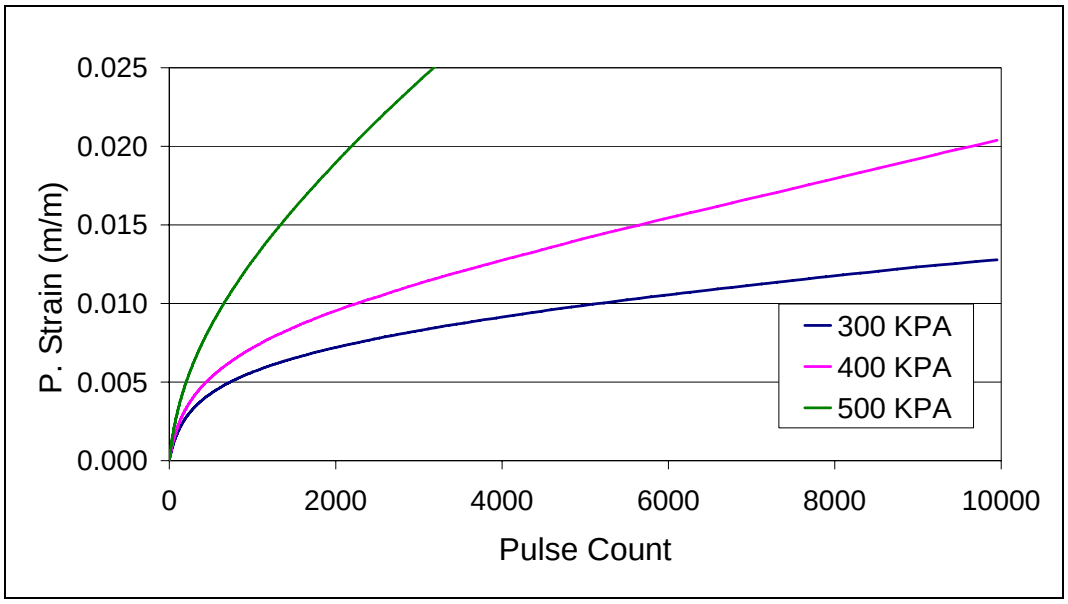

a) Under 0.2 sec pulse width and 0.8 sec pulse period

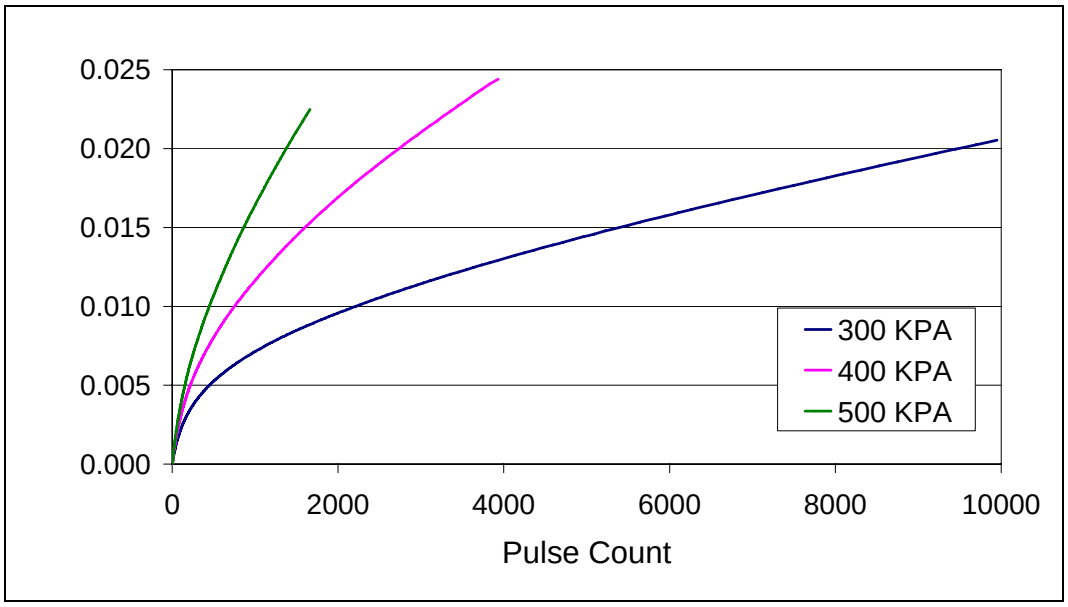

b) Under 0.8 sec pulse width and 1.8 sec pulse period

Figure 5.7: Creep curves for specimens with 5.25% bitumen content tested at 40°C

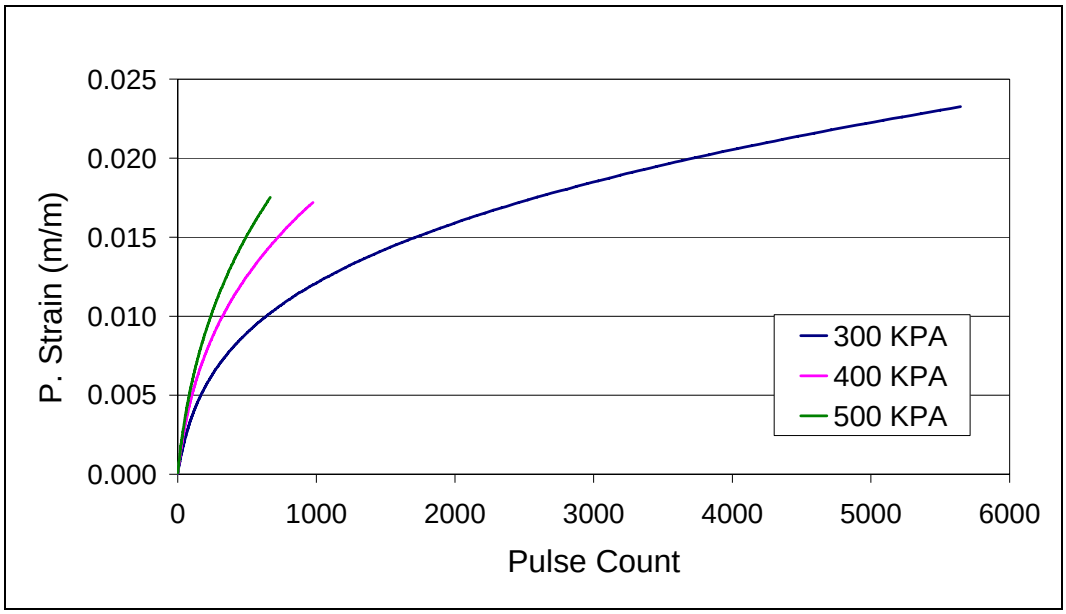

a) Under 0.2 sec pulse width and 0.8 sec pulse period

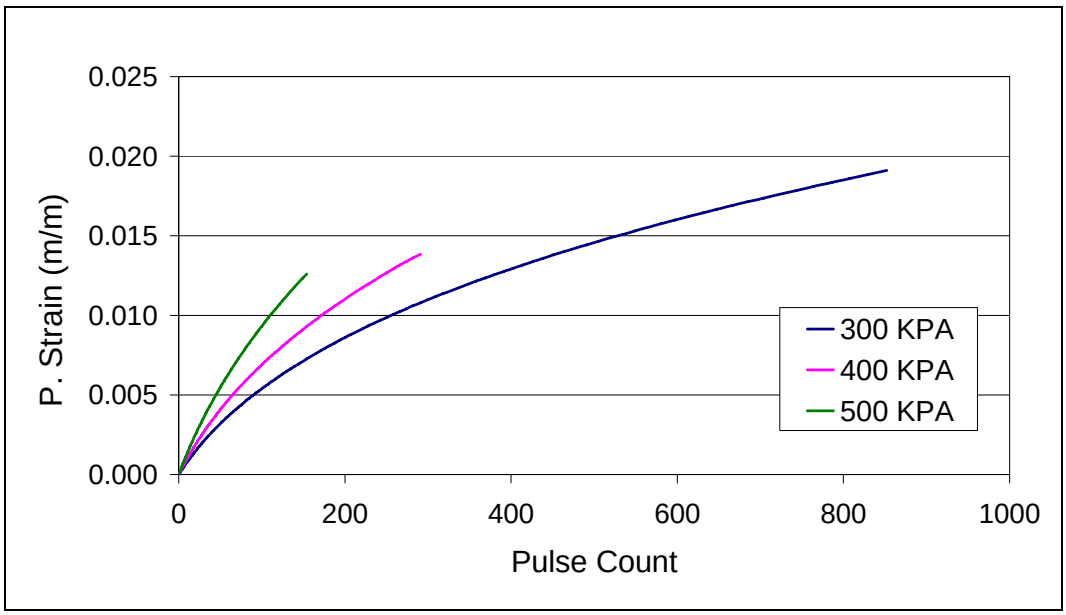

b) Under 0.8 sec pulse width and 1.8 sec pulse period

Figure 5.8: Creep curves for specimens with 5.75% bitumen content tested at 40°C

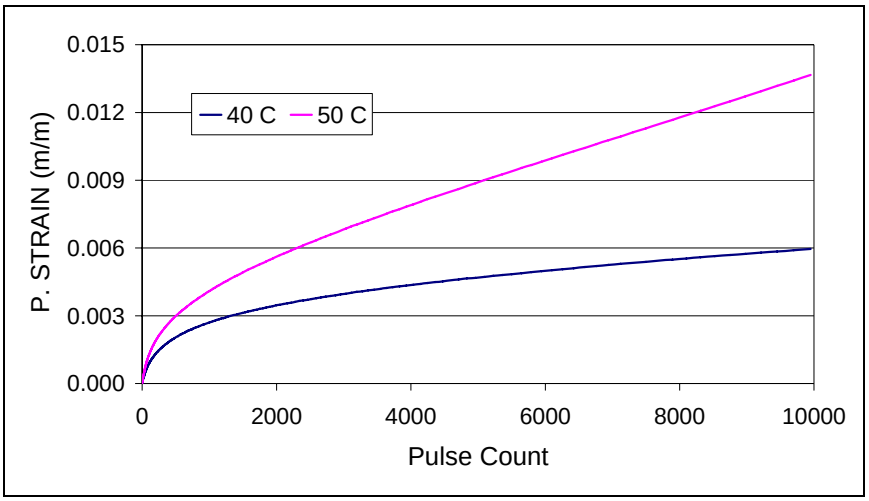

a) For 300 KPa Stress

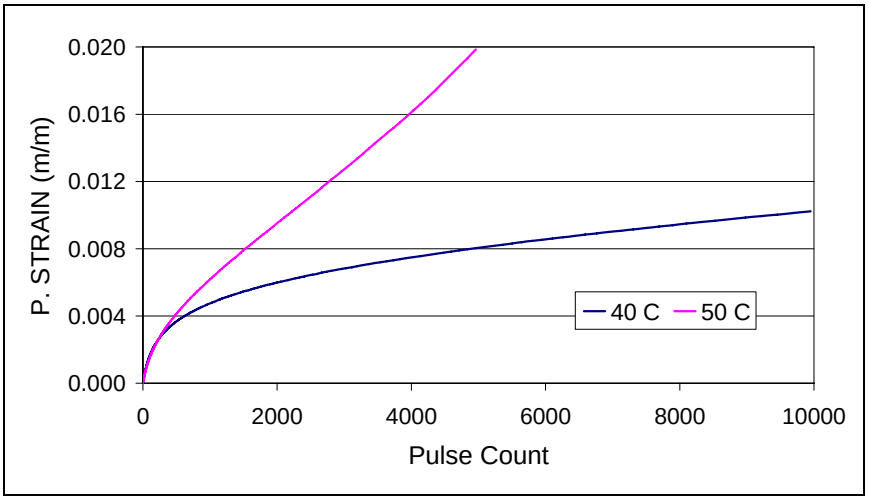

b) For 400 KPa Stress

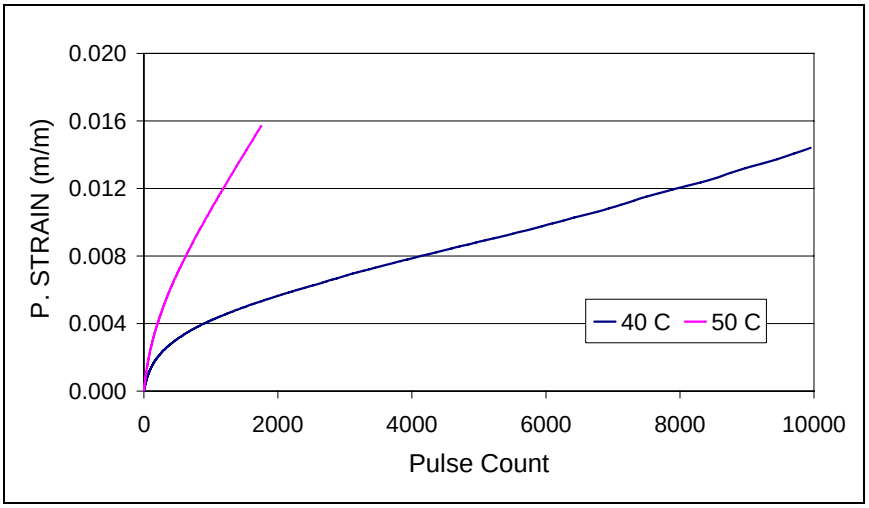

c) For 500 KPa Stress

Figure 5.9: Creep curves for specimens with 4.75% bitumen content tested under 0.2 sec pulse width and 0.8 sec pulse period

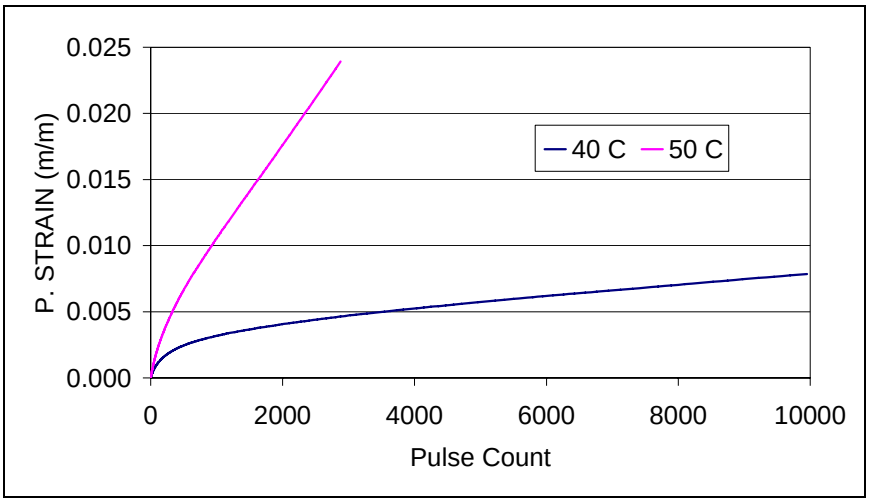

a) For 300 KPa Stress

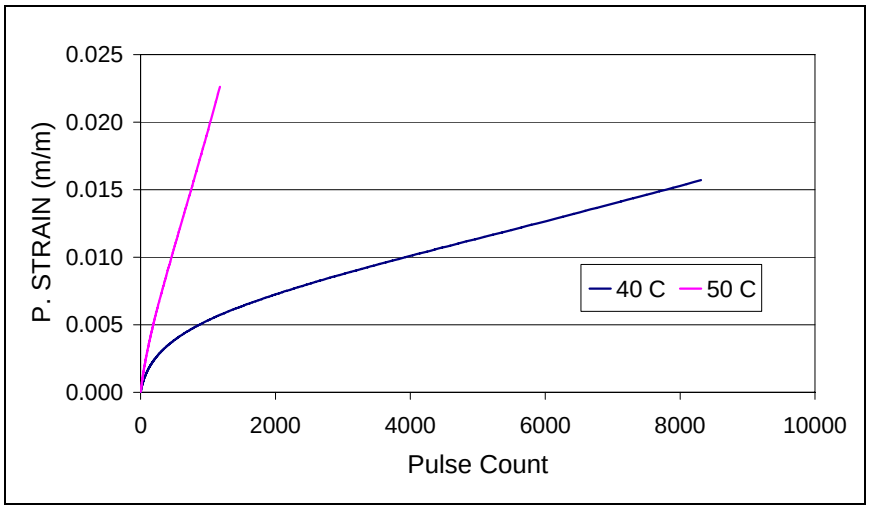

b) For 400 KPa Stress

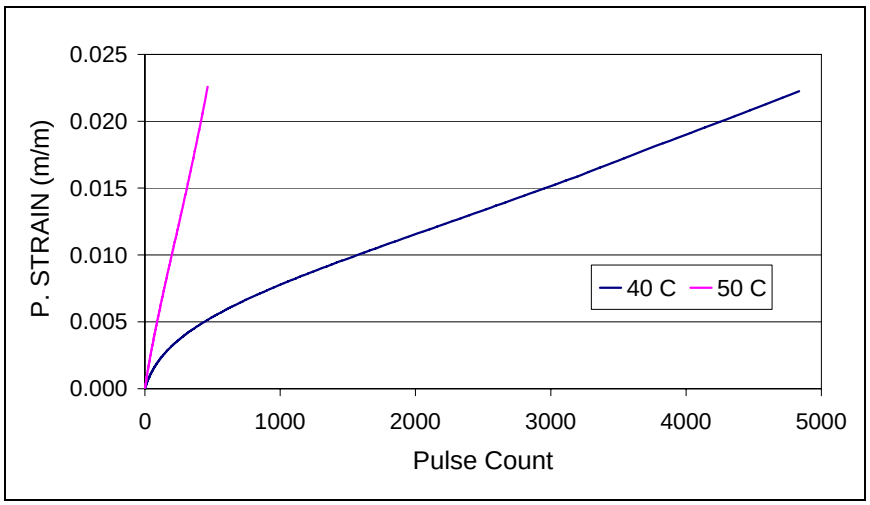

c) For 500 KPa Stress

Figure 5.10: Creep curves for specimens with 4.75% bitumen content tested under 0.8 sec pulse width and 1.8 sec pulse period

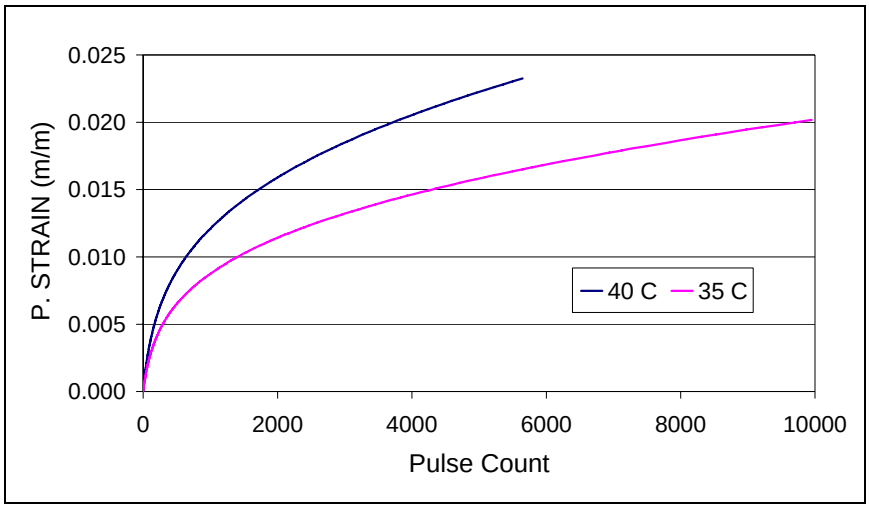

a) For 300 KPa Stress

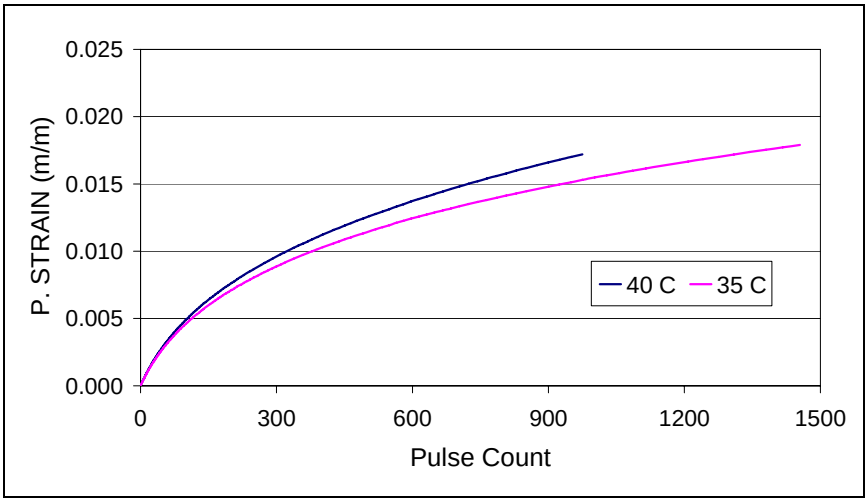

b) For 400 KPa Stress

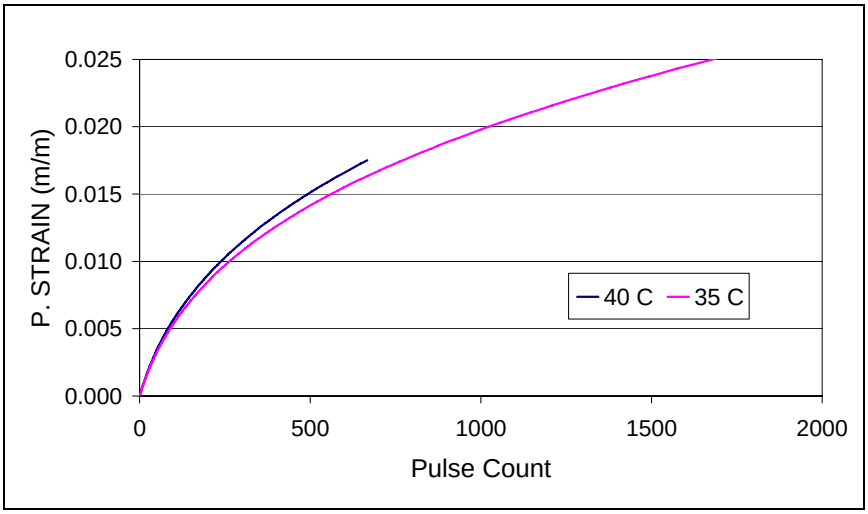

c) For 500 KPa Stress

Figure 5.11: Creep curves for specimens with 5.75% bitumen content tested under 0.2 sec pulse width and 0.8 sec pulse period

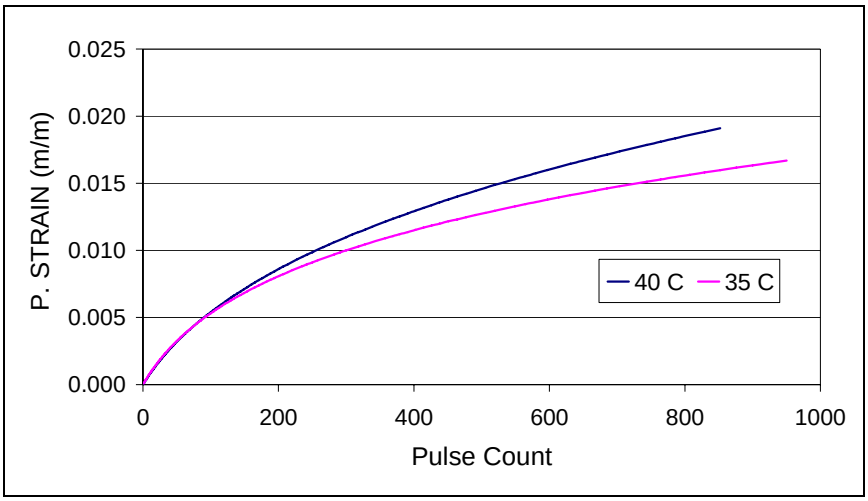

a) For 300 KPa Stress

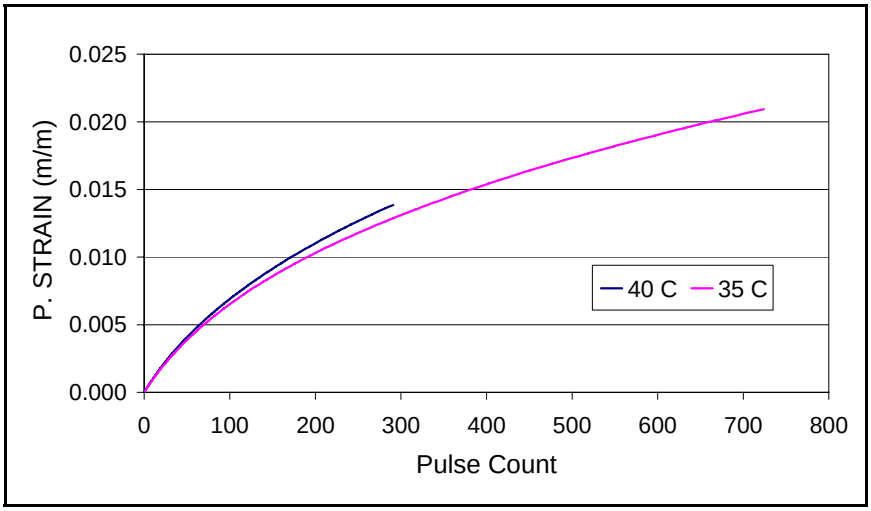

b) For 400 KPa Stress

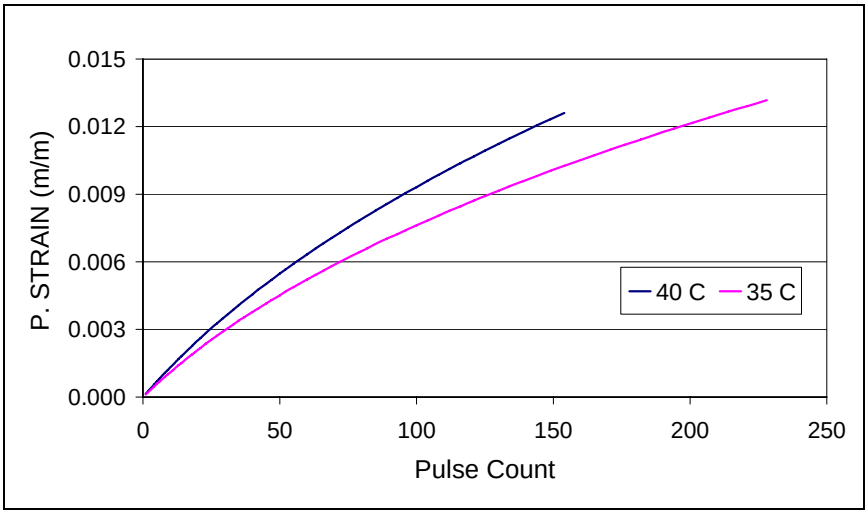

c) For 500 KPa Stress

Figure 5.12: Creep curves for specimens with 5.75% bitumen content tested under 0.8 sec pulse width and 1.8 sec pulse period

5.2 Mathematical Models and Parametric Studies

5.2.1 General

The primary objective of this study is to search for correlations between the parameters of the selected mathematical models and the factors effecting creep behavior, in relation to bitumen content, applied load and frequency. The second initial objective is, if possible, to formulate some primitive constitutive equations for mathematical model parameters as functions of factors affecting the creep behavior. But, because of limited data, no attempt for this objective could be possible within the scope of this thesis.

In Section 5.1, asphalt concrete creep behavior is examined on the plots of creep curves for the specimens with three different bitumen contents under various test conditions. The trends observed in the mean creep curves indicate that the tested specimen exhibit expected creep behaviors.

The second step is to study the mean creep curve data analytically. In literature, there are many attempts to represent the creep behavior by mathematical models for this purpose. Various mathematical models are suggested to represent the time dependent behavior of asphalt concrete as discussed in Chapter 2.

Initially two mathematical creep models are selected from the literature for analytical study. The first one is the model suggested by Beckedahl et al. (1992). This model represents well all the three stages of a typical creep curve. The second model is the power model suggested by Monismith et al. (1975). This model is also a very popular, and a well-known model. It is generally used for representing only the secondary stage of the creep curve.

A third model is suggested by the author and used within the scope of this study. This model is obtained by modifying the model suggested by Beckedahl et al. (1992) as explained later in this chapter. It is observed that

this model is successful in representing both primary and secondary stage in a typical creep curve.

In the following sections, three selected mathematical models are studied and the parameters of the models are determined for the mean creep curves selected for the statistical analysis. The model parameters are determined by regression analyses performed by using the nonlinear regression tool box of the software SPSS.

5.2.2 Model Proposed by Beckedahl et al

A typical creep curve normally has three parts; consolidation, deformation and plastic failure. Likewise, a creep model may also be formed to have three parts of known and approved functions to represent those three parts of a typical creep curve. Such a closed mathematical model composed of three components was developed by Beckedahl et al. (1992) to represent any complete typical creep behavior. The model fits well with the experimental creep data. The suggested model by Beckedahl et al is given in Equation 5.1.

$$\varepsilon(n) = E0 + An^{k} + B(e^{nC} + 1) \qquad \text{(Eqn. 5.1)}$$

n = Pulse Count (number of load applications)
ε(n) = Strain after load application n
E0, A, B, C,k = Parameters

The first component “E0” stands for the consolidation. This part is affected not only by the specimen properties and experiment conditions but also by surface irregularities, and friction between platens and the specimen.

The second component “An^{k}” expresses the creep deformation, which represents the normal load-number function of the permanent deformation. During this section, the volume of the specimen does not change.

The third component "B(e^{nC}+1)" represents the plastic failure part. Mostly, this part is only observed in triaxial tests. (Beckedahl et al. 1992).

In Figure 5.13, three components of the model are plotted separately. The horizontal line represents the consolidation, "E0". The section between the straight line and the middle line is equal to the permanent deformation due to repeated loading. And lastly, the section between the middle and upper line gives the permanent deformation from plastic failure. (Beckedahl et al 1992)

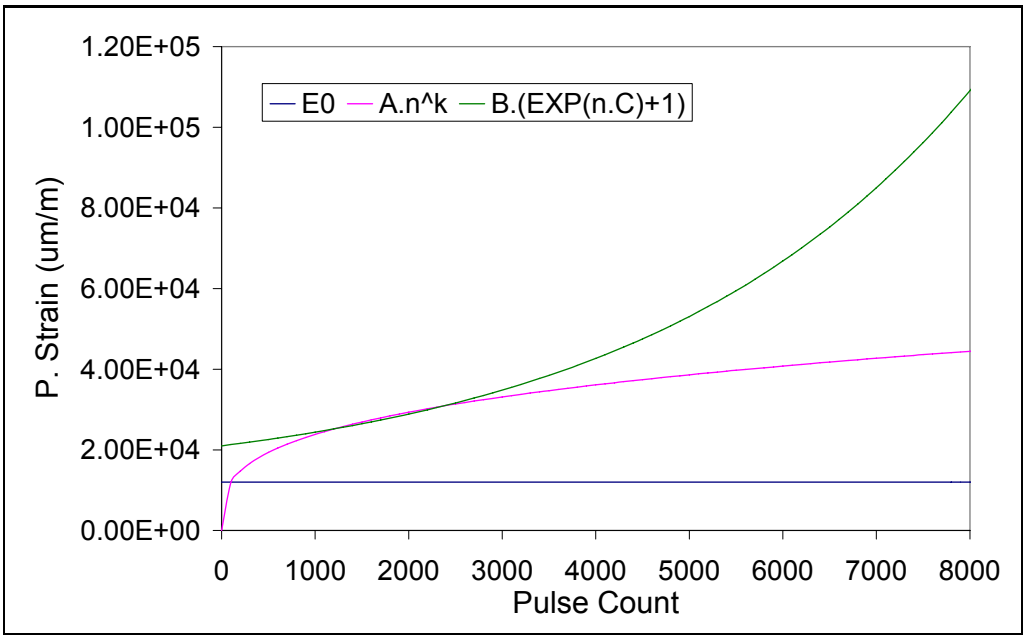

Figure 5.13: Three parts of equation (schematic plot)

5.2.2.1 Parameters of Model Proposed by Beckedahl et al

The parameters E0, A, B, C and k of the model given by Equation 5.1 are determined by the regression analysis. The parameters for the designated mean creep curves and the correlation of deviation (R^2) values are given in Table 5.1. R^2 is the interaction of variability in a data set.

Table 5.1: Parameters of the model given by Equation 5.1 fit to mean creep curves of each replicate and correlation of deviation R^2.

Rep. No.	A400208300	A400208400	A400208500	A400818300	A400818400	A400818500
E0	-1.55E-02	-1.89E-02	-1.89E-03	-8.96E-04	-1.18E-03	-3.73E-03
A	1.37E-04	3.32E-04	3.98E-04	4.91E-04	3.79E-04	3.31E-04
B	7.64E-03	9.13E-03	5.82E-04	2.40E-05	2.22E-04	1.53E-03
C	-1.08E-04	-1.39E-04	2.16E-04	3.52E-04	3.12E-04	3.58E-04
k	4.80E-01	4.33E-01	3.59E-01	3.03E-01	3.98E-01	4.57E-01
R2	0.99974	0.99959	0.99976	0.99913	0.99977	0.99983
Rep. No.	**B400208300**	**B400208400**	**B400208500**	**B400818300**	**B400818400**	**B400818500**
E0	-2.99E-02	-1.51E-03	-6.88E-04	-1.78E-03	-8.38E-04	-6.32E-01
A	2.90E-04	6.61E-04	3.10E-04	5.96E-04	3.80E-04	1.64E-04
B	1.46E-02	1.05E-04	2.60E-05	3.14E-04	1.00E-06	3.16E-01
C	-1.23E-04	3.21E-04	1.00E-03	2.13E-04	1.60E-03	-1.18E-04
k	4.79E-01	3.67E-01	5.44E-01	3.79E-01	5.06E-01	8.33E-01
R2	0.99965	0.99955	0.99993	0.99969	0.99985	0.99996
Rep. No.	**C400208300**	**C400208400**	**C400208500**	**C400818300**	**C400818400**	**C400818500**
E0	-1.42E-01	-2.69E-01	-3.52E-01	-3.13E-01	-6.83E-01	-9.61E-01
A	3.29E-04	3.15E-04	3.25E-04	3.24E-04	3.21E-04	3.80E-04
B	7.05E-02	1.34E-01	1.76E-01	1.56E-01	3.41E-01	4.80E-01
C	-1.09E-04	-1.72E-04	-1.83E-04	-1.65E-04	-1.86E-04	-2.06E-04
K	5.96E-01	6.99E-01	7.34E-01	7.16E-01	8.14E-01	8.54E-01
R2	0.99981	0.99974	0.99970	0.99966	0.99967	0.99970

5.2.3 Mathematical Model $E= E0 + A.n^k$

Since the experiments are terminated after 10.000 pulse cycles, the tertiary stage of the creep does not reached in most of the experiments. Therefore; a simpler model that is only capable of representing the primary and secondary stages of the creep model is proposed. The suggested model is a modified

form of the model given by Beckedahl et al obtained by eliminating the third part of the mathematical expression of the model given by Equation 5.1. Thus the mathematical expression of the derived model in this manner takes the form given in Equation 5.2. Similar to original model given by Equation 5.2, the first component "E0" represents the consolidation and the second component "An^k" represents the creep deformation.

$$\varepsilon(n) = E0 + A * n^k \qquad \text{(Eqn. 5.2)}$$

n = Pulse Count (number of load applications)

ε(n) = Strain after load application n

E0, A, k = Parameters

5.2.3.1 Parameters of Mathematical Model $E= E0+ A.n^k$

The Parameters E0, A and k of the model are determined by the regression analysis. The parameters for the designated mean creep curves and R^2 values are given in Table 5.2.

If the two mathematical models are compared, the reduction in the R^2 value can be observed. However, the model is statistically significant since the R^2 values are not less than 99%. Besides, this model is not successful in fitting the tertiary stage of creep as expected. The graphical analysis shows that this model successfully fits the first stage of creep curves.

Table 5.2: Parameters of the model given by Equation 5.2 fit to mean creep curves of each replicate and correlation of deviation, R^2.

Rep. No.	A400208300	A400208400	A400208500	A400818300	A400818400	A400818500
E0	-8.53E-04	-1.61E-03	1.59E-04	-5.78E-04	-1.79E-04	2.86E-04
A	4.76E-04	9.60E-04	1.01E-04	3.52E-04	1.91E-04	8.60E-05
K	2.89E-01	2.72E-01	5.29E-01	3.41E-01	4.84E-01	6.46E-01
R^2	0.99869	0.99869	0.99439	0.99816	0.99782	0.99672
Rep. No.	**B400208300**	**B400208400**	**B400208500**	**B400818300**	**B400818400**	**B400818500**
E0	-1.62E-03	-7.09E-04	-5.06E-04	-6.37E-04	-7.84E-04	-6.29E-04
A	8.88E-04	4.30E-04	2.78E-04	3.97E-04	3.65E-04	2.85E-04
K	3.02E-01	4.18E-01	5.60E-01	4.29E-01	5.11E-01	5.93E-01
R2	0.99873	0.99838	0.99987	0.99901	0.99983	0.99987
Rep. No.	**C400208300**	**C400208400**	**C400208500**	**C400818300**	**C400818400**	**C400818500**
E0	-2.94E-03	-1.55E-03	-1.25E-03	-1.41E-03	-7.25E-04	-4.92E-04
A	1.46E-03	7.46E-04	6.14E-04	6.42E-04	4.11E-04	3.64E-04
K	3.36E-01	4.71E-01	5.29E-01	5.16E-01	6.32E-01	7.14E-01
R2	0.99842	0.99849	0.99883	0.99870	0.99921	0.99951

5.2.4 Power Model ($E=an^b$)

The relationship between the permanent strain and the number of load applications can successfully be expressed by the classical power model. Equation 5.3 is the developed mathematical formula for creep analysis. On a log-log scale, the intercept “a” states the permanent strain at n=1 and the slope “b” expresses the rate of change of the permanent strain. The model equation is plotted in Figure 5.14. on a log-log scale. The linear part of the experimental data of the creep test represents the secondary phase of the creep curve. The point or the pulse count, where the linearity is lost, is determined as the starting point of the tertiary phase. In the literature, this point is defined as Flow Number (FN).

$$\varepsilon_p = an^b \qquad \text{(Eqn 5.3)}$$

n = Pulse Count (number of load applications)

ε_p = Permanent Strain

a, b = Parameters

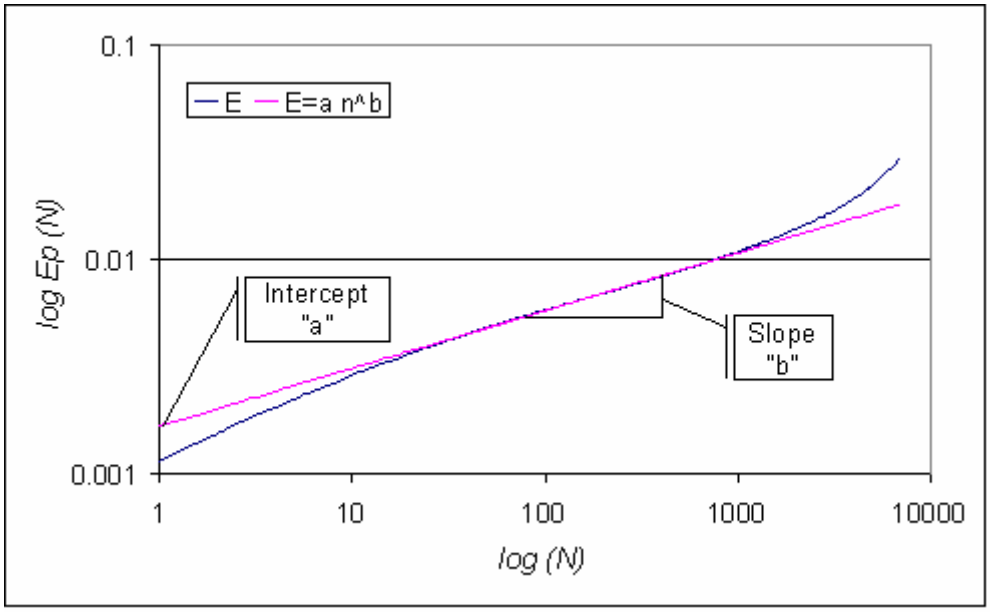

Figure 5.14: Regression constants a and b plotted on a log-log scale

5.2.4.1 Power Model Parameters

Power model given by Equation 5.3 is linear in log-log scale and can only be used to represent the linear part of the creep curve in log-log scale. For this reason, a prior step before using the model should be detected and the linear section of the creep curve should be extracted in the log-log scale. For this purpose a Matlab code written by Asst. Prof. Dr. M. Guler is modified and used to analyze the mean creep curves (Guler 2002).The purpose of the code is to achieve the zone nearest to R^2=1.0 to get the linear part of the creep curve.

The flow numbers are not calculated since the tertiary phase of the creep is not observed in most of the experiments.

The parameters a and b of the power model are determined by regression analysis for each mean creep curve. The parameters for the designated mean creep curves and R^2 values are given in Table 5.3.

Table 5.3: Parameters of the power model given by Equation 5.3 fit to mean creep curves of each replicate and correlation of deviation, R^2.

Rep. No.	**A400208300**	**A400208400**	**A400208500**	**A400818300**	**A400818400**	**A400818500**
a	2.38E-04	3.86E-04	9.90E-05	1.57E-04	1.69E-04	2.40E-05
b	3.50E-01	3.56E-01	5.28E-01	4.22E-01	4.93E-01	8.04E-01
R2	0.99969	0.99995	0.99988	0.99991	0.99992	0.99999
Rep. No.	**B400208300**	**B400208400**	**B400208500**	**B400818300**	**B400818400**	**B400818500**
a	4.45E-04	1.03E-04	2.01E-04	2.84E-04	2.93E-04	2.30E-04
b	3.64E-01	5.74E-01	5.98E-01	4.61E-01	5.34E-01	6.18E-01
R2	0.99994	0.99994	0.99999	0.99999	0.99999	0.99999
Rep. No.	**C400208300**	**C400208400**	**C400208500**	**C400818300**	**C400818400**	**C400818500**
a	1.03E-03	4.65E-04	6.43E-04	6.61E-04	1.16E-04	3.14E-04
b	3.61E-01	5.31E-01	5.08E-01	4.99E-01	9.30E-01	7.36E-01
R2	0.99999	0.99994	0.99996	0.99999	0.99999	0.99992

5.3. Studies on Model Parameters

5.3.1. General

The variations of the model parameters are studied graphically by generating the plots of the model parameters versus the test condition parameters in order to examine the correlations between them. However, the trends observed in these plots do not have definite paths in general. For this reason, it is decided to carry out 3-Way ANOVA analysis for evaluating these trends.

5.3.2. Analysis of Variance (ANOVA)

ANOVA is a common way of analyzing correlation between a dependent variable and independent variables. The variations of the means through the analysis of the sum of squares are concerned in the ANOVA analysis. In statistical terminology, an independent variable is named as a factor. A factor is an independent treatment variable whose settings (values) are controlled and varied by the experimenter. There are two types of factors: experimental and classification. The experimental factors are under the control of experimenter. The classification factors come out randomly.

In this study, the dependent variables are defined as model parameters and independent variables are the test conditions (load frequency, applied load, and bitumen content). Since the values are fixed in this study, the independent variables are the experimental factors. 3-way ANOVA analyses are carried out by N-way analysis tool of Matlab software. (Neter, Wasserman, Whitmore 1978)

The experimental layout is given in Figure 5.15. Factor B refers to the bitumen content in asphalt concrete specimens. Factor L refers to the applied load of uniaxial repeated load creep tests and Factor F refers to the frequency of the applied load.

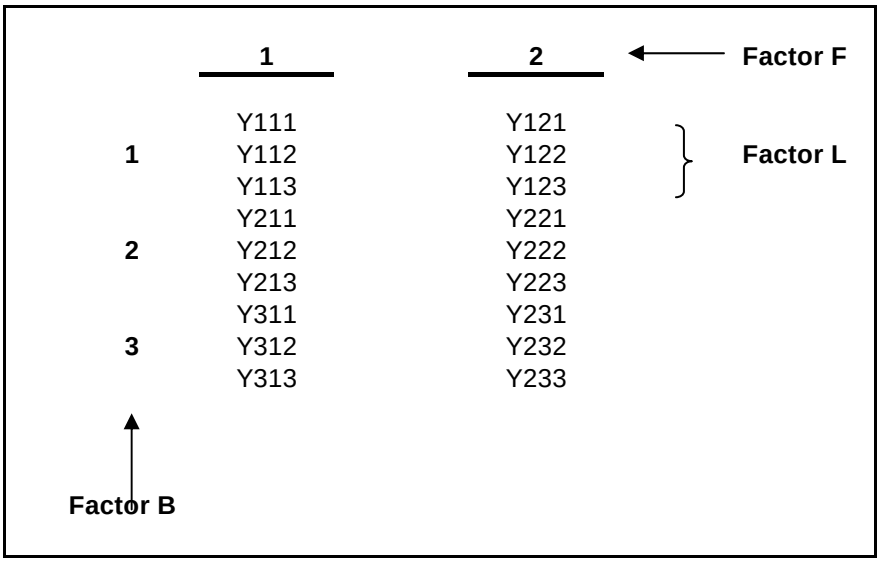

Figure 5.15: The experimental layout

The mean squares are obtained by dividing the sum of squares by the corresponding degrees of freedoms. With the help of F-test, the p-values are calculated for each independent factor. The calculations of a 3-way ANOVA are summarized in Table 5.4.

Table 5.4: ANOVA Table for three factor study

Source	**Degrees of Freedom**	**Sum of Squres**	**Means Square**	**F value**	**P-value**
X1(Bitumen Content)	B-1	SSB	MSB=(SSB/(B-1))	MSB/MSE	<0.05
X2(Frequency)	F-1	SSF	MSF=(SSF/(F-1))	MSF/MSE	<0.05
X3(Load)	L-1	SSL	MSL=(SSL/(L-1))	MSL/MSE	<0.05
Error	B * F * L	SSE	MSE=(SSE/(BFL(n-1))		
Total	N-1	SST			

If p-value is less than 0.05, which is equal to 95% confidence interval, the independent variable is statistically significant.

The ANOVA tables for analyzing the correlations between the selected model parameters and test variables at 40°C are given in Tables D1 to D10 in Appendix D. The plots showing the variation of the model parameters with the test condition variables are also prepared for three different bitumen contents and given in Figures D1 to D20 in Appendix D. In the following Sections, the results of ANOVA analysis are discussed and the trends which are found to be statistically significant are examined graphically.

5.3.3 Parametric Study of Proposed Model by Beckedahl et al.

According to ANOVA tables from Table D1 to D5 given in Appendix D, only the bitumen content is statistically significant for the parameters “E0”, “B” and “k” of the proposed model by Beckedahl et al. The trends of these parameters with respect to the bitumen content can be observed from Figure 5.16 to Figure 5.18.

It is clear from Figure 5.16 that the increase in bitumen content causes reduction in the value of parameter “E0”. On the contrary, the increase in bitumen content results with an increase in the value of parameter “B” as seen in Figure 5.17. If the mathematical model is examined in its open form given in Equation 5.4, it can be concluded that parameters “E0” and “B” interact oppositely.

$$\varepsilon(n) = E0 + An^{k} + Be^{nC} + B \qquad \text{(Eqn. 5.4)}$$

The trends observed in Figure 5.18 point out that an increase in bitumen content causes generally an increase in the value of parameter “k”.

However, the trends observed graphically and the results of ANOVA analyses only provide some clue upon the general behavior of parameters. No constitutive relation between the model parameters and the bitumen content of specimens can be developed due to limited data points available.

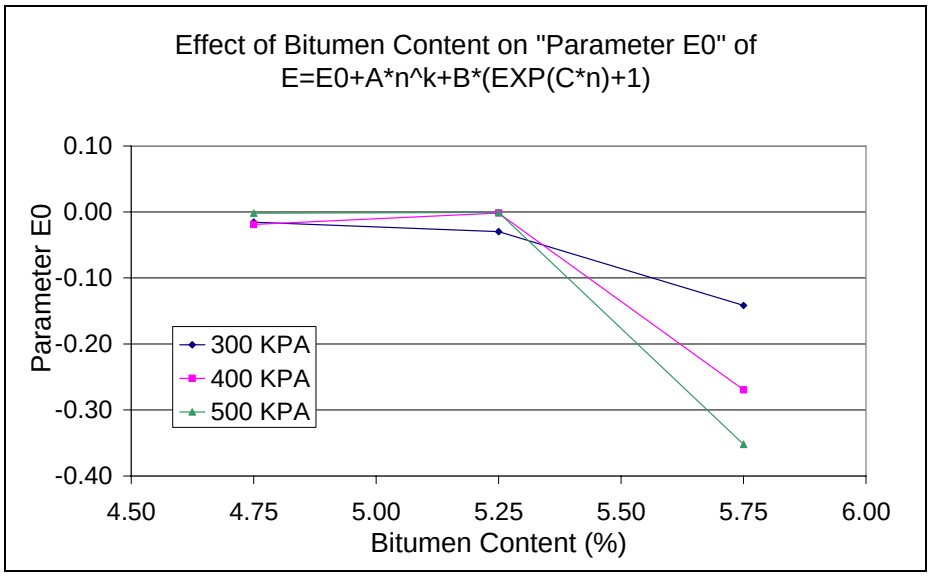

a) Under 0.2 sec pulse width and 0.8 sec pulse period

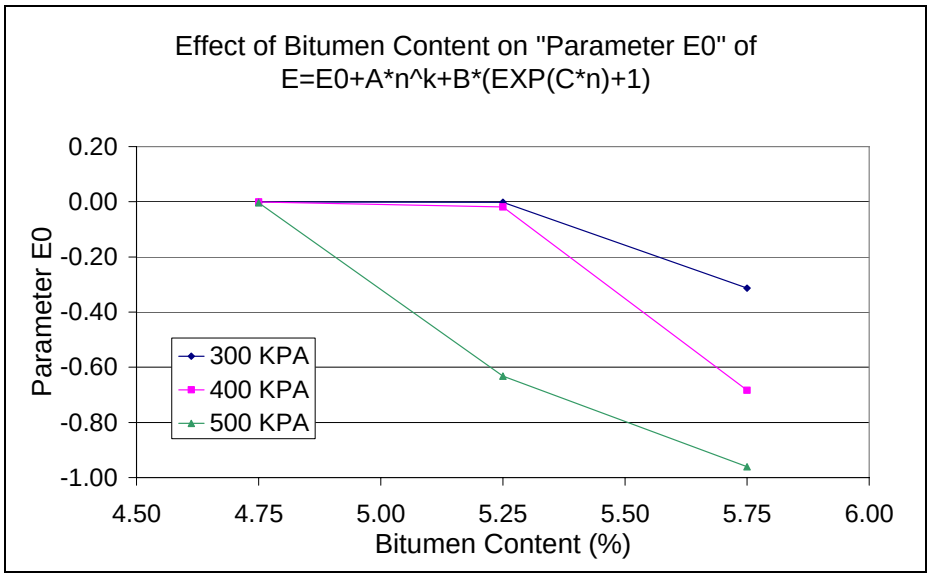

b) Under 0.8 sec pulse width and 1.8 sec pulse period

Figure 5.16: Variation of model parameter “E0” with bitumen content for specimens tested at 40°C

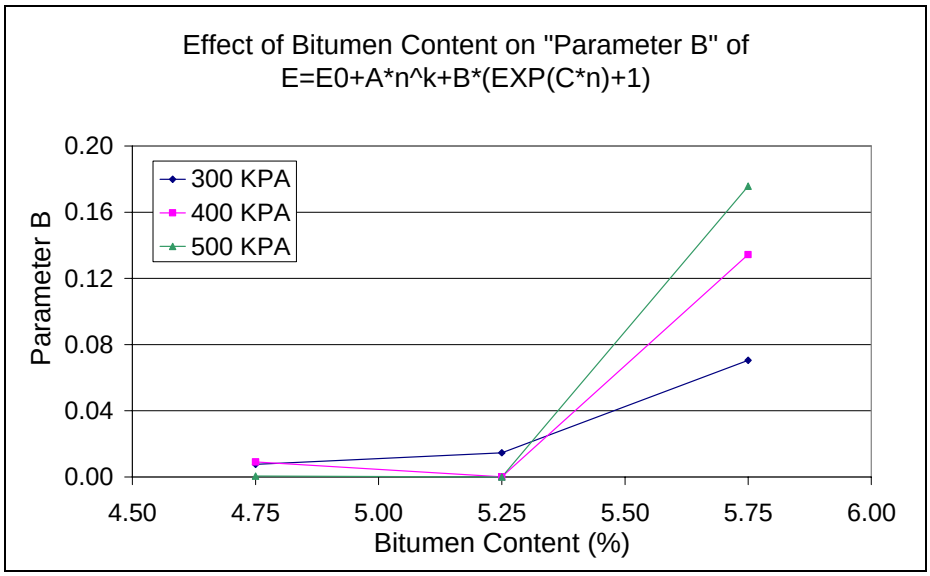

a) Under 0.2 sec pulse width and 0.8 sec pulse period

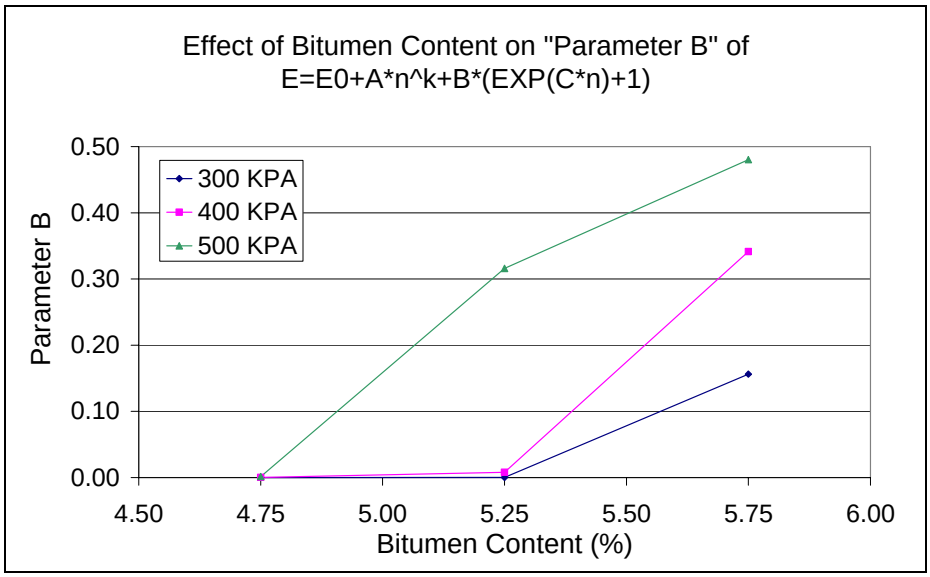

b) Under 0.8 sec pulse width and 1.8 sec pulse period

Figure 5.17: Variation of model parameter “B” with bitumen content for specimens tested at 40°C

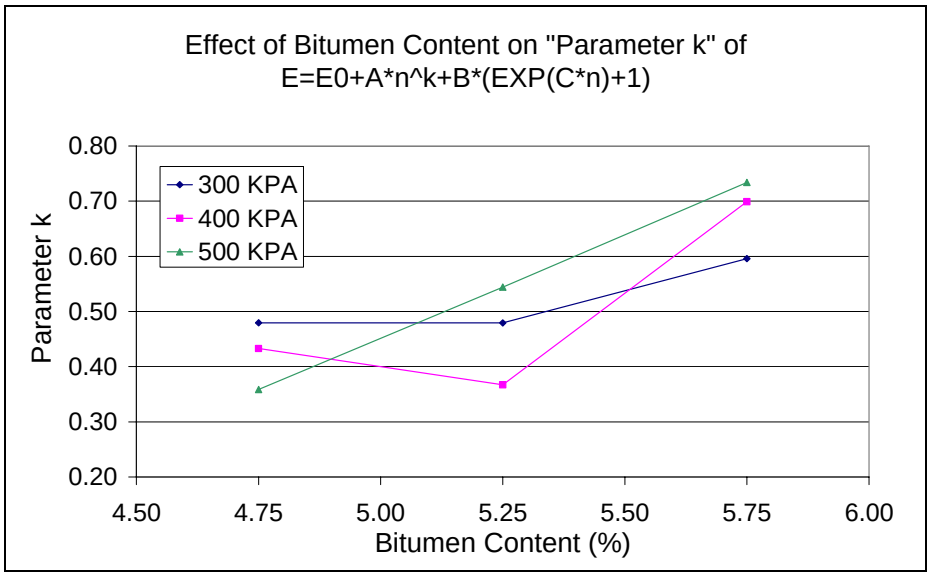

a) Under 0.2 sec pulse width and 0.8 sec pulse period

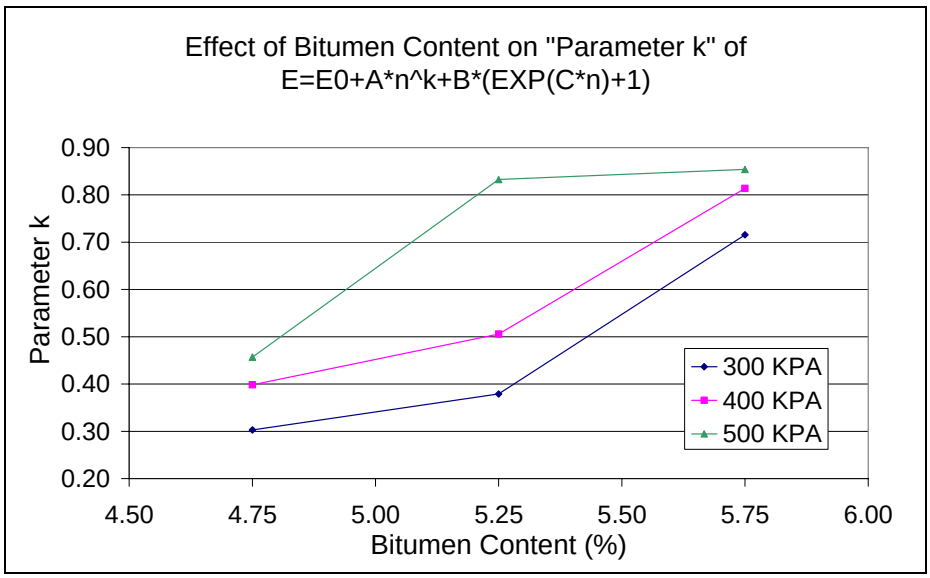

b) Under 0.8 sec pulse width and 1.8 sec pulse period

Figure 5.18: Variation of model parameter “k” with bitumen content for specimens tested at 40°C

5.3.4 Parametric Study of Proposed Model $E=E0+An^k$

According to ANOVA tables from Table D6 to D8 given in Appendix D, the interactions between the parameters of the model and test condition variables are totally changed after eliminating the last term "$B(e^{nC}+1)$" of the proposed model by Beckedahl et al.

The bitumen content and the test condition variables, applied load and load frequency, are also found to be statistically significant for model parameter "E0" since all p-values of these independent factors are smaller than 0.05 as seen in Table D6.

In Figure 5.19, it is observed that an increase in bitumen content generally cause a reduction in the value of parameter "E0", similar to the trend observed for the parameter "E0" of the proposed model of Beckedahl et al.

The variation of parameter "E0" with respect to the load frequency is shown in Figure 5.20. Generally, the value of parameter "E0" increases with the reduction in the load frequency. However, the variation of parameter "E0" for specimens containing 5.25% bitumen tested under both 400 kPa and 500 kPa stresses do not follow this trend.

In Figure 5.21, the change in parameter "E0" with respect to the applied load can be examined. The variations of parameter "E0" for specimens containing 4.75% bitumen tested under 0.2 sec pulse width and 0.8 sec pulse period, and 300 kPa stress and specimens containing 5.25% bitumen tested under 0.8 sec pulse width and 1.8 sec pulse period, and 300 kPa stress do not follow a consistent trend. Although, it is not possible to detect and qualify a common trend for the behavior parameter "E0" with respect to the applied load for all test conditions, it can be concluded that the value of parameter "E0" generally increases with the applied load.

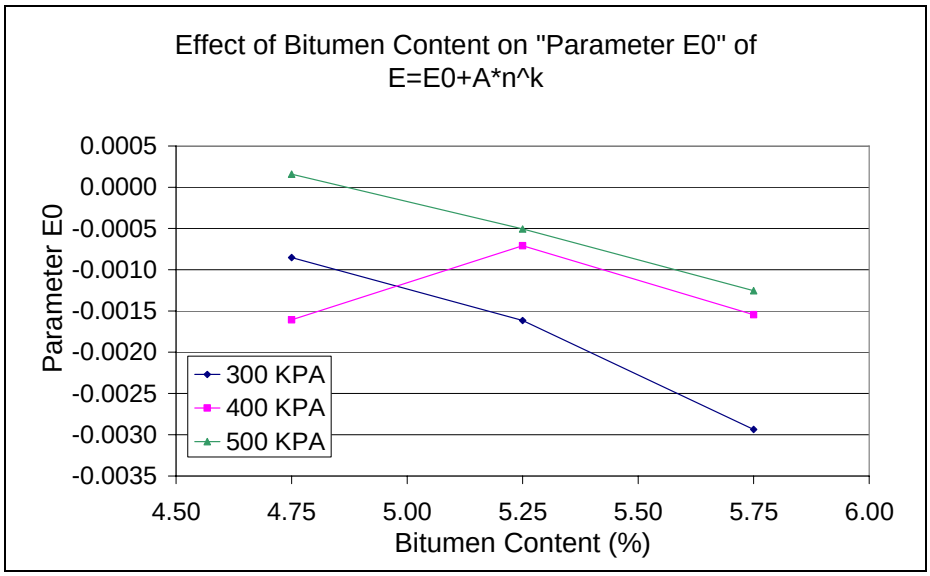

a) Under 0.2 sec pulse width and 0.8 sec pulse period

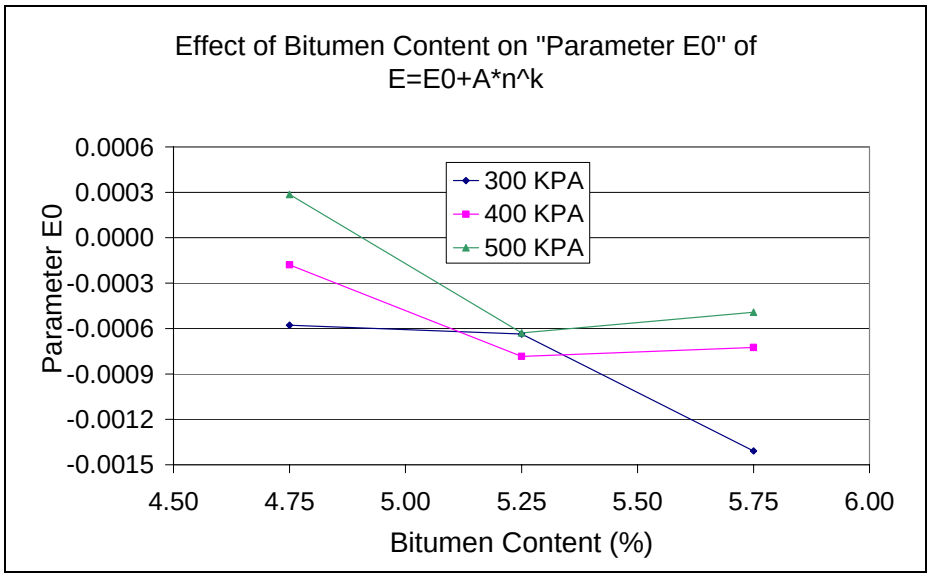

b) Under 0.8 sec pulse width and 1.8 sec pulse period

Figure 5.19: Variation of model parameter “E0” with bitumen content for specimens tested at 40°C

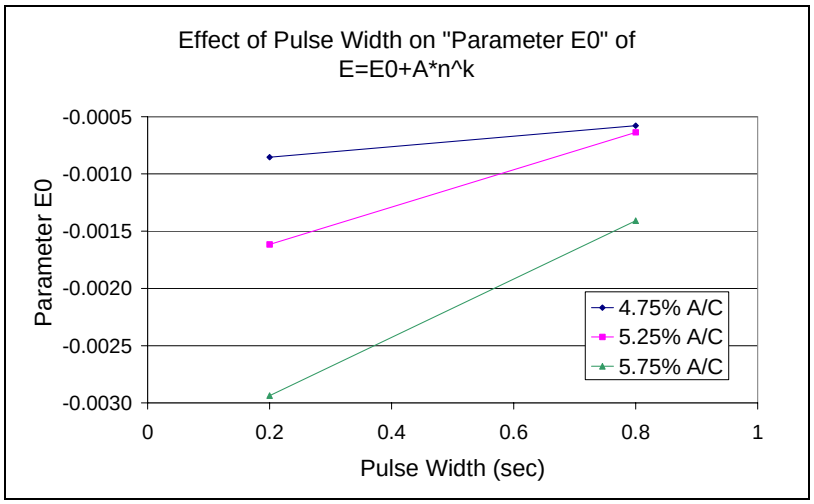

a) Under 300 kPa stress

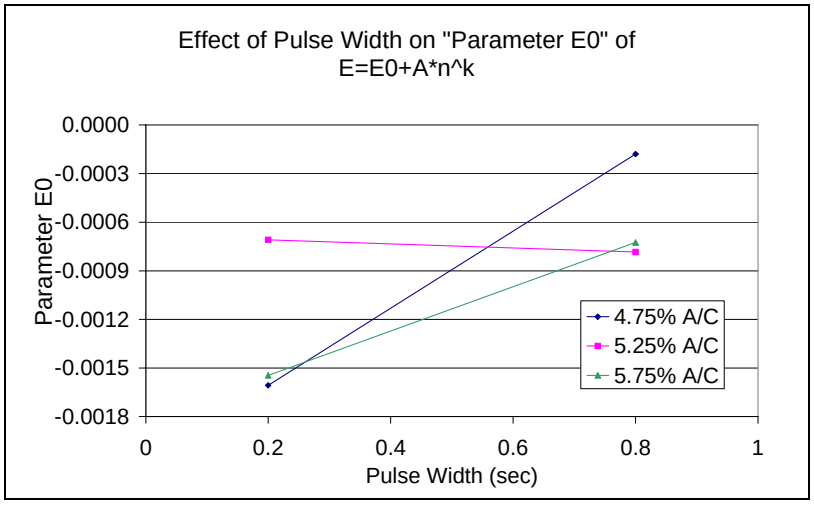

b) Under 400 kPa stress

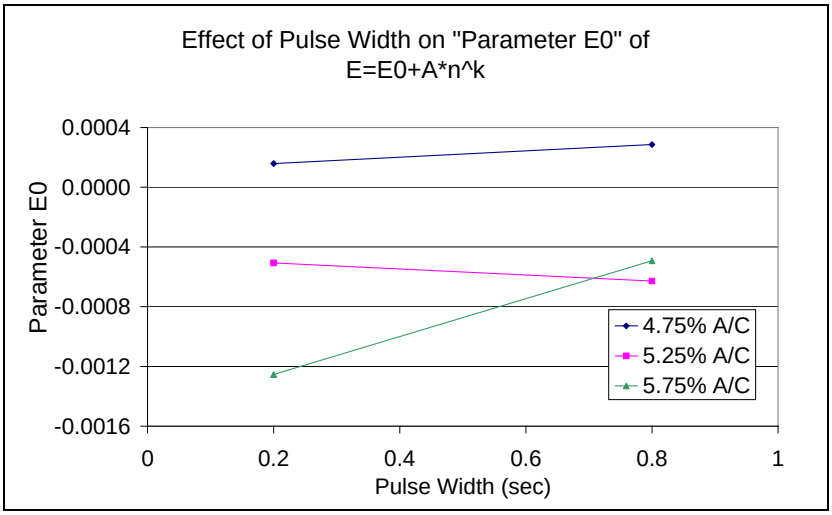

c) Under 500 kPa stress

Figure 5.20: Variation of model parameter “E0” with load frequency for specimens tested at 40°C

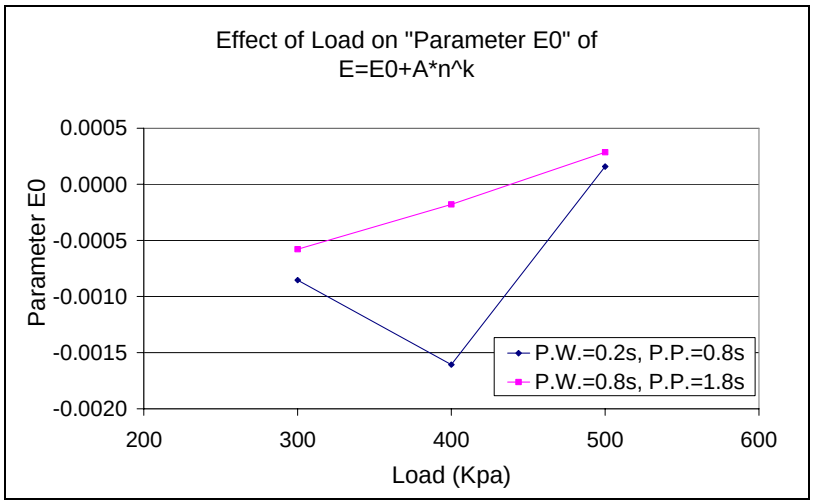

a) 4.75% A\C

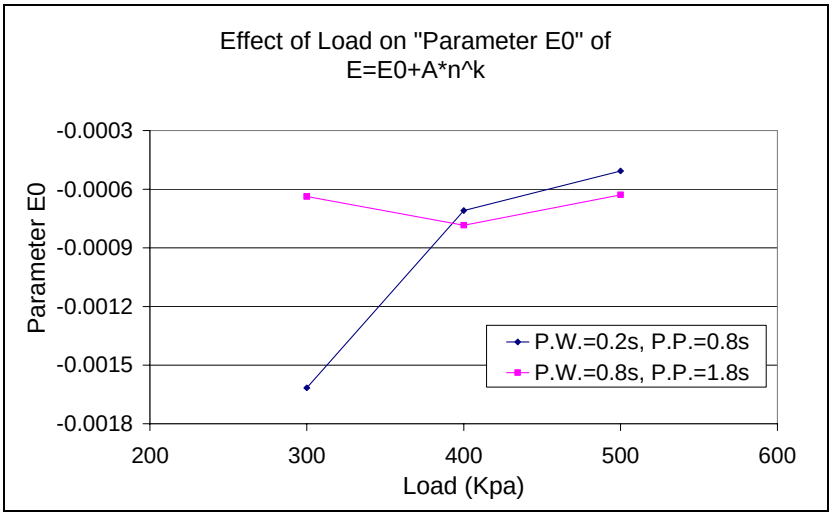

b) 5.25% A\C

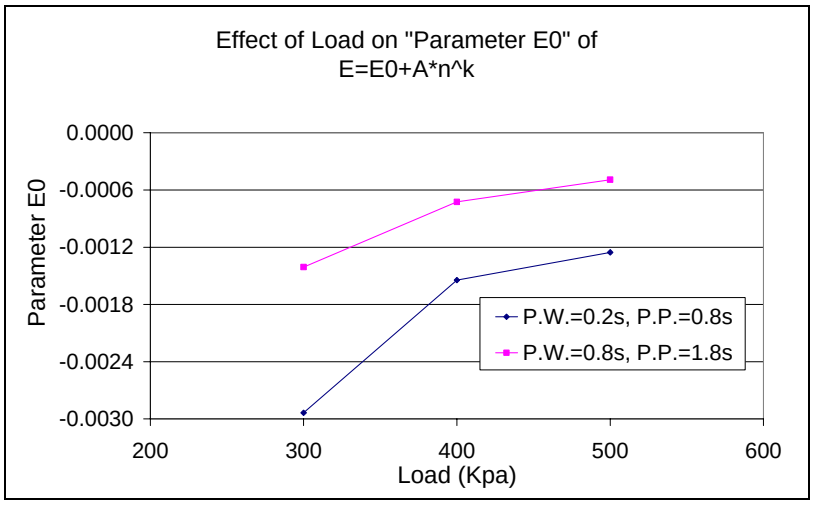

c) 5.75% A\C

Figure 5.21: Variation of model parameter “E0” with applied load for specimens tested at 40°C

According to ANOVA Table D.6, load frequency and applied load are two independent factors that are statistically significant for parameter A.

It is clearly seen from Figure 5.22 that there is a consistent interaction between parameter “A” and load frequency. The value of parameter A decreases with the reduction of load frequency.

The change in parameter “A” with respect to applied load is given in Figure 5.23. Although the variations of parameter “A” for specimens containing 4.75% bitumen tested under 0.2 sec pulse width and 0.8 sec pulse period, and 300 kPa stress have irregular pattern, the general trend is that the value of parameter “A” decreases with increase in the applied load.

According to ANOVA Table D.7, bitumen content of specimens, load frequency and applied load are statistically significant for parameter “k”.

The variation of parameter “k” with respect to the bitumen content is shown in Figure 5.24. From this figure, it is seen that the parameter “k” shows an inconsistent behavior for the specimens containing 5.75% bitumen tested under 0.2 sec pulse width and 0.8 sec pulse period and 500 kPa stress and tested under 0.8 sec pulse width and 1.8 sec pulse period and 300 kPa stress. Roughly, a general trend of an increase of parameter “k” with an increase in the bitumen content can be mentioned.

In Figure 5.25, a more definite trend in between parameter “k” and the load frequency is observed. The value of parameter k increases with the reduction of the load frequency.

Generally, the value of parameter “k” also increases with the increase of applied load. However, only for these specimens containing 4.75% bitumen tested under 0.2 sec pulse width and 0.8 sec pulse period and 400 kPa stress, the parameter shows an irregular pattern.

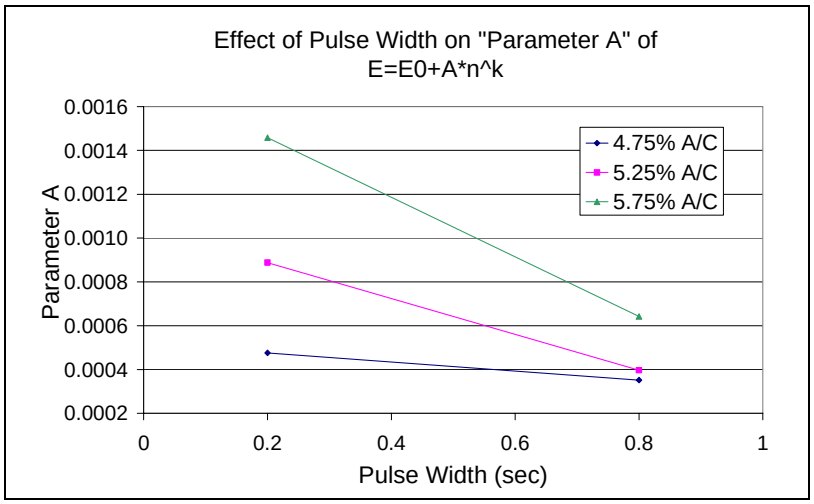

a) Under 300 kPa stress

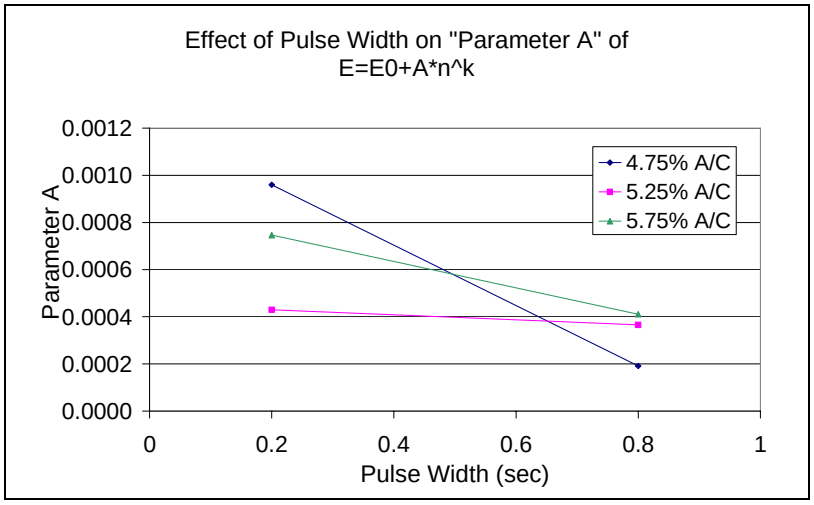

b) Under 400 kPa stress

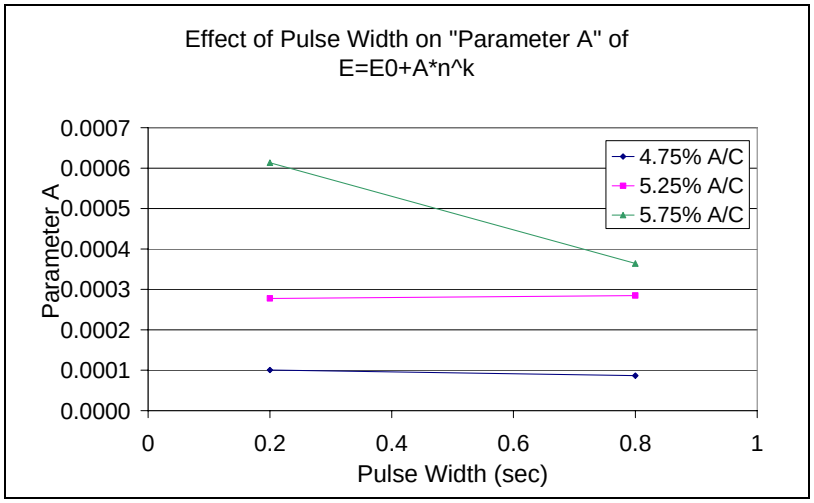

c) Under 500 kPa stress

Figure 5.22: Variation of model parameter “A” with load frequency for specimens tested at 40°C

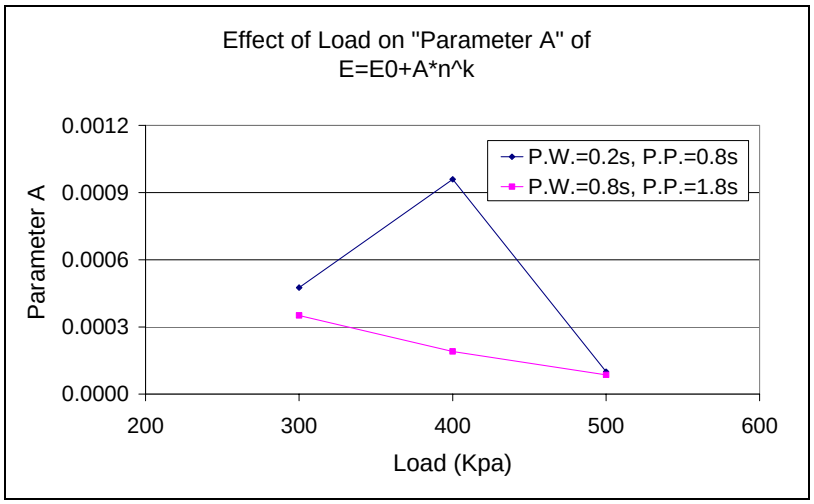

a) 4.75% A\C

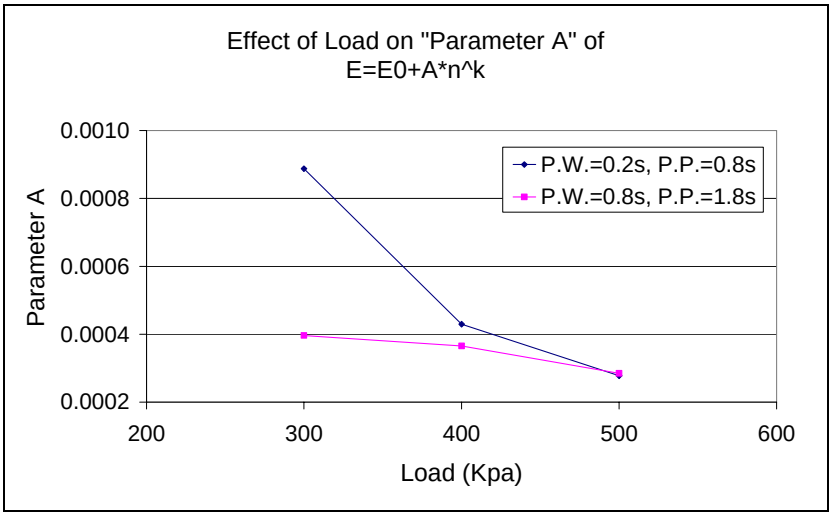

b) 5.25% A\C

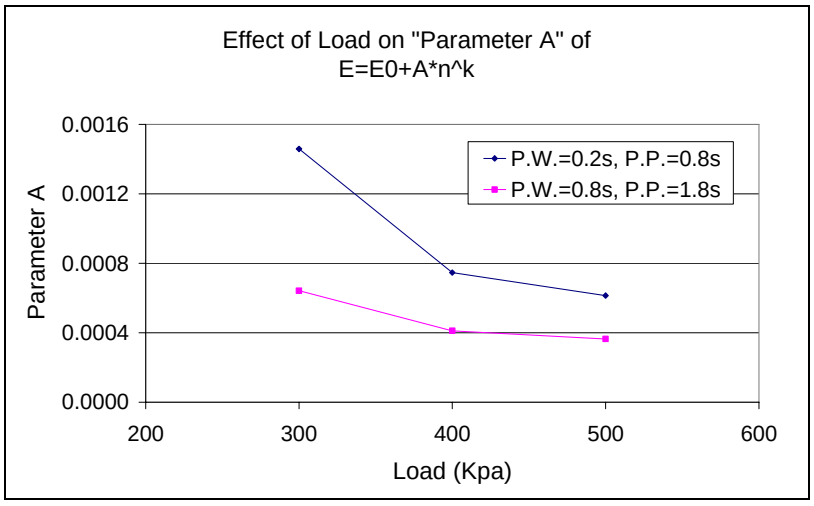

c) 5.75% A\C

Figure 5.23: Variation of model parameter “A” with applied load for specimens tested at 40°C

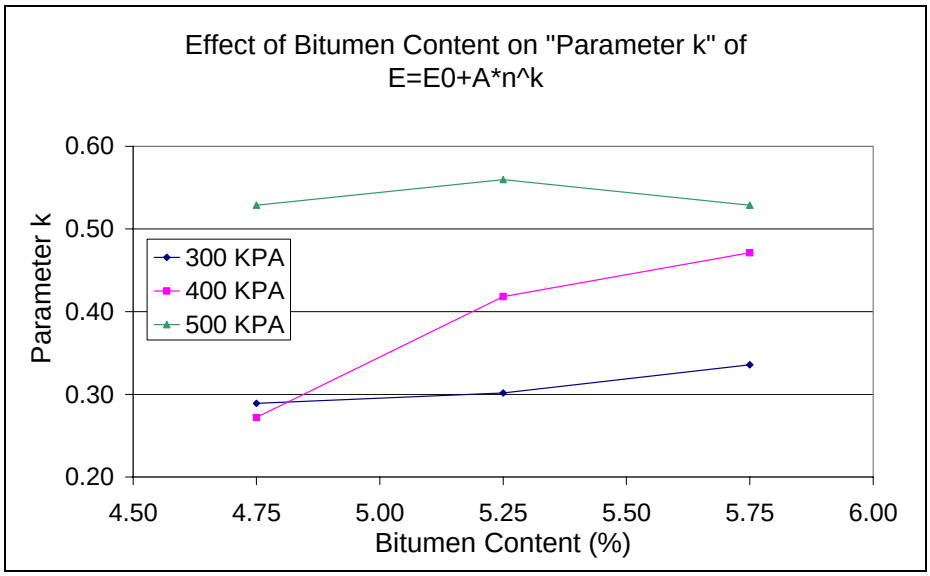

a) Under 0.2 sec pulse width and 0.8 sec pulse period

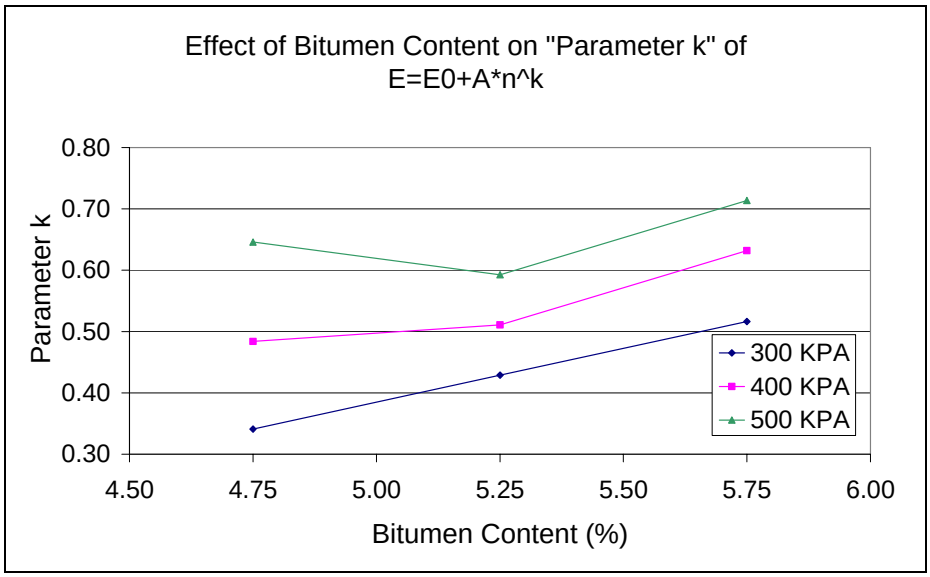

b) Under 0.8 sec pulse width and 1.8 sec pulse period

Figure 5.24: Variation of model parameter “k” with bitumen content for specimens tested at 40°C

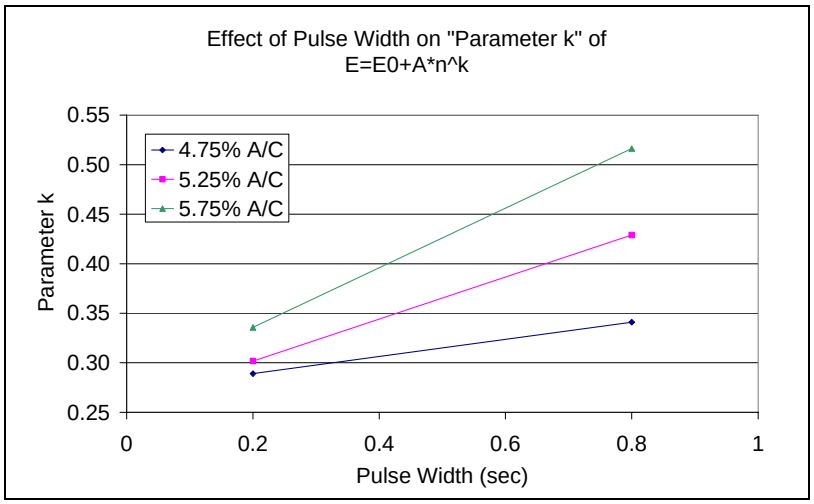

a) Under 300 kPa stress

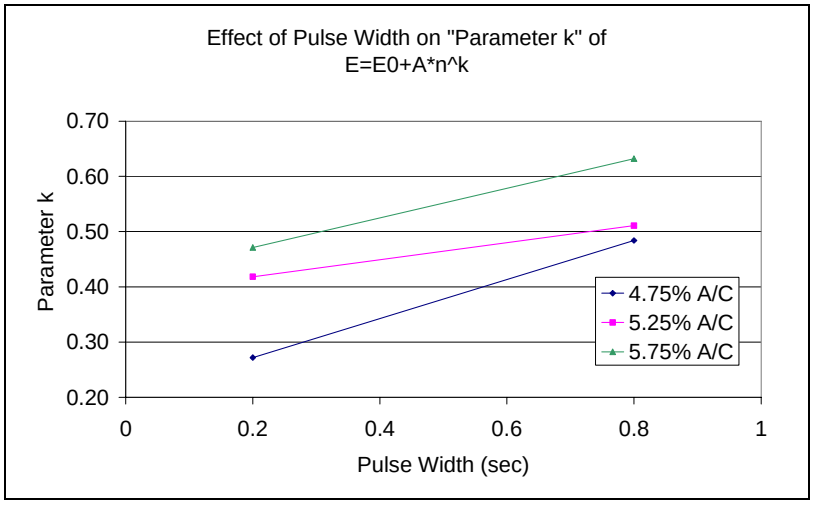

b) Under 400 kPa stress

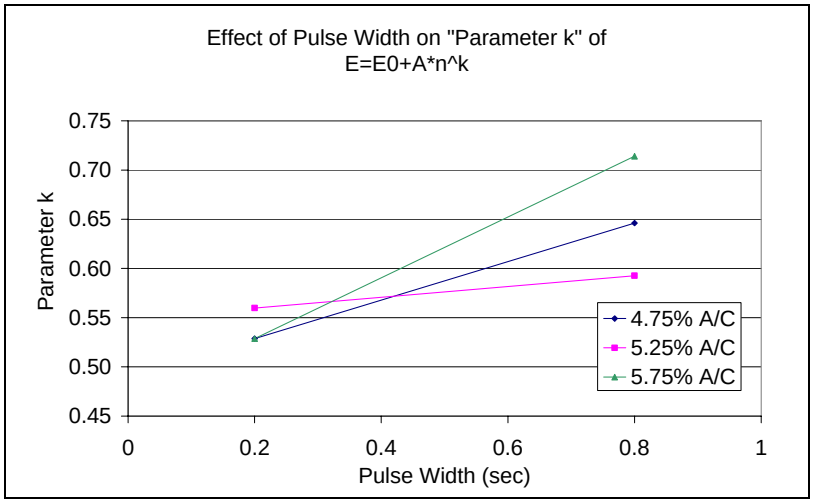

c) Under 500 kPa stress

Figure 5.25: Variation of model parameter “k” with load frequency for specimens tested at 40°C

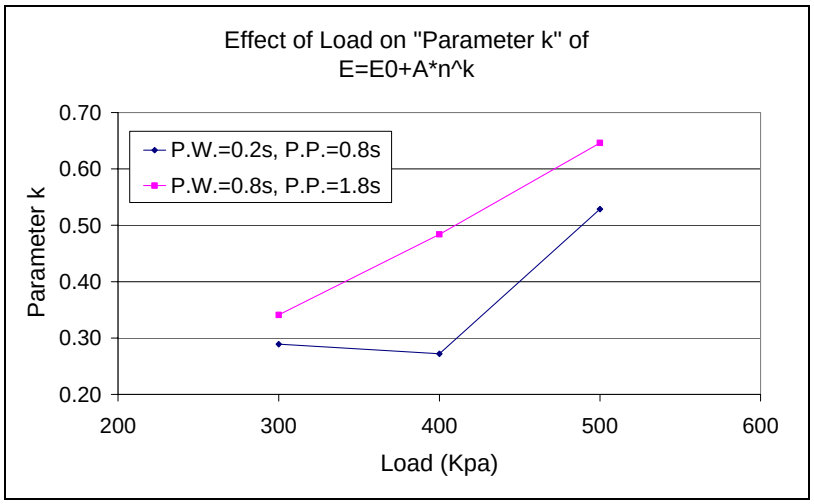

a) 4.75% A\C

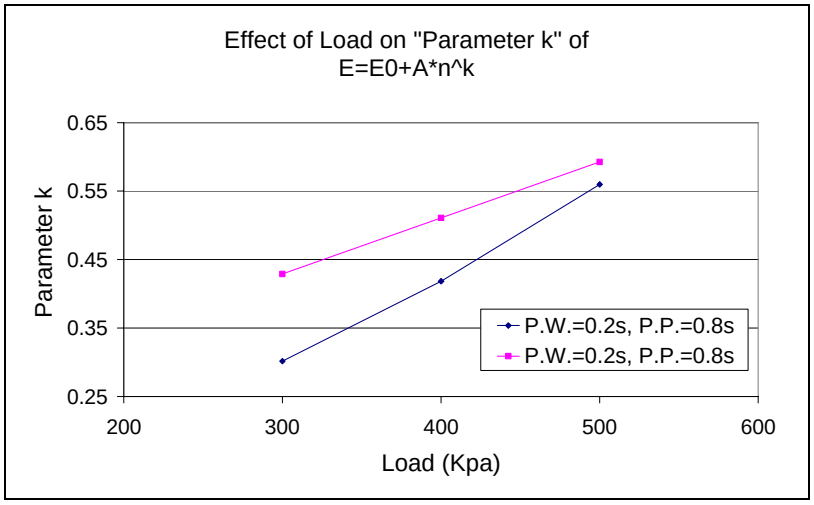

b) 5.25% A\C

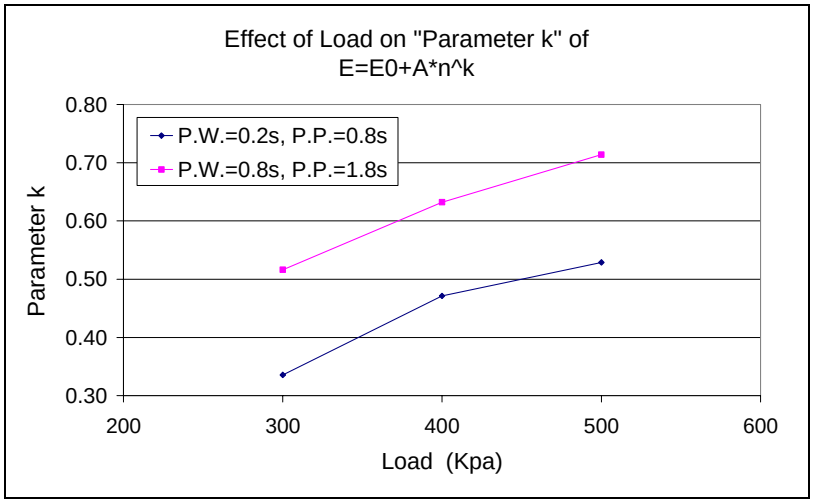

c)5.75% A\C

Figure 5.26: Variation of model parameter “k” with applied load for specimens tested at 40°C

5.3.5 Parametric Study of Power Model:

The ANOVA tables for the parameters of the Power model are given from D9 to D10 in Appendix D.

According to ANOVA Table D9, only the bitumen content is statistically significant for parameter “a” since the p-values are less than 0.05. The general trend of the value of parameter “a” is that its value increases with the increase in the bitumen content as seen in Figure 5.27. However, the behavior of the parameter for specimens containing 4.75% bitumen tested under 0.2 sec pulse width and 0.8 sec pulse period, and 400 kPa and the behavior of specimens containing 5.75% bitumen tested under 0.8 sec pulse width and 1.8 sec pulse period, and 400 kPa is not regular.

The load frequency and the applied load are statistically significant for parameter “b” since the p-values are less than 0.05 as seen in Table D10. The value of parameter “b” generally increases with the reduction of load frequency as shown in Figure 5.28. However, for the specimens containing 5.25% bitumen tested under 400 kPa stress and 500 kPa, the parameter does not show regular variation pattern.

Although, it is generally observed that the value of parameter “b” increases with the increase of the applied load, it is obvious from Figure 5.29 that the parameter does not show consistent behavior for all specimens containing 5.75% bitumen tested under 500 kPa.

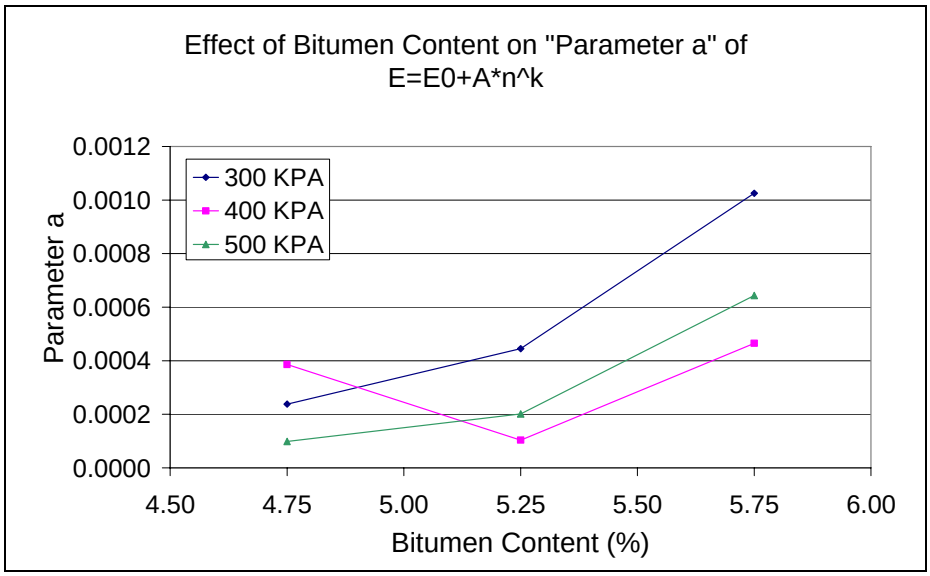

a) Under 0.2 sec pulse width and 0.8 sec pulse period

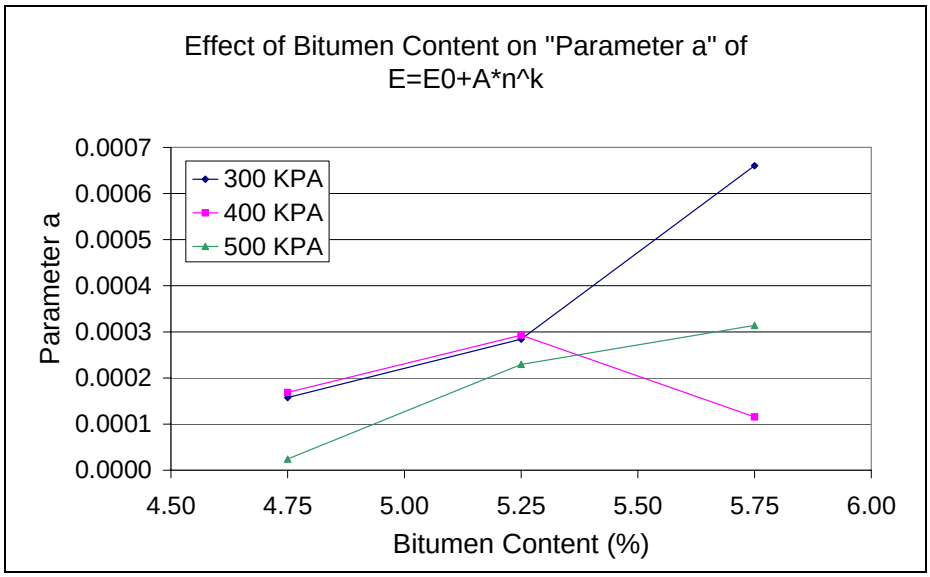

b) Under 0.8 sec pulse width and 1.8 sec pulse period

Figure 5.27: Variation of model parameter “a” with bitumen content for specimens tested at 40°C

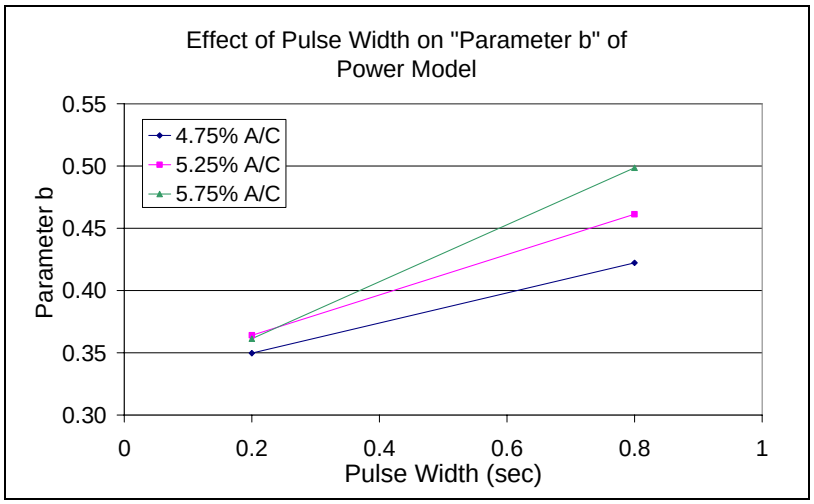

a) Under 300 kPa stress

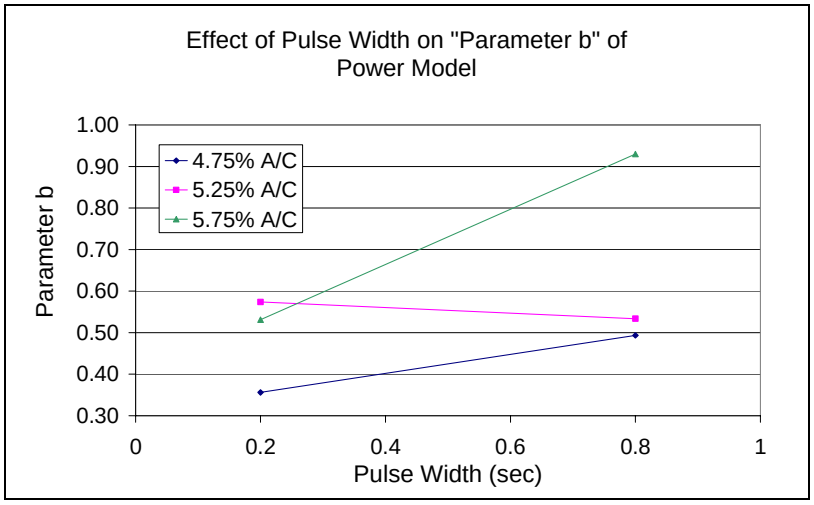

b) Under 400 kPa stress

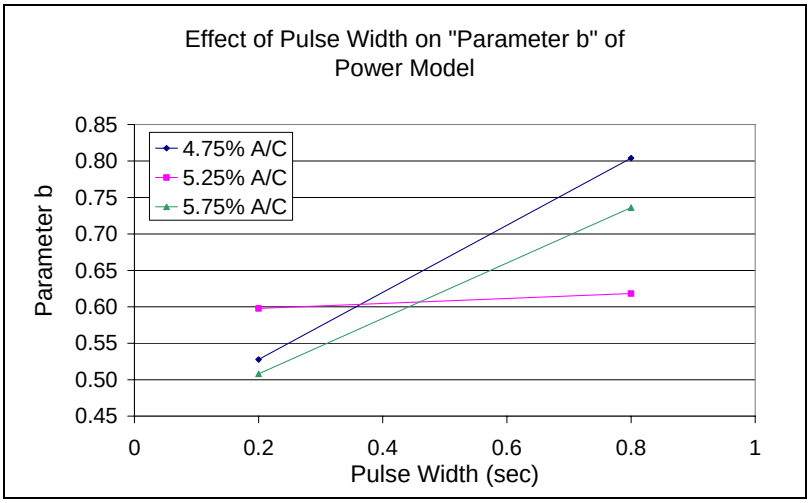

c) Under 500 kPa stress

Figure 5.28: Variation of model parameter “b” with load frequency for specimens tested at 40°C

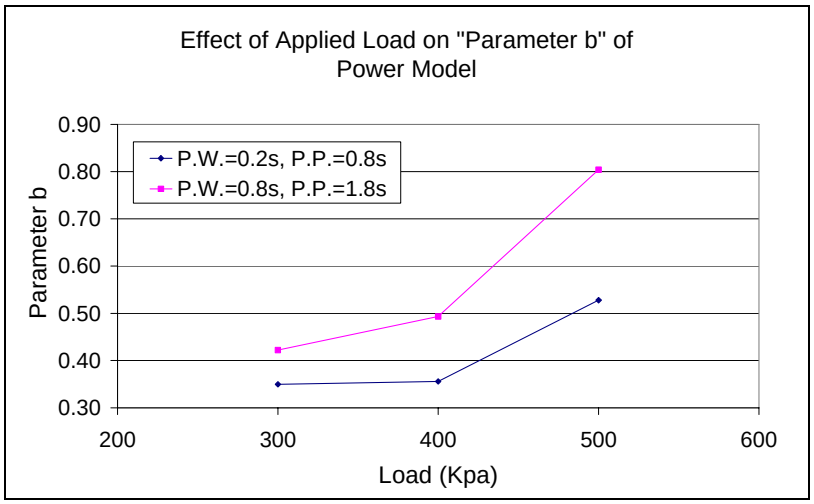

a) 4.75% A\C

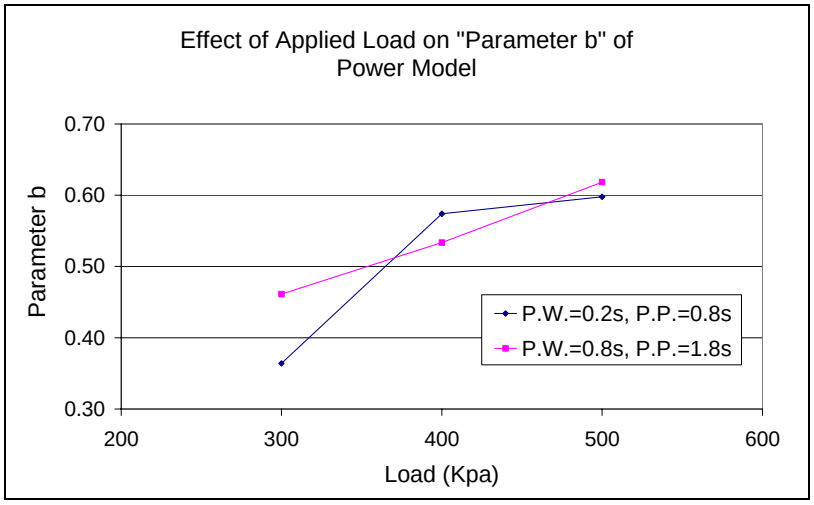

b) 5.25% A\C

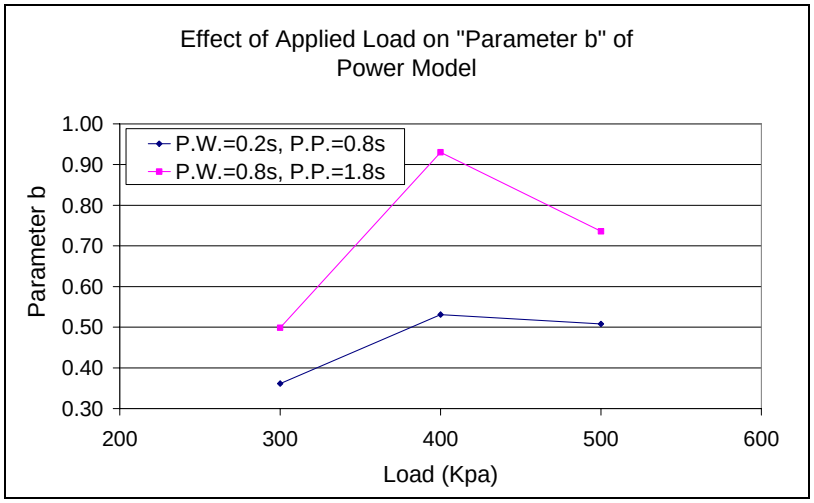

c)5.75% A\C

Figure 5.29: Variation of model parameter “b” with applied load for specimens tested at 40°C

CHAPTER 6

CONCLUSION

6.1 General

A large number of Marshall specimens were prepared and tested in the laboratory to determine the optimum bitumen content, to calibrate the UMATTA instrument and to study the dynamic creep behavior of asphalt concrete. The test data recorded for 54 specimens were used for analyzing the dynamic creep behavior of asphalt concrete. The same data are also used for the parametric studies on the selected mathematical creep models.

A single material property and three test condition parameters were varied within the planned creep test program. All individual creep curves were found to be representative of typical dynamic creep behavior of asphalt concrete. However, the tertiary stage was not reached for the tests conducted at 40^{o}C and 35^{o}C since all the tests are terminated before 10.000 pulse counts. On the other hand, the tertiary stages were reached and also the specimens were failed before 10.000 pulses for the tests conducted at 50^{o}C.

Two well-known mathematical models and a modified model suggested by the author were used to represent every single creep curve recorded during this study. All of these models were found to be successful in representing the experimental data. The interactions between the parameters of these three models and the variables of the test programs were also studied both graphically and statistically.

The outcomes of this study and the recommendations for further studies derived from these outcomes are summarized as follows.

6.2 Outcomes

1. The following expected dynamic creep behavior of asphalt concrete are confirmed by the results of the tests conducted in laboratory:
   a) When the bitumen content and other test conditions except temperature are fixed, the rate of permanent deformation increases as the test temperature increases. For the tests conducted at 50^{o}C for which the failures are observed, failure pulse counts are significantly reduced.
   b) When the bitumen content and other test conditions except applied load are fixed, the rate of permanent strain increases as the applied load increases. For the tests conducted at 50^{o}C for which the failures are observed, failure pulse counts are reduced with increased load.
   c) The rate of permanent strain increase with increase in bitumen content for the tests conducted without changing the other test condition variables.
   d) When only the load frequency is varied, for a given pulse count the accumulated permanent strains for the tests conducted at low frequency of load corresponding to slow traffic are greater then the accumulated strains for the tests conducted at high frequency of the load corresponding to fast traffic.

2. The effect of the temperature on the creep of asphalt concrete is found to be different at different temperature ranges. When only test temperature is changed and other test conditions are fixed, the creep behaviors of similar specimens tested at 35^{o}C and 40^{o}C temperatures do not differ from each other considerably. On the other hand the creep behaviors of similar specimens tested at 40^{o}C and 50^{o}C temperatures, when other test conditions are fixed, are completely different from each other. All specimens tested at 50^{o}C reach tertiary stage and also fail very quickly,

whereas the specimens tested at 40^{o}C do not even reach the tertiary stage before 10.000 pulses.

3. The three models selected for representing the dynamic creep behavior of asphalt concrete have the following mathematical forms:

   The Model Proposed by Beckedahl et al : $\varepsilon(n) = E0 + An^{k} + B(e^{nC} + 1)$

   The Model suggested by author : $\varepsilon(n) = E0 + An^{k}$

   The Power Model : $\varepsilon(n) = an^{b}$

   As it is seen the Power Model with two parameters only, a" and "b", is the simplest one among these. For the model proposed within this study, the added term "E0" becomes the third parameter of the model. The model proposed by Beckedahl et al being the most complex one among the three, includes two more parameters, "B" and "C", within the additional third term. The performance of these three models in representing dynamic creep behavior of the specimens tested is summarized as follows.

   a) Proposed Model by Beckedahl et al. represents well all the three stages of a typical creep curve. But it is not stable and the model may fit to the recorded data at two extremes with two different parameters set. For this reason this model is not found to be suitable for parametric study.
   b) Proposed Model "E=E0+an^{k}" successfully fits to a typical creep curve with primary and secondary stages.
   c) Power model is capable to represent only the secondary stage extracted from a given typical creep curve.

4. The interaction of model parameters with bitumen content and test condition parameters were studied graphically and also statistically by conducting analysis of variance to support graphically observed trends. The results of parametric studies for the selected mathematical models are summarized as follows:

a) The model parameters “E0”, “B” and “k” of the model proposed by Beckedahl et al. are found to be effected by the bitumen content. However, the parameters of this model do not show consistent trends because the model is unstable.
b) The parameter “E0” and “k” of the model proposed by the author are affected by the variations of bitumen content, load frequency, and applied load. Whereas, the Parameter “A” of the proposed model is found to be affected by the changes in load frequency and applied load but not affected by bitumen content. .
c) The variations in the bitumen content affect the parameter “a” of the power model. Parameter “b” is affected by both the frequency and the magnitude of the applied load.

5. Among the selected models, the Power model is the most suitable model for parametric study. Additionally, this model is more stable than the other two models. The behavior observed for Power Model parameters can be stated as follows:
   a) It is found out that the parameter “a” which is the intercept of the model presented in log-log scale increases with the increase in the bitumen content. This parameter is directly related to the permanent strain accumulated during the primary stage. It is obvious that increase in bitumen content is expected to cause an increase in accumulated permanent strain during primary stage. Therefore the trends observed for parameter “a” of the Power model is conforming to the expectations.
   b) The parameter “b” of the model which represents the slope of the creep curve is highly affected by the magnitude of the repeated load. It is observed that an increase in the applied repeated stress results in an increase in the value of parameter “b”. This observed behavior is found to be meaningful.
   c) It is known that the rate of increase in permanent strain of asphalt concrete layers under fast traffic is lower than the rate under slow traffic. In other words, the slope of the creep curve on a log-log scale

is expected to be lower for high frequency loading and to be higher for low frequency loading. It is observed that for a fixed stress magnitude, as the frequency of the load repetition increased, the value of the parameter “b” of the power model is decreased. The behavior of parameter “b” of the model in this manner is also found to be conforming to expectations.

6.3 Recommendations for Further Studies

1. In order to detect and develop mathematical relations to represent interactions between mathematical creep model parameters and test parameters, the spectra of applied load, load frequency, and bitumen content must be widened.

2. For the limited laboratory dynamic creep test data recorded during this study, the Power model which has very simple mathematical expression was found to be stable and also the parameters of the model showed consistent trends. For this reason, the Power model can be selected as the basic model fort further studies aiming to develop constitutive relations for dynamic creep modeling.

REFERENCES

Abdullah W. S., Obaidat M. T., Abu-Sa'da N. M., "Influence of Aggregate Type and Gradation on Voids of Asphalt Concrete Pavements", Journal of Materials in Civil Engineering, Vol.10, No.2, May 1998

Abdulshafi A. A., "Viscoelastic/plastic characterization, rutting and fatigue of flexible pavements", PhD. Dissertation, Ohio State University, USA, 1983

Barksdale R.D., "Test device for evaluating rutting of asphalt concrete mixes", Transportation Research Record 1418, National Research Council, Washington D.C., 1993

Brown E. R. and Foo K.Y., "Comparison of unconfined and confined creep tests for hot mix asphalt", Journal of Materials in Civil Engineering Vol.6 No.2 pages 307-326, 1994

Brown E. R., Kandhal P. S., Zhang J., "Performance Testing for Hot Mix Asphalt", NCAT Report 01-05, November 2001

Cheung C.Y., "The mechanical behavior of bitumens and bituminous mixes", PHD thesis, University of Cambridge, 1995

Dawley C. B., Hogewiede B.L.,and Anderson K.O., "Mitigation of Instability Rutting of Asphalt Concrete Pavements in Lethbridge, Alberta, Canada" The Asphalt Paving Technology, Volume 59 Pages 481-505, 1990

De Vos K. B., "UMMATA Universal Materials Testing Apparatus for Asphalt and Unbound Specimens Reference and Operating Manual", Industrial Process Control Ltd., Australia, 1992

Deshpnde V.S., ”Steady-state deformation behavior of bituminous mixes”, PHD thesis, University of Cambridge, 1997

Foo K.Y., “Predicting rutting in hot mix asphalts”, PHD Dissertation, Auburn University,1994

Gabrielson J.R.,” Evaluation of hot mix asphalt (HMA) under static creep and repeated load tests”, PHD Dissertation, Auburn University,1992

Guler M., “Characterization of hot mix asphalt shear resistance and correlation with rutting performance”, PHD Dissertation, The University of Wisconsin – Madision, 2002

Kraus Harry, “Creep Analysis”, John Wiley & Sons, page 1-10, 1980.

Lai J.S., and Hufferd W. L., “Predicting permanent deformation of asphalt concrete from creep tests”, Transportation Research Record.616, page 41-53, Transportation Research Board, Washington, D.C., 1976

Marks V. J., Monroe R. W., Adams J. F., ”Relating Creep Testing to rutting of Asphalt Concrete Mixes”, Iowa Department of Transportation, Paper No: 910460, January 13-17 1991

Monismith C.L., Hicks, R.G., Finn F.N., Sousa J., Harvey J., Weissman S., Deacon J., Coplantz J., Paulsen G., “Permanent Deformation Response of Asphalt Aggregate Mixes”, SHRP-A-415, August 1994

Neter J., Wasserman W., Whitmore G.A., “Applied Statistics”, Allyn and Bacon Inc., pp.522-548, 1978

NCHRP 9-19,"Standard Test Method for Simple Performance Test for Permanent Deformation Based Upon Dynamic Modulus of Asphalt Concrete Mixtures", 2000

NCHRP Project 1-37A, "Development of the 2002 Guide for the Design of New and Rehabilitated Pavement Structures", Module 3-3 Rutting in Flexible Pavements, 2005

NIH, "Pavement Analysis and Design Check", Federal Highway Administration, NIH Training Courses, pp (2-3.15)-(2-3.24), June 1993

Perl M., Uzan J., and Sides A., "A visco-elasto-plastic constitutive law for a bituminous mixture under repeated loading", Transportation Research Record.911, page 20-27, Transportation Research Board, Washington, D.C., 1983

Sides A., Uzan J., and Perl M., "A comprehensive visco-elasto-plastic characterization of sand-asphalt under compression and tension cycle loading". Journal Test Evaluation, Vol. 13(1), pages 49-59, 1985

Szydlo A., Mackiewicz P., "Asphalt Mixes Deformation Sensitivity to Change in Rheological Parameters", Journal of Materials in Civil Engineering, Vol.17, No.1, January-February 2005

Tapkın Hasan, "Mathematical Creep Models for Asphaltic Mixtures", METU, Turkey, 1980.

Tarefder R.A., Zaman M. and Hobson K., "A laboratory and statistical evaluation of factors Affecting Rutting", The International Journal of Pavement Engineering Vol.4(1) pp. 59-68, March 2003

Uluğtekin Erkan, "Creep Properties of Asphaltic Concrete under Repeated Load" MS. Dissertation, METU, 1999

Uzan J., Sides A., and Perl M., “Viscoelastoplastic model for predicting performance of asphaltic mixtures”, Transportation Research Record.1043, page 78-79, Transportation Research Board, Washington, D.C., 1985

Uzan J., “Viscoelastic-Viscoplastic Model with Damage for Asphalt Concrete”, Journal of Materials in Civil Engineering Vol. 17, No.5 page 528-534, 2005.

Zhou F., Scullion T., “Discussion: Three stage of permanent deformation curve and rutting model”, The International Journal of Pavement Engineering Vol.3(4), pp.251-260, 2002

Zhu L. Y., Fwa T. F., Liu Y., ”Rutting Potential Evaluation of Asphalt Mixtures by Repeated-Load Creep Test”, TRB Annual Meeting CD-ROM, 2002

APPENDIX A

MARSHALL MIX DESIGN AND PHYSICAL PROPERTIES OF SPECIMENS

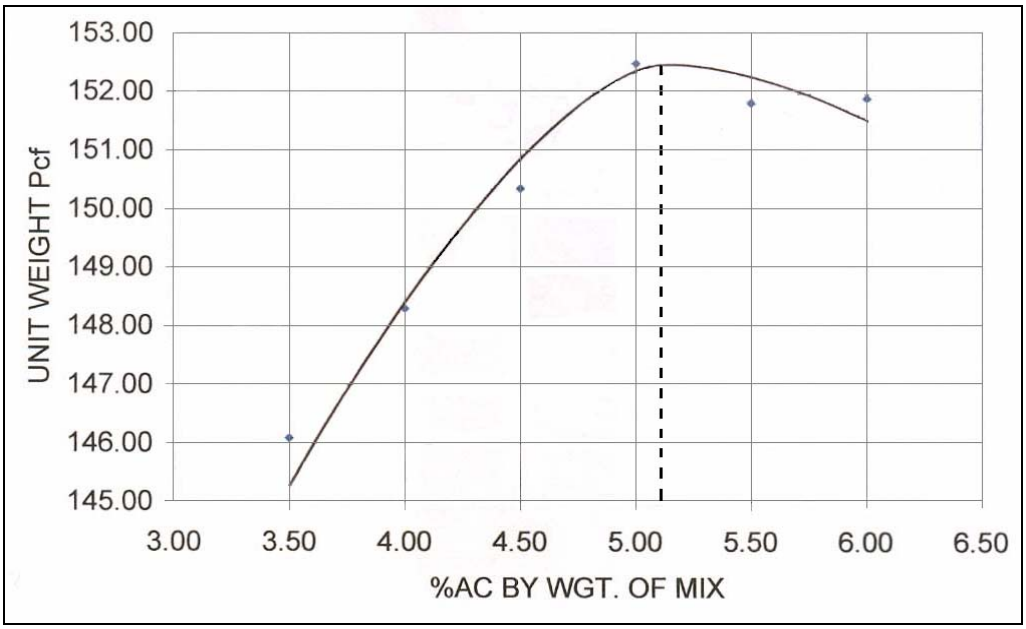

a) Unit Weight vs. % AC by Weight of Mix

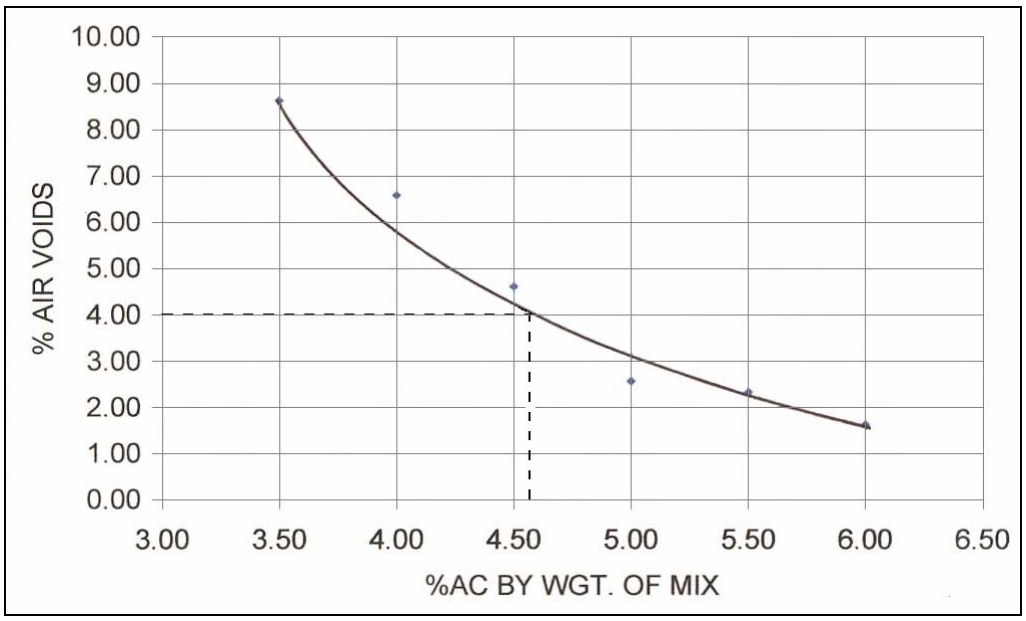

b) % Air Voids vs. % AC by Weight of Mix

Figure A1: Test Results from the Marshall Mix Design (cont'd)

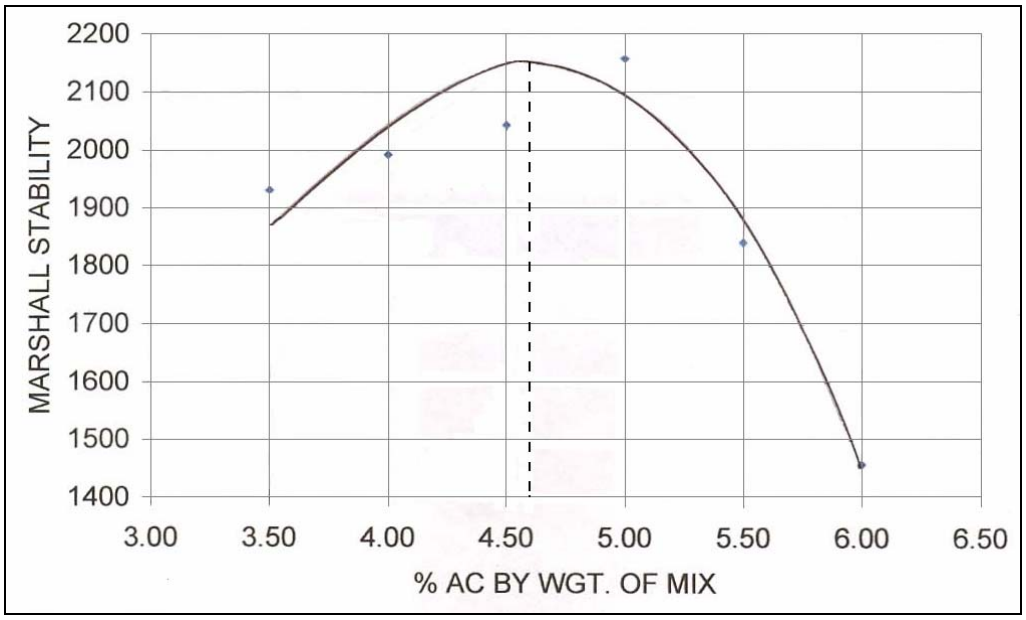

c) Stability vs. % AC by Weight of Mix

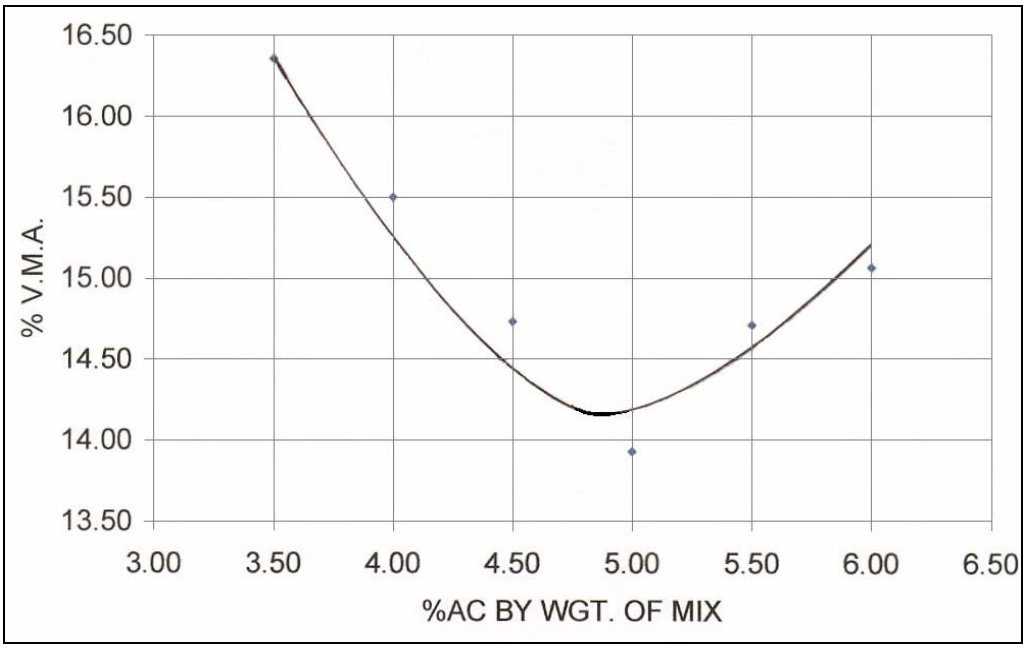

d) % V.M.A. vs. % AC by Weight of Mix

Figure A1: Test Results from the Marshall Mix Design (cont'd)

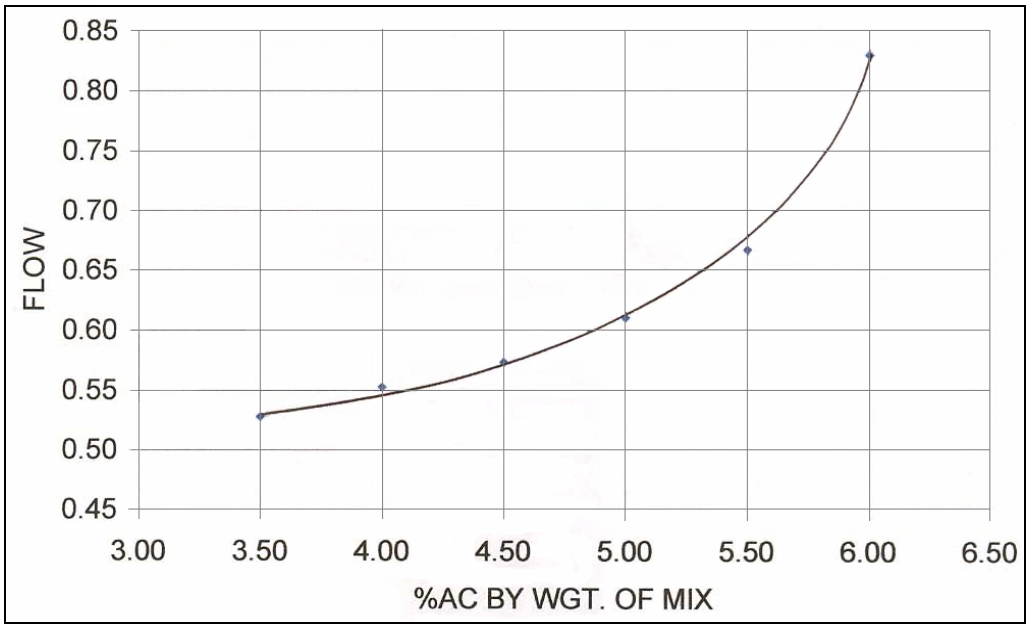

e) Flow vs. % AC by Weight of Mix

Figure A1: Test Results from the Marshall Mix Design

Table A1: Marshall Test Data

SPECIMEN NUMBER	AC	AC	SPEC.	WEIGHT (gr)		VOLUME	SPECIFIC GRAVITY		VOLUME wrt TOTAL %			VOID PERCENTAGES(%)			UNIT	STABILITY		FLOW	
	(%)	(%)	HEIGHT	In Air	In Water	(cm3)	Mixture	Mixture (theoric)	Asphalt	Aggregate	Air Void	Aggregate	Fill with asphalt	Total mixture	WEIGHT (pcf)	Exp.	Corr.	1/100"	mm
	a	b	C	d	e	f	g	h	i	j	k	l	m	n	o	p	q	r	s
	wrt aggregate weight	a/(100+a)				d-e	d/(d-e)		b*g/ (SGasp)	(100-b)*g/ SGagg	100-i-j	100-j	i/l	100-100g/h	62.4*g		p*c.factor		r*0.254
1A	3.50	3.38	60.00	1129.80	650.20	479.60	2.36	2.56	7.78	84.16	8.06	15.84	49.10	8.06	147.00	2025.00	2227.50	2.42	0.61
1B	3.50	3.38	60.00	1131.50	648.10	483.40	2.34	2.56	7.73	83.62	8.65	16.38	47.19	8.65	146.06	1771.00	1948.10	2.03	0.52
1C	3.50	3.38	60.00	1133.60	649.50	484.10	2.34	2.56	7.73	83.66	8.61	16.34	47.31	8.61	146.12	1739.00	1912.90	2.13	0.54
Avg. curve	3.50	3.38	60.00	1132.55	648.80	483.75	2.34	2.56	7.73	83.64	8.63	16.36	47.25	8.63	146.09	1755.00	1930.50	2.08	0.53
2A	4.00	3.85	60.00	1144.30	663.30	481.00	2.38	2.54	8.93	84.58	6.48	15.42	57.94	6.48	148.45	1784.00	1962.40	2.03	0.52
2B	4.00	3.85	60.00	1134.50	657.00	477.50	2.38	2.54	8.92	84.47	6.61	15.53	57.46	6.61	148.26	1800.00	1980.00	2.13	0.54
2C	4.00	3.85	60.00	1144.30	662.50	481.80	2.38	2.54	8.92	84.44	6.64	15.56	57.33	6.64	148.20	1850.00	2035.00	2.37	0.60
Avg. curve	4.00	3.85	60.00	1141.03	660.93	480.10	2.38	2.54	8.93	84.50	6.58	15.50	57.58	6.58	148.30	1811.33	1992.47	2.18	0.55
3A	4.50	4.31	59.00	1134.20	661.80	472.40	2.40	2.53	10.09	84.95	4.95	15.05	67.09	4.95	149.82	1758.00	1986.54	2.42	0.61
3B	4.50	4.31	60.00	1135.40	663.80	471.60	2.41	2.53	10.12	85.19	4.69	14.81	68.34	4.69	150.23	1755.00	1930.50	0.91	0.23
3C	4.50	4.31	60.00	1131.40	663.60	467.80	2.42	2.53	10.17	85.58	4.25	14.42	70.50	4.25	150.92	1910.00	2101.00	2.10	0.53
Avg. curve	4.50	4.31	59.50	1132.80	662.70	470.10	2.41	2.53	10.13	85.26	4.60	14.74	68.79	4.60	150.37	1834.00	2043.77	2.26	0.57
4A	5.00	4.76	58.50	1147.90	677.80	470.10	2.44	2.51	11.35	85.99	2.66	14.01	81.03	2.66	152.37	1813.00	2175.60	2.38	0.60
4B	5.00	4.76	59.00	1149.80	679.80	470.00	2.45	2.51	11.37	86.15	2.48	13.85	82.12	2.48	152.65	1895.00	2141.35	2.43	0.62
4C	5.00	4.76	60.00	1143.90	674.80	469.10	2.44	2.51	11.34	85.87	2.79	14.13	80.25	2.79	152.16	1515.00	1621.05	2.59	0.66
Avg. curve	5.00	4.76	58.75	1148.85	678.80	470.05	2.44	2.51	11.36	86.07	2.57	13.93	81.57	2.57	152.51	1854.00	2158.48	2.41	0.61
5A	5.50	5.21	59.00	1146.50	674.00	472.50	2.43	2.49	12.35	85.04	2.61	14.96	82.57	2.61	151.41	1586.00	1792.18	2.24	0.57
5B	5.50	5.21	60.00	1155.20	681.80	473.40	2.44	2.49	12.42	85.52	2.05	14.48	85.81	2.05	152.27	1627.00	1789.70	3.21	0.82
5C	5.50	5.21	58.50	1147.80	676.10	471.70	2.43	2.49	12.39	85.28	2.33	14.72	84.16	2.33	151.84	1618.00	1941.60	2.44	0.62
Avg. curve	5.50	5.21	59.17	1149.83	677.30	472.53	2.43	2.49	12.39	85.28	2.33	14.72	84.18	2.33	151.84	1610.33	1841.16	2.63	0.67
6A	6.00	5.66	60.00	1158.00	683.00	475.00	2.44	2.47	13.47	85.04	1.49	14.96	90.06	1.49	152.12	1219.00	1340.90	3.52	0.89
6B	6.00	5.66	60.00	1153.30	678.00	475.30	2.43	2.47	13.41	84.64	1.95	15.36	87.32	1.95	151.41	1399.00	1538.90	2.66	0.68
6C	6.00	5.66	60.00	1157.90	683.30	474.60	2.44	2.47	13.48	85.10	1.41	14.90	90.52	1.41	152.24	1359.00	1494.90	3.63	0.92
Avg. curve	6.00	5.66	60.00	1156.40	681.43	474.97	2.43	2.47	13.46	84.93	1.62	15.07	89.30	1.62	151.93	1325.67	1458.23	3.27	0.83

Table A2: Physical properties of specimens

SPECIMEN	AC	AC	SPECIMEN	WEIGHT (gr)		VOLUME	SPECIFIC GRAVITY		VOLUME wrt TOTAL %			VOID PERCENTAGES(%)			UNIT WEIGHT
	(%)	(%)	HEIGHT	In Air	In Water	(cm3)	Mixture	Mixture (theoric)	Asphalt	Aggregate	Air Void	Aggregate	Fill with asphalt	Total mixture	pcf
	a	b	C	d	e	f	g	h	i	j	k	l	m	n	o
	wrt agg. weight	a/(100+a)				d-e	d/(d-e)		b*g/ (SGasp)	(100-b) *g/SGagg	100-i-j	100-j	i/l	100-100g/h	62.4*g
A4008183001	4,75	4,5346	59,00	1146,10	675,50	470,60	2,435	2,517	10,7827	85,97	3,25	14,03	76,84	3,25	151,97
A4008183002	4,75	4,5346	59,00	1145,10	675,90	469,20	2,441	2,517	10,8055	86,15	3,05	13,85	78,01	3,05	152,29
A4008184001	4,75	4,5346	58,00	1146,20	679,50	466,70	2,456	2,517	10,8738	86,69	2,43	13,31	81,71	2,43	153,25
A4008184002	4,75	4,5346	58,00	1145,80	678,70	467,10	2,453	2,517	10,8607	86,59	2,55	13,41	80,98	2,55	153,07
A4008185001	4,75	4,5346	58,00	1149,60	681,70	467,90	2,457	2,517	10,8781	86,73	2,39	13,27	81,96	2,39	153,31
A4008185002	4,75	4,5346	58,50	1146,70	680,30	466,40	2,459	2,517	10,8855	86,79	2,33	13,21	82,38	2,33	153,42
A5008183001	4,75	4,5346	58,50	1145,10	673,80	471,30	2,430	2,517	10,7573	85,76	3,48	14,24	75,57	3,48	151,61
A5008183002	4,75	4,5346	59,00	1144,60	675,90	468,70	2,442	2,517	10,8123	86,20	2,99	13,80	78,36	2,99	152,39
A5008184001	4,75	4,5346	60,00	1147,60	674,50	473,10	2,426	2,517	10,7398	85,62	3,64	14,38	74,71	3,64	151,36
A5008184002	4,75	4,5346	59,50	1151,40	679,20	472,20	2,438	2,517	10,7959	86,07	3,13	13,93	77,51	3,13	152,15
A5008185001	4,75	4,5346	60,00	1150,20	679,20	471,00	2,442	2,517	10,8121	86,20	2,99	13,80	78,36	2,99	152,38
A5008185002	4,75	4,5346	60,00	1147,80	677,90	469,90	2,443	2,517	10,8148	86,22	2,96	13,78	78,50	2,96	152,42

Table A2: Physical properties of specimens (cont'd)

SPECIMEN	AC	AC	SPECIMEN	WEIGHT (gr)		VOLUME	SPECIFIC GRAVITY		VOLUME wrt TOTAL %			VOID PERCENTAGES(%)			UNIT WEIGHT
	(%)	(%)	HEIGHT	In Air	In Water	(cm3)	Mixture	Mixture (theoric)	Asphalt	Aggregate	Air Void	Aggregate	Fill with asphalt	Total mixture	pcf
	a	b	C	d	e	f	g	h	i	j	k	l	m	n	o
	wrt agg. weight	a/(100+a)				d-e	d/(d-e)		b*g/ (SGasp)	(100-b) *g/SGagg	100-i-j	100-j	i/l	100-100g/h	62.4*g
A4002083001	4,75	4,5346	60,00	1148,50	675,30	473,20	2,427	2,517	10,7459	85,67	3,58	14,33	75,01	3,58	151,45
A4002083002	4,75	4,5346	59,00	1149,00	675,80	473,20	2,428	2,517	10,7506	85,71	3,54	14,29	75,24	3,54	151,52
A4002084001	4,75	4,5346	59,00	1145,20	678,00	467,20	2,451	2,517	10,8527	86,52	2,62	13,48	80,54	2,62	152,95
A4002084002	4,75	4,5346	58,00	1147,50	680,40	467,10	2,457	2,517	10,8768	86,72	2,41	13,28	81,88	2,41	153,29
A4002085001	4,75	4,5346	60,00	1150,30	678,10	472,20	2,436	2,517	10,7856	85,99	3,22	14,01	76,98	3,22	152,01
A4002085002	4,75	4,5346	58,50	1147,50	678,30	469,20	2,446	2,517	10,8281	86,33	2,84	13,67	79,20	2,84	152,61
A5002083001	4,75	4,5346	58,50	1145,90	677,10	468,80	2,444	2,517	10,8222	86,28	2,90	13,72	78,89	2,90	152,53
A5002083002	4,75	4,5346	59,00	1150,70	680,80	469,90	2,449	2,517	10,8421	86,44	2,72	13,56	79,96	2,72	152,81
A5002084001	4,75	4,5346	58,00	1147,80	676,60	471,20	2,436	2,517	10,7850	85,98	3,23	14,02	76,95	3,23	152,00
A5002084002	4,75	4,5346	58,00	1148,00	679,50	468,50	2,450	2,517	10,8490	86,50	2,66	13,50	80,34	2,66	152,90
A5002085001	4,75	4,5346	60,00	1151,70	680,20	471,50	2,443	2,517	10,8147	86,22	2,96	13,78	78,49	2,96	152,42
A5002085002	4,75	4,5346	58,00	1146,10	680,50	465,60	2,462	2,517	10,8985	86,89	2,21	13,11	83,13	2,21	153,60

Table A2: Physical properties of specimens (cont'd)

SPECIMEN	AC	AC	SPECIMEN	WEIGHT (gr)		VOLUME	SPECIFIC GRAVITY		VOLUME wrt TOTAL %			VOID PERCENTAGES(%)			UNIT WEIGHT
	(%)	(%)	HEIGHT	In Air	In Water	(cm3)	Mixture	Mixture (theoric)	Asphalt	Aggregate	Air Void	Aggregate	Fill with asphalt	Total mixture	pcf
	a	b	C	d	e	f	g	h	i	j	k	l	m	n	o
	wrt agg. weight	a/(100+a)				d-e	d/(d-e)		b*g/ (SGasp)	(100-b) *g/SGagg	100-i-j	100-j	i/l	100-100g/h	62.4*g
C4002083001	5,75	5,4374	58,00	1158,20	685,90	472,30	2,452	2,483	13,0188	85,74	1,24	14,26	91,32	1,24	153,02
C4002083002	5,75	5,4374	58,00	1157,60	685,80	471,80	2,454	2,483	13,0258	85,79	1,18	14,21	91,67	1,18	153,10
C4002084001	5,75	5,4374	60,00	1158,20	685,10	473,10	2,448	2,483	12,9968	85,60	1,40	14,40	90,25	1,40	152,76
C4002084002	5,75	5,4374	60,00	1163,50	688,30	475,20	2,448	2,483	12,9986	85,61	1,39	14,39	90,33	1,39	152,78
C4002085001	5,75	5,4374	59,00	1155,30	685,20	470,10	2,458	2,483	13,0470	85,93	1,02	14,07	92,72	1,02	153,35
C4002085002	5,75	5,4374	59,00	1157,40	685,60	471,80	2,453	2,483	13,0236	85,77	1,20	14,23	91,55	1,20	153,08
C4008183001	5,75	5,4374	59,00	1163,30	689,30	474,00	2,454	2,483	13,0292	85,81	1,16	14,19	91,83	1,16	153,14
C4008183002	5,75	5,4374	58,00	1158,50	685,90	472,60	2,451	2,483	13,0139	85,71	1,27	14,29	91,08	1,27	152,96
C4008184001	5,75	5,4374	59,00	1158,80	684,90	473,90	2,445	2,483	12,9816	85,50	1,52	14,50	89,52	1,52	152,58
C4008184002	5,75	5,4374	59,00	1159,80	687,20	472,60	2,454	2,483	13,0285	85,81	1,16	14,19	91,80	1,16	153,13
C4008185001	5,75	5,4374	58,00	1157,40	685,00	472,40	2,450	2,483	13,0071	85,67	1,33	14,33	90,74	1,33	152,88
C4008185002	5,75	5,4374	58,00	1162,10	687,90	474,20	2,451	2,483	13,0103	85,69	1,30	14,31	90,90	1,30	152,92

Table A2: Physical properties of specimens (cont'd)

SPECIMEN	AC	AC	SPECIMEN	WEIGHT (gr)		VOLUME	SPECIFIC GRAVITY		VOLUME wrt TOTAL %			VOID PERCENTAGES(%)			UNIT WEIGHT
	(%)	(%)	HEIGHT	In Air	In Water	(cm3)	Mixture	Mixture (theoric)	Asphalt	Aggregate	Air Void	Aggregate	Fill with asphalt	Total mixture	pcf
	a	b	C	d	e	f	g	h	i	j	k	l	m	n	o
	wrt agg. weight	a/(100+a)				d-e	d/(d-e)		b*g/ (SGasp)	(100-b) *g/SGagg	100-i-j	100-j	i/l	100-100g/h	62.4*g
C3502083001	5,75	5,4374	58,00	1159,90	687,10	472,80	2,453	2,483	13,0241	85,78	1,20	14,22	91,58	1,20	153,08
C3502084001	5,75	5,4374	59,00	1159,00	685,90	473,10	2,450	2,483	13,0058	85,66	1,34	14,34	90,68	1,34	152,87
C3502085001	5,75	5,4374	59,00	1162,00	686,80	475,20	2,445	2,483	12,9818	85,50	1,52	14,50	89,53	1,52	152,59
C3508183001	5,75	5,4374	59,00	1159,70	686,30	473,40	2,450	2,483	13,0054	85,65	1,34	14,35	90,66	1,34	152,86
C3508184001	5,75	5,4374	59,00	1159,90	686,70	473,20	2,451	2,483	13,0131	85,71	1,28	14,29	91,04	1,28	152,95
C3508185001	5,75	5,4374	58,50	1160,00	686,80	473,20	2,451	2,483	13,0142	85,71	1,27	14,29	91,09	1,27	152,97
B4002083001	5,25	4,9881	58,00	1152,80	681,70	471,10	2,447	2,500	11,9178	85,97	2,11	14,03	84,93	2,11	152,70
B4002083002	5,25	4,9881	59,00	1157,60	686,10	471,50	2,455	2,500	11,9573	86,25	1,79	13,75	86,98	1,79	153,20
B4002084001	5,25	4,9881	59,00	1157,40	685,20	472,20	2,451	2,500	11,9375	86,11	1,95	13,89	85,94	1,95	152,95
B4002084002	5,25	4,9881	59,00	1156,00	683,50	472,50	2,447	2,500	11,9155	85,95	2,13	14,05	84,81	2,13	152,67
B4002085001	5,25	4,9881	59,00	1151,90	680,70	471,20	2,445	2,500	11,9060	85,88	2,21	14,12	84,33	2,21	152,54
B4002085002	5,25	4,9881	60,00	1152,60	681,10	471,50	2,445	2,500	11,9056	85,88	2,21	14,12	84,32	2,21	152,54

Table A2: Physical properties of specimens (cont'd)

SPECIMEN	AC	AC	SPECIMEN	WEIGHT (gr)		VOLUME	SPECIFIC GRAVITY		VOLUME wrt TOTAL %			VOID PERCENTAGES(%)			UNIT WEIGHT
	(%)	(%)	HEIGHT	In Air	In Water	(cm3)	Mixture	Mixture (theoric)	Asphalt	Aggregate	Air Void	Aggregate	Fill with asphalt	Total mixture	pcf
	a	b	C	d	e	f	g	h	i	j	k	l	m	n	o
	wrt agg. weight	a/(100+a)				d-e	d/(d-e)		b*g/ (SGasp)	(100-b) *g/SGagg	100-i-j	100-j	i/l	100-100g/h	62.4*g
B4008183001	5,25	4,9881	59,00	1153,20	682,90	470,30	2,452	2,500	11,9422	86,14	1,91	13,86	86,19	1,91	153,01
B4008183002	5,25	4,9881	59,00	1152,00	681,40	470,60	2,448	2,500	11,9222	86,00	2,08	14,00	85,15	2,08	152,75
B4008184001	5,25	4,9881	59,00	1152,70	683,30	469,40	2,456	2,500	11,9599	86,27	1,77	13,73	87,12	1,77	153,23
B4008184002	5,25	4,9881	58,50	1155,00	684,20	470,80	2,453	2,500	11,9482	86,19	1,87	13,81	86,50	1,87	153,08
B4008185001	5,25	4,9881	59,00	1152,80	682,90	469,90	2,453	2,500	11,9482	86,19	1,86	13,81	86,50	1,86	153,09
B4008185002	5,25	4,9881	58,00	1153,90	682,60	471,30	2,448	2,500	11,9241	86,01	2,06	13,99	85,25	2,06	152,78

APPENDIX B

CREEP CURVES OF TESTS

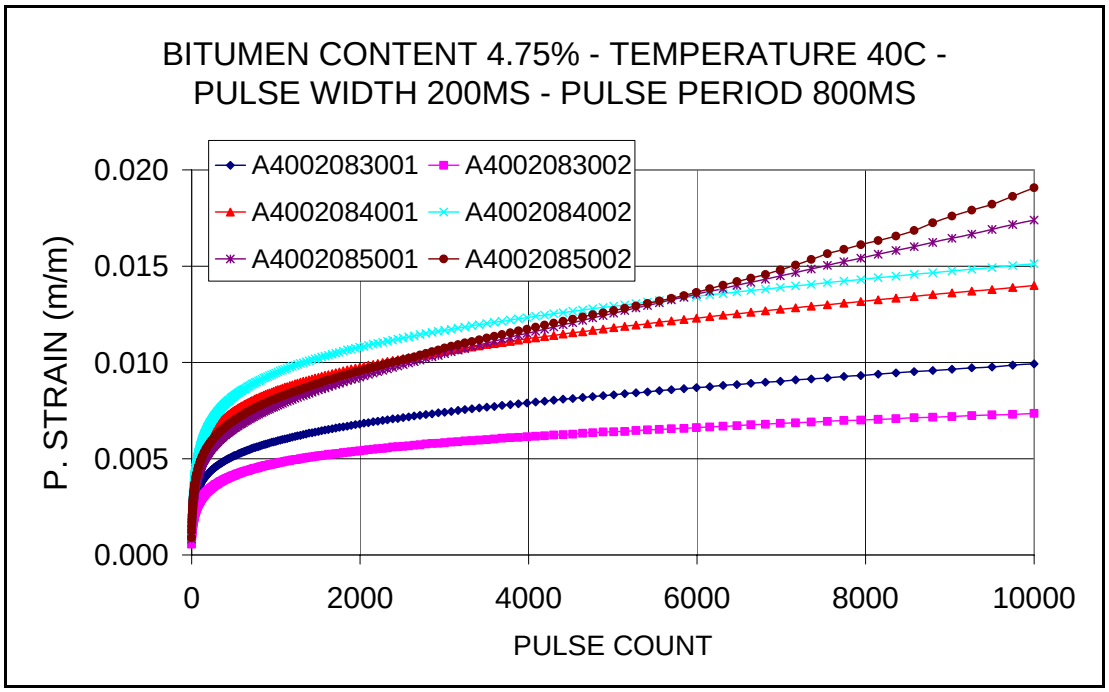

Figure B1: Creep curves for specimens with 4.75% bitumen content tested under 0.2 sec pulse width and 0.8 sec pulse period at 40°C

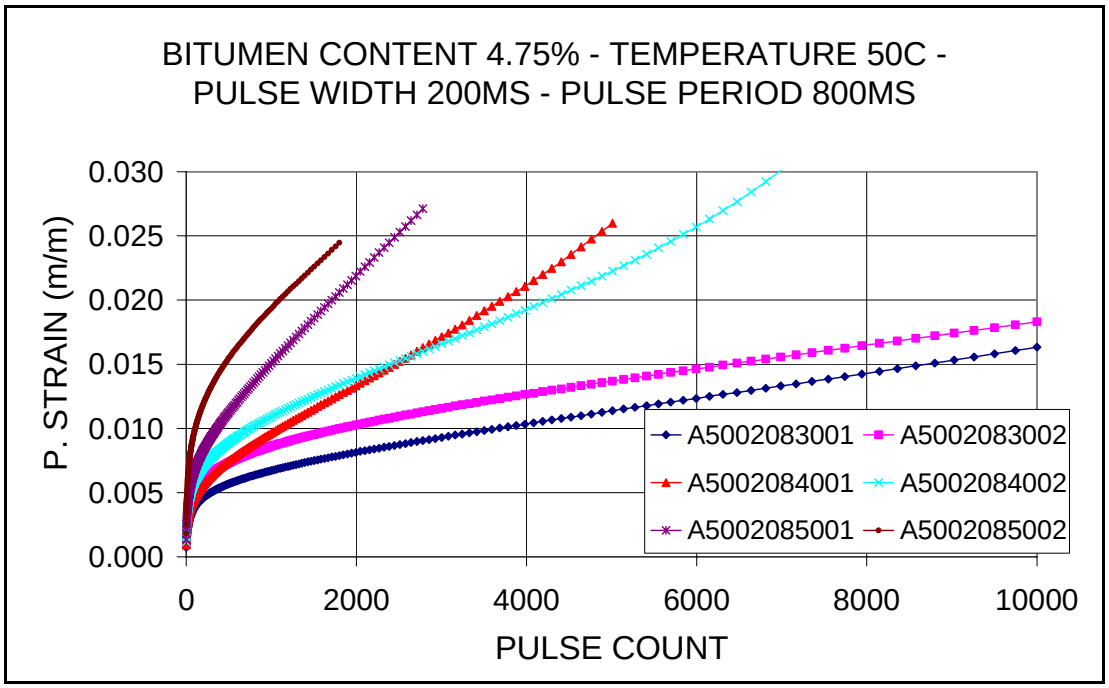

Figure B2: Creep curves for specimens with 4.75% bitumen content tested under 0.2 sec pulse width and 0.8 sec pulse period at 50°C

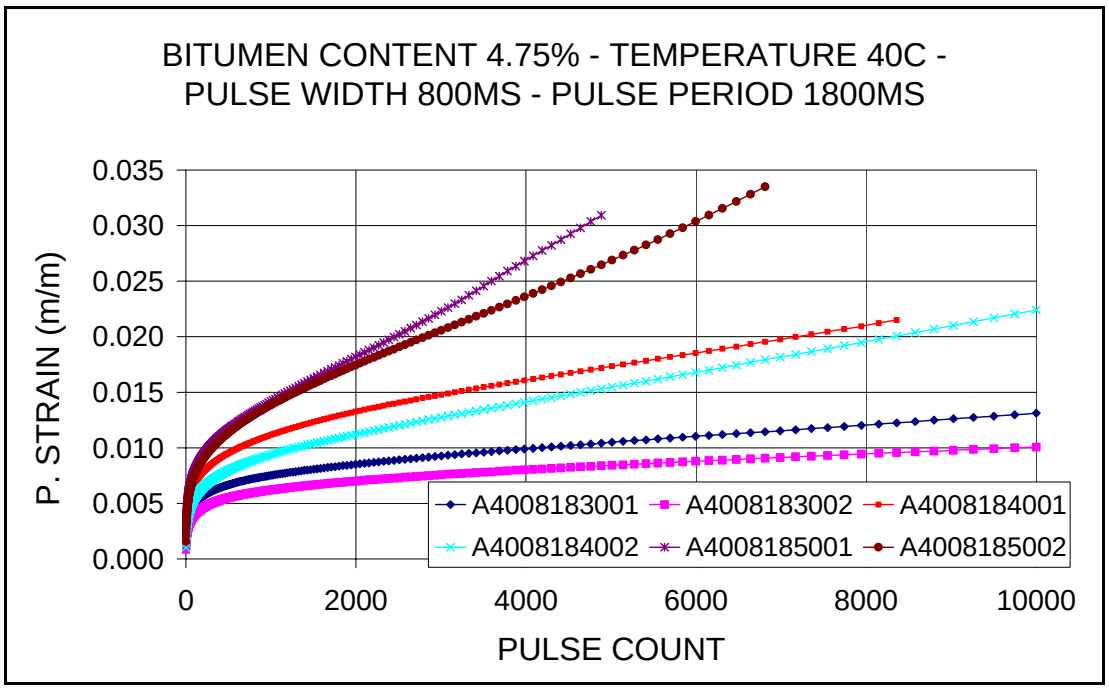

Figure B3: Creep curves for specimens with 4.75% bitumen content tested under 0.8 sec pulse width and 1.8 sec pulse period at 40°C

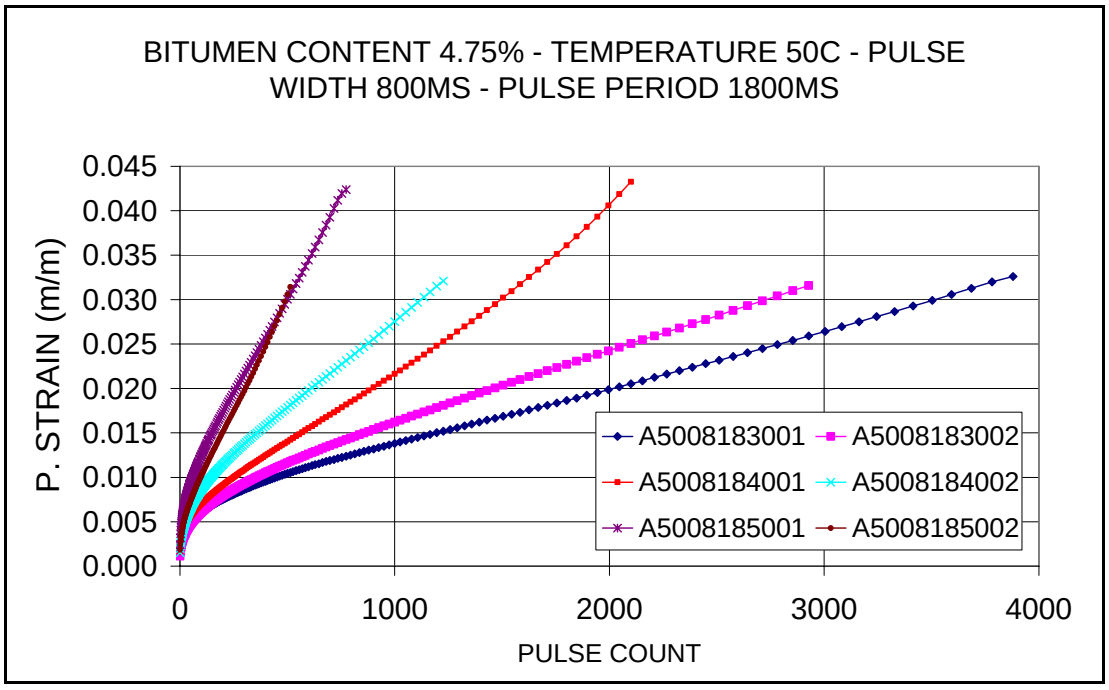

Figure B4: Creep curves for specimens with 4.75% bitumen content tested under 0.8 sec pulse width and 1.8 sec pulse period at 50°C

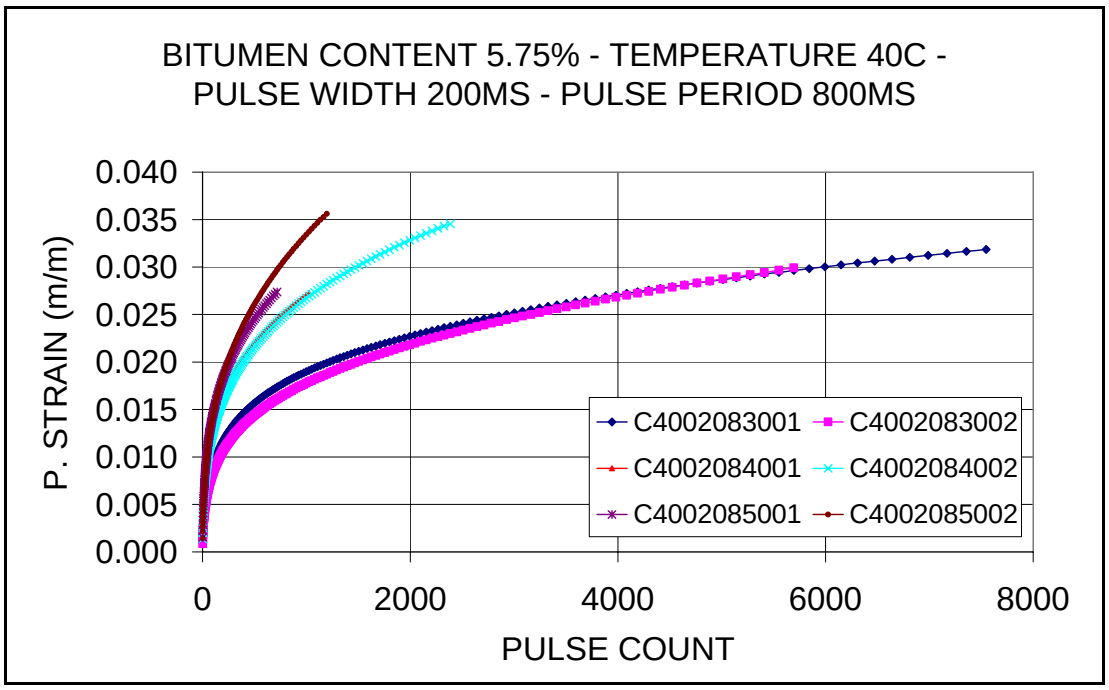

Figure B5: Creep curves for specimens with 5.75% bitumen content tested under 0.2 sec pulse width and 0.8 sec pulse period at 40°C

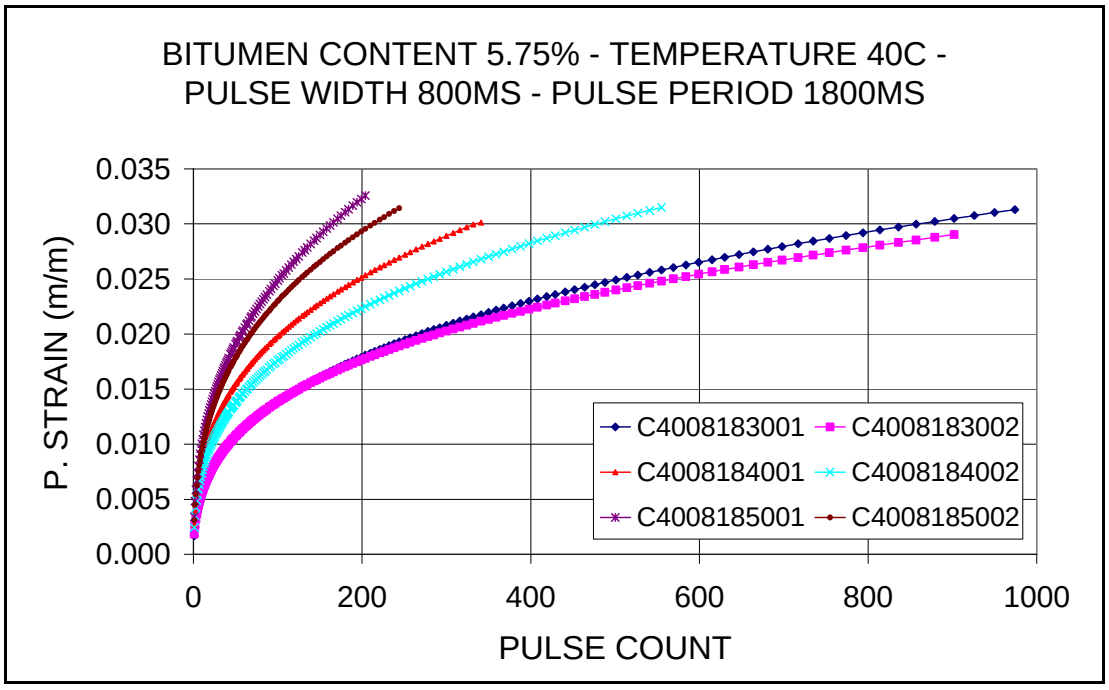

Figure B6: Creep curves for specimens with 5.75% bitumen content tested under 0.8 sec pulse width and 1.8 sec pulse period at 40°C

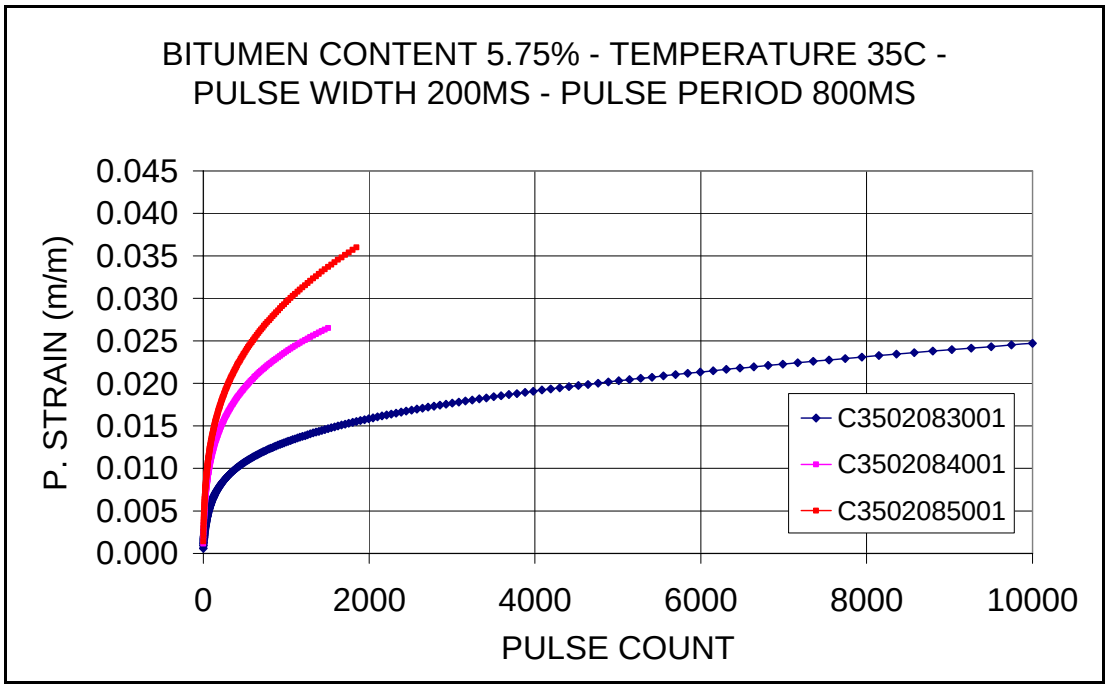

Figure B7: Creep curves for specimens with 5.75% bitumen content tested under 0.2 sec pulse width and 0.8 sec pulse period at 35°C

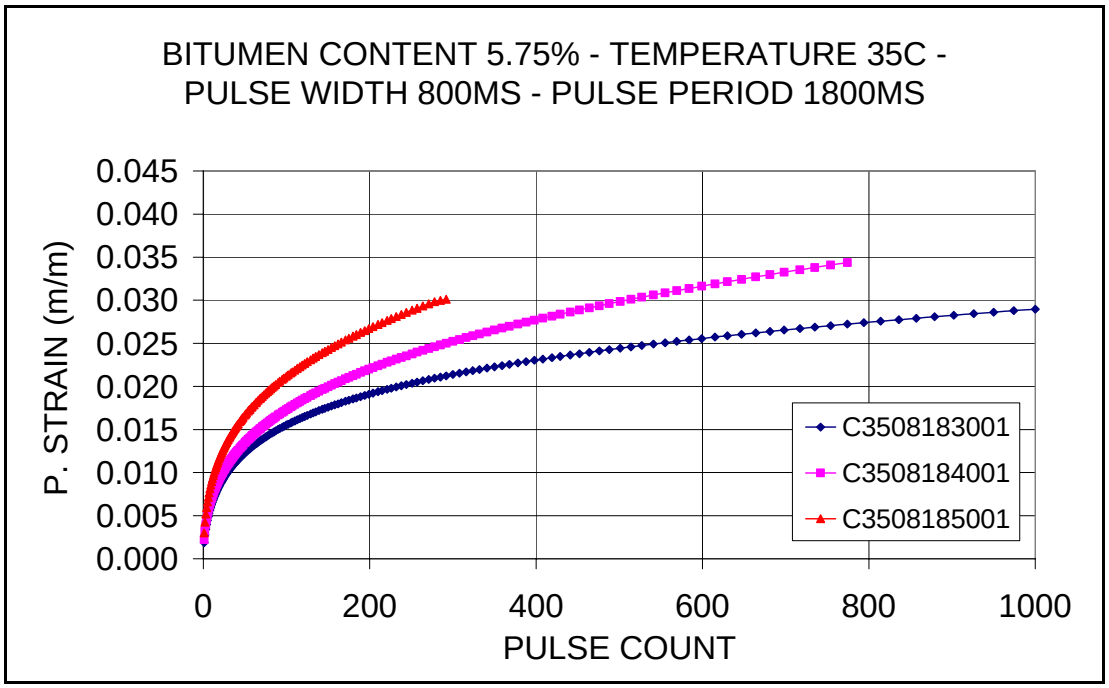

Figure B8: Creep curves for specimens with 5.75% bitumen content tested under 0.8 sec pulse width and 1.8 sec pulse period at 35°C

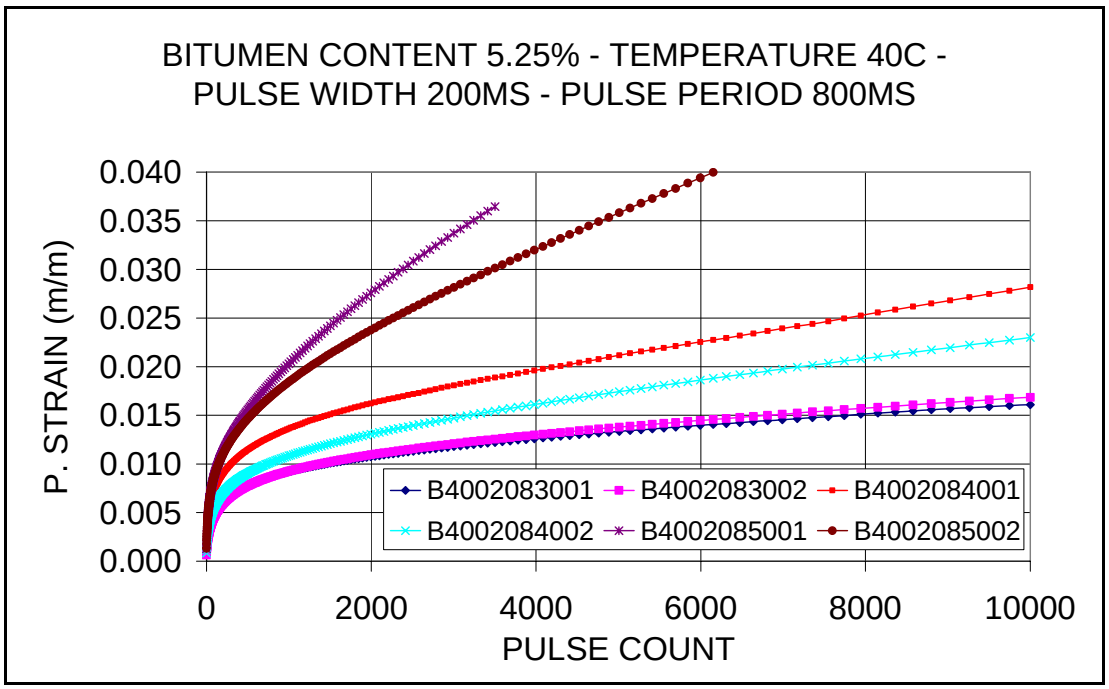

Figure B9: Creep curves for specimens with 5.25% bitumen content tested under 0.2 sec pulse width and 0.8 sec pulse period at 40°C

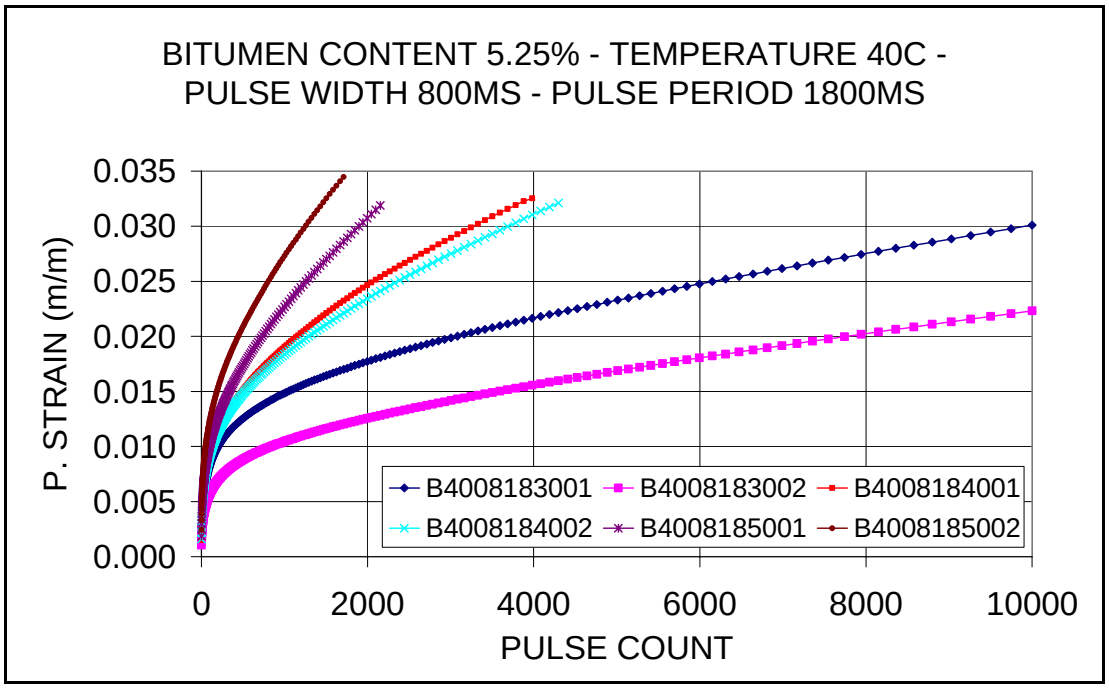

Figure B10: Creep curves for specimens with 5.25% bitumen content tested under 0.8 sec pulse width and 1.8 sec pulse period at 40°C

APPENDIX C

ASPHALT REPEATED LOAD CREEP TEST OUTPUT FILE EXAMPLE

INDUSTRIAL PROCESS CONTROLS Limited REPEATED LOAD ASPHALT CREEP TEST
Universal Material Testing Apparatus Thursday August 2 2007 11:00 AM
specimen identification: denms3
comment: #
comment:
comment:
specimen length (mm): 60.0
specimen diameter (mm): 100.0
set temperature (øC): 40.0
pulse width (ms): 200
pulse period (ms): 800
test termination strain (æî): 100000
... or terminal pulse count: 100000
conditioning stress (kPa): 100
test loading stress (kPa): 500
conditioning time (minutes): 1
preload rest time (minutes): 2
recovery time (minutes): 15
binary file name: C:\HANDE\DENMS3.BIN
ASCII output data file name: C:\HANDE\DENMS3.CSV

final reading of measured parameters:
conditioning strain (um/m) 3534 condition time (hh:mm:ss) 00:01:00
preload rest strain (um/m) 2039 rest time (hh:mm:ss) 00:02:00
loading strain (um/m) 36556 loading time (hh:mm:ss) 00:47:32
recovery strain (um/m) 35619 recovery time (hh:mm:ss) 00:15:00
conditioning stress (kPa) 97 total loading pulse count 3566
peak loading stress (kPa) 484 skin temperature (øC) 40.6
resilient strain (æî) 954 core temperature (øC) 41.0
resilient modulus (MPa) 507.0

Pulse Count	TotVFrc (N)	PermStrn (um/m)	ResiStrn (um/m)	ResiMod (Mpa)	SkinTemp (degC)
1	3851	1280	2073	236.5	40.6
2	3892	1797	2152	230.3	40.6
3	3898	2170	2161	229.7	40.6
4	3896	2467	2196	226	40.6
5	3903	2738	2188	227.2	40.6
6	3901	2967	2206	225.2	40.6
7	3903	3162	2223	223.5	40.6
8	3898	3357	2215	224.1	40.6
9	3903	3535	2216	224.3	40.6
10	3898	3705	2225	223.1	40.6
11	3901	3857	2234	222.4	40.6
12	3898	4001	2226	223	40.6

APPENDIX D

ANOVA TABLES & GRAPHICAL ANALYSIS

D.1 Proposed model by Beckedahl et al.

Table D.1: Analysis of Variance - E0

Analysis of Variance - E0					
Source	**Sum Sq.**	**d.f.**	**Mean Sq.**	**F**	**Prob>F**
X1(Bitumen Content)	6.54E-01	2	3.27E-01	8.87E+00	**0.004318**
X2(Frequency)	1.73E-01	1	1.73E-01	4.70E+00	0.051040
X3(Load)	1.82E-01	2	9.09E-02	2.46E+00	0.126900
Error	4.43E-01	12	3.69E-02		
Total	1.45E+00	17			
Constrained (Type III) sums of squares.					

Table D.2: Analysis of Variance - A

Analysis of Variance - A					
Source	**Sum Sq.**	**d.f.**	**Mean Sq.**	**F**	**Prob>F**
X1(Bitumen Content)	1.57E-08	2	7.85E-09	4.08E-01	0.674050
X2(Frequency)	4.04E-09	1	4.04E-09	2.10E-01	0.655210
X3(Load)	1.92E-08	2	9.59E-09	4.98E-01	0.619910
Error	2.31E-07	12	1.93E-08		
Total	2.70E-07	17			
Constrained (Type III) sums of squares.					

Table D.3: Analysis of Variance - B

Analysis of Variance - B					
Source	**Sum Sq.**	**d.f.**	**Mean Sq.**	**F**	**Prob>F**
X1(Bitumen Content)	1.64E-01	2	8.18E-02	8.86E+00	**0.004340**
X2(Frequency)	4.33E-02	1	4.33E-02	4.69E+00	0.051208
X3(Load)	4.55E-02	2	2.28E-02	2.46E+00	0.126950
Error	1.11E-01	12	9.24E-03		
Total	3.63E-01	17			
Constrained (Type III) sums of squares.					

Table D.4: Analysis of Variance – C

Analysis of Variance - C					
Source	**Sum Sq.**	**d.f.**	**Mean Sq.**	**F**	**Prob>F**
X1(Bitumen Content)	1.28E-06	2	6.41E-07	3.40E+00	0.067825
X2(Frequency)	1.18E-07	1	1.18E-07	6.24E-01	0.444930
X3(Load)	2.38E-07	2	1.19E-07	6.31E-01	0.548770
Error	2.26E-06	12	1.89E-07		
Total	3.90E-06	17			
Constrained (Type III) sums of squares.					

Table D.5: Analysis of Variance - k

Analysis of Variance - k					
Source	**Sum Sq.**	**d.f.**	**Mean Sq.**	**F**	**Prob>F**
X1(Bitumen Content)	3.38E-01	2	1.69E-01	1.58E+01	**0.000440**
X2(Frequency)	1.79E-02	1	1.79E-02	1.67E+00	0.220630
X3(Load)	5.96E-02	2	2.98E-02	2.78E+00	0.102030
Error	1.29E-01	12	1.07E-02		
Total	5.45E-01	17			
Constrained (Type III) sums of squares.					

D.2 Proposed model $E=E0+An^k$

Table D.6: Analysis of Variance - E0

Analysis of Variance - E0					
Source	**Sum Sq.**	**d.f.**	**Mean Sq.**	**F**	**Prob>F**
X1(Bitumen Content)	2.65E-06	2	1.33E-06	6.21E+00	**0.014062**
X2(Frequency)	1.82E-06	1	1.82E-06	8.52E+00	**0.012878**
X3(Load)	2.62E-06	2	1.31E-06	6.13E+00	**0.014661**
Error	2.56E-06	12	2.14E-07		
Total	9.65E-06	17			
Constrained (Type III) sums of squares.					

Table D.7: Analysis of Variance - A

Analysis of Variance – A					
Source	**Sum Sq.**	**d.f.**	**Mean Sq.**	**F**	**Prob>F**
X1(Bitumen Content)	3.92E-07	2	1.96E-07	3.81E+00	0.052328
X2(Frequency)	4.54E-07	1	4.54E-07	8.82E+00	**0.011690**
X3(Load)	5.17E-07	2	2.58E-07	5.02E+00	**0.025984**
Error	6.17E-07	12	5.14E-08		
Total	1.98E-06	17			
Constrained (Type III) sums of squares.					

Table D.8 Analysis of Variance - k

Analysis of Variance - k					
Source	**Sum Sq.**	**d.f.**	**Mean Sq.**	**F**	**Prob>F**
X1(Bitumen Content)	3.43E-02	2	1.72E-02	8.05E+00	**0.006053**
X2(Frequency)	7.48E-02	1	7.48E-02	3.51E+01	**0.000070**
X3(Load)	1.55E-01	2	7.73E-02	3.63E+01	**0.000008**
Error	2.56E-02	12	2.13E-03		
Total	2.89E-01	17			
Constrained (Type III) sums of squares.					

D.3 Power Model

Table D.9: Analysis of Variance – a

Analysis of Variance - a					
Source	**Sum Sq.**	**d.f.**	**Mean Sq.**	**F**	**Prob>F**
X1(Bitumen Content)	4.25E-07	2	2.12E-07	7.23E+00	**0.008694**
X2(Frequency)	1.02E-07	1	1.02E-07	3.49E+00	0.086301
X3(Load)	1.85E-07	2	9.23E-08	3.14E+00	0.079785
Error	3.52E-07	12	2.94E-08		
Total	1.06E-06	17			
Constrained (Type III) sums of squares.					

Table D.10: Analysis of Variance - b

Analysis of Variance - b					
Source	**Sum Sq.**	**d.f.**	**Mean Sq.**	**F**	**Prob>F**
X1(Bitumen Content)	3.26E-02	2	1.63E-02	1.39E+00	0.285510
X2(Frequency)	9.79E-02	1	9.79E-02	8.37E+00	**0.013484**
X3(Load)	1.58E-01	2	7.90E-02	6.76E+00	**0.010835**
Error	1.40E-01	12	1.17E-02		
Total	4.29E-01	17			
Constrained (Type III) sums of squares.					

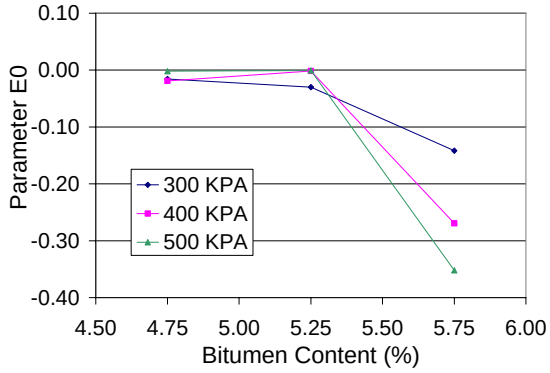

a) Under 0.2 sec pulse width and 0.8 sec pulse period

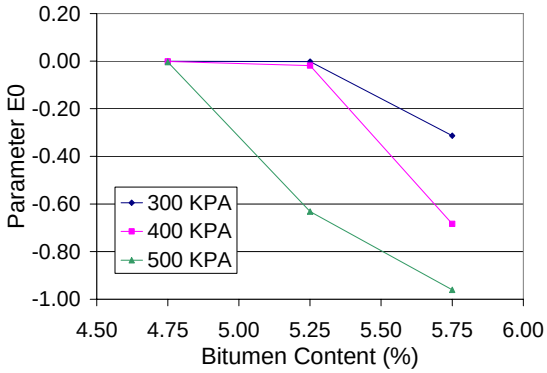

b) Under 0.8 sec pulse width and 1.8 sec pulse period

Figure D.1: Variation of model parameter E0 with applied load for specimens tested at 40°C

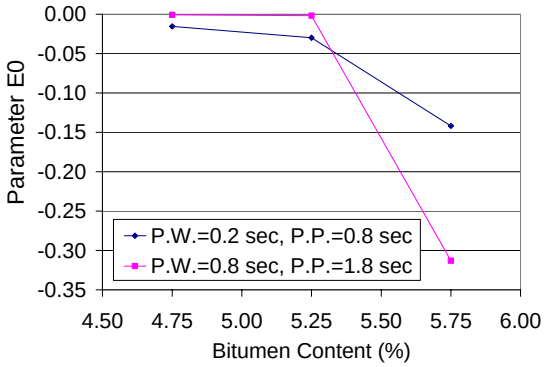

a) Under 300 Kpa stress

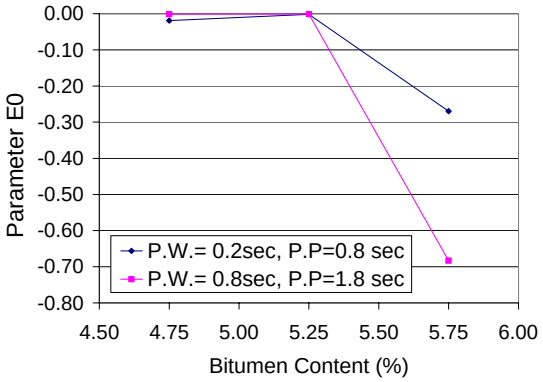

b) Under 400 Kpa stress

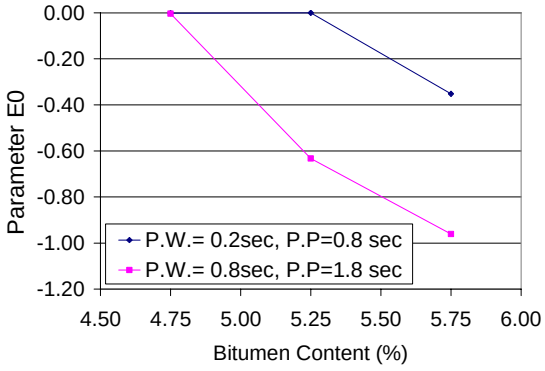

c) Under 500 Kpa stress

Figure D.2: Variation of model parameter E0 with load frequency for specimens tested at 40°C

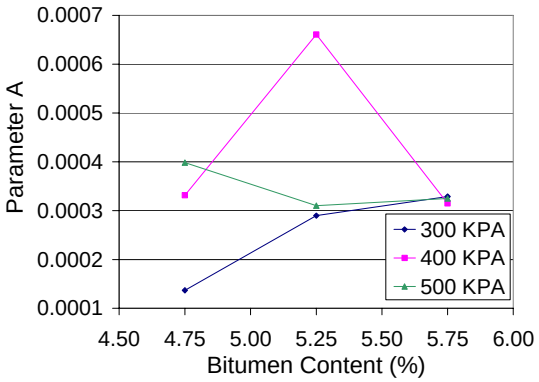

a) Under 0.2 sec pulse width and 0.8 sec pulse period

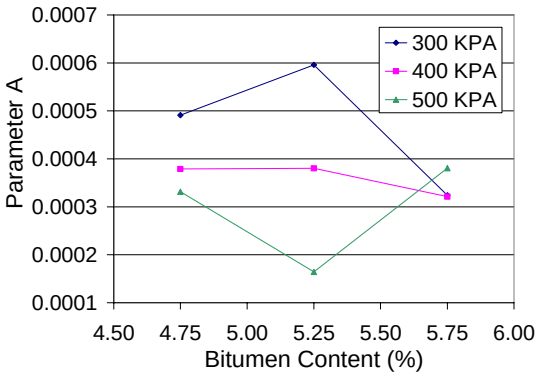

b) Under 0.8 sec pulse width and 1.8 sec pulse period

Figure D.3: Variation of model parameter A with applied load for specimens tested at 40°C

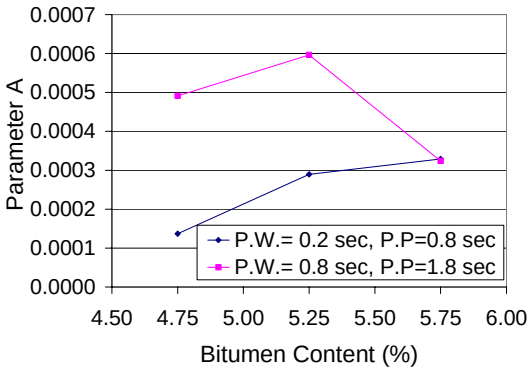

a) Under 300 Kpa stress

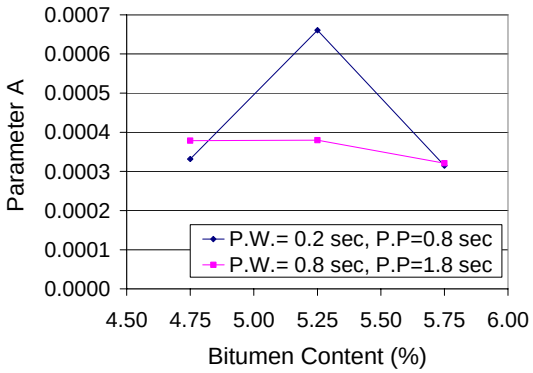

b) Under 400 Kpa stress

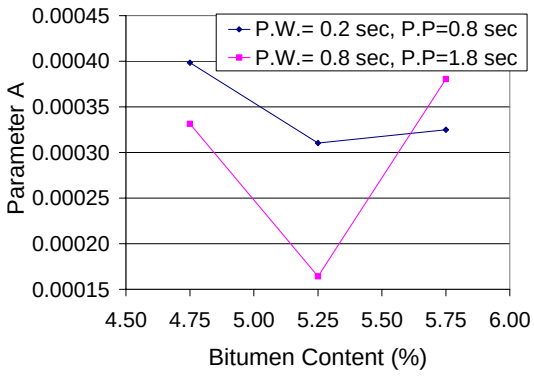

c) Under 500 Kpa stress

Figure D.4: Variation of model parameter A with load frequency for specimens tested at 40°C

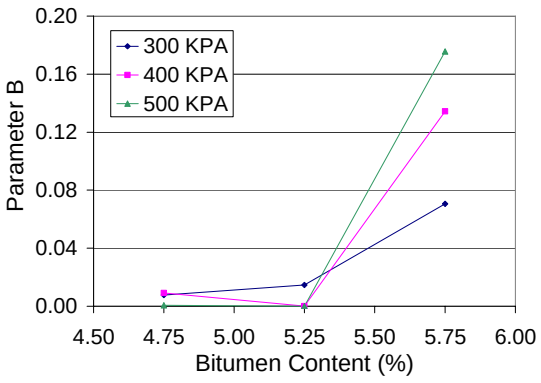

a) Under 0.2 sec pulse width and 0.8 sec pulse period

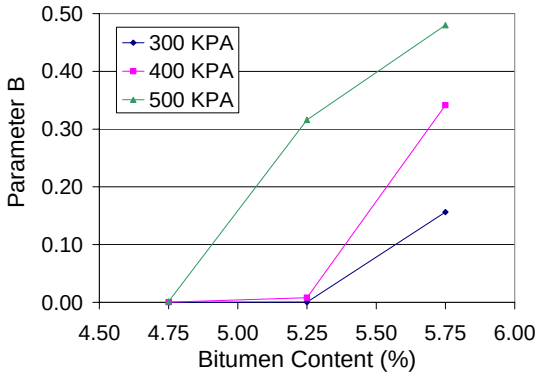

b) Under 0.8 sec pulse width and 1.8 sec pulse period

Figure D.5: Variation of model parameter B with applied load for specimens tested at 40°C

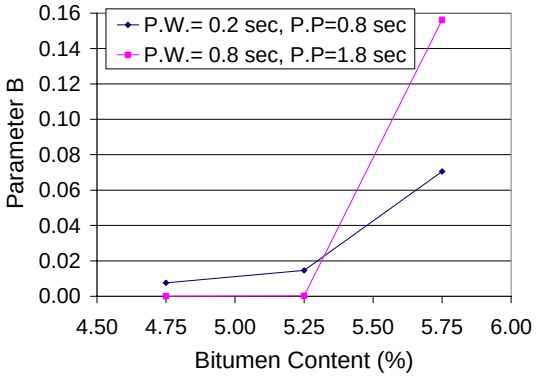

a) Under 300 Kpa stress

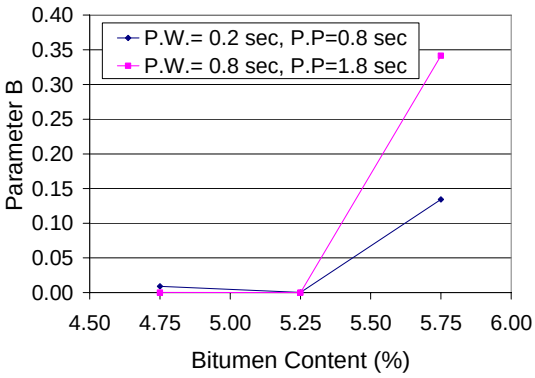

b) Under 400 Kpa stress

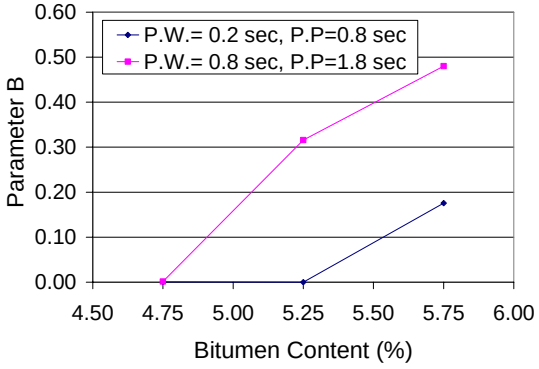

c) Under 500 Kpa stress

Figure D.6: Variation of model parameter B with load frequency for specimens tested at 40°C

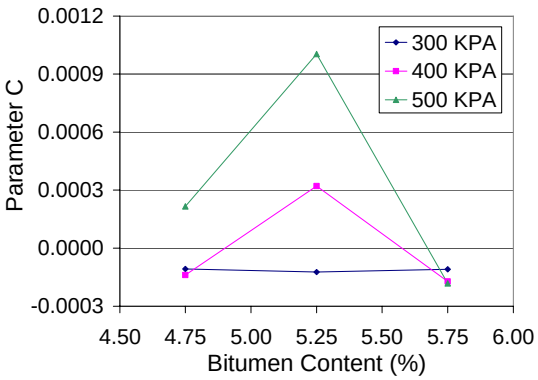

a) Under 0.2 sec pulse width and 0.8 sec pulse period

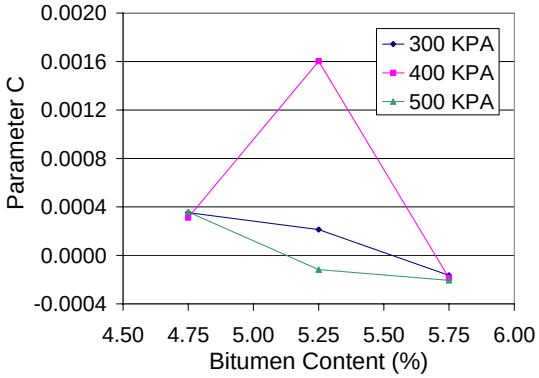

b) Under 0.8 sec pulse width and 1.8 sec pulse period

Figure D.7: Variation of model parameter C with applied load for specimens tested at 40°C

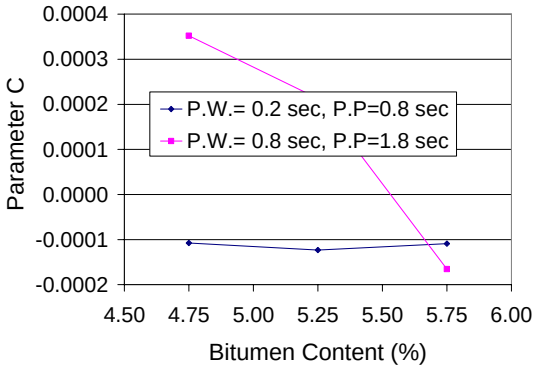

a) Under 300 Kpa stress

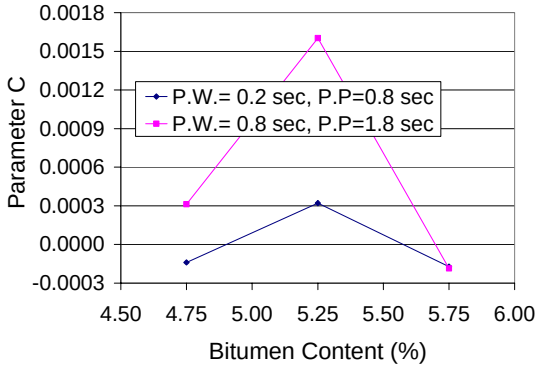

b) Under 400 Kpa stress

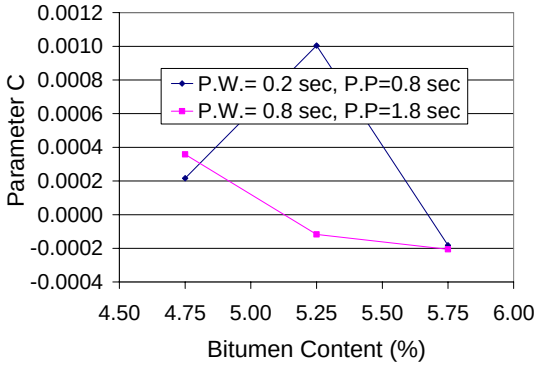

c) Under 500 Kpa stress

Figure D.8: Variation of model parameter C with load frequency for specimens tested at 40°C

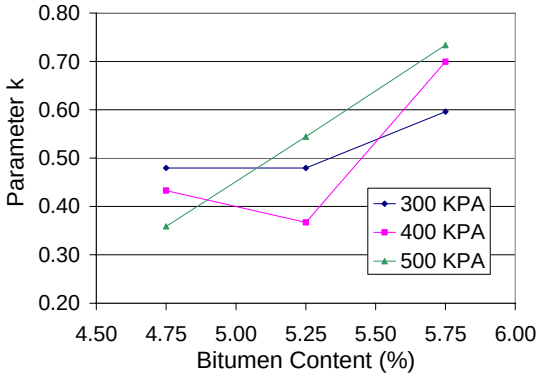

a) Under 0.2 sec pulse width and 0.8 sec pulse period

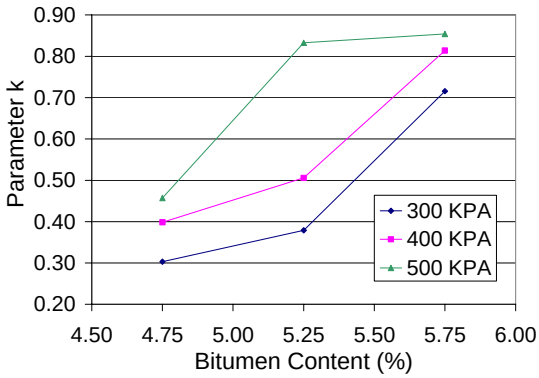

b) Under 0.8 sec pulse width and 1.8 sec pulse period

Figure D.9: Variation of model parameter k with applied load for specimens tested at 40°C

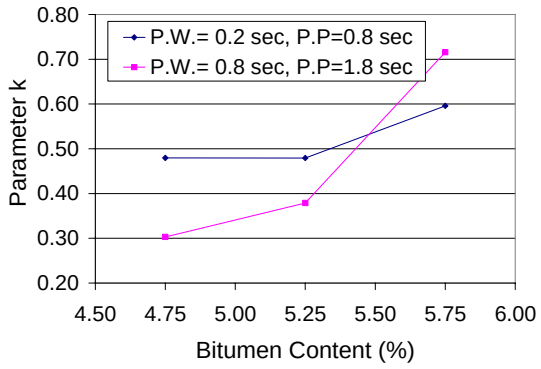

a) Under 300 Kpa stress

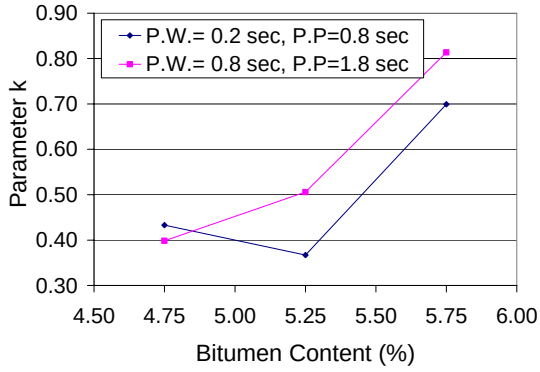

b) Under 400 Kpa stress

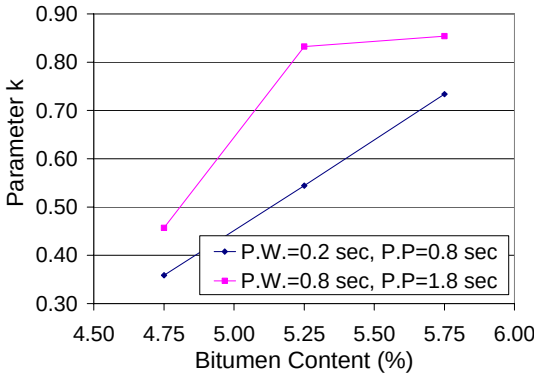

c) Under 500 Kpa stress

Figure D.10: Variation of model parameter k with load frequency for specimens tested at 40°C

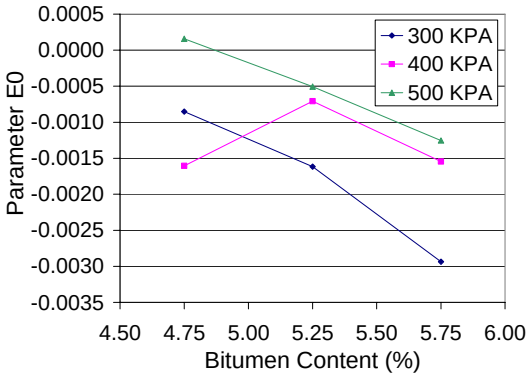

a) Under 0.2 sec pulse width and 0.8 sec pulse period

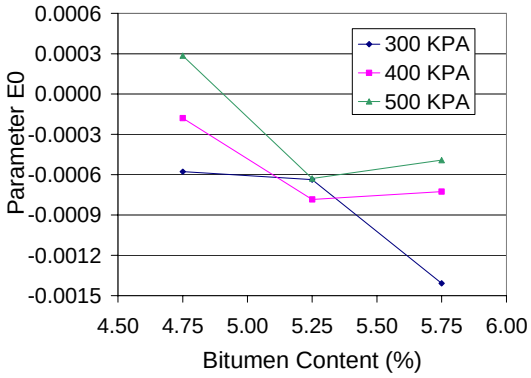

b) Under 0.8 sec pulse width and 1.8 sec pulse period

Figure D.11: Variation of model parameter E0 with applied load for specimens tested at 40°C

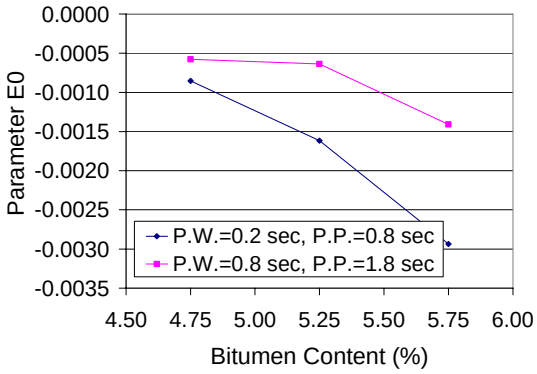

a) Under 300 Kpa stress

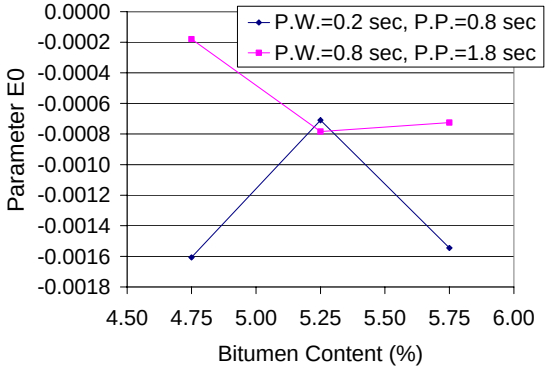

b) Under 400 Kpa stress

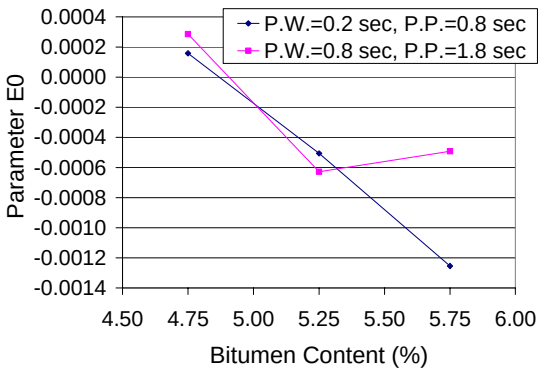

c) Under 500 Kpa stress

Figure D.12: Variation of model parameter E0 with load frequency for specimens tested at 40°C

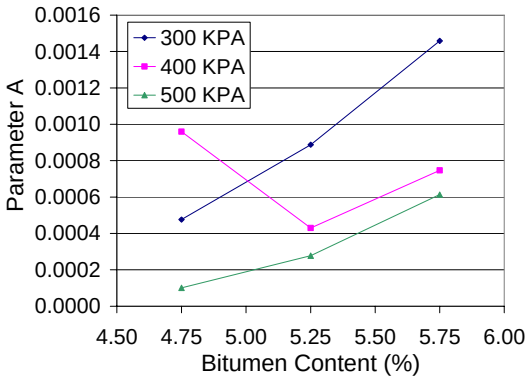

a) Under 0.2 sec pulse width and 0.8 sec pulse period

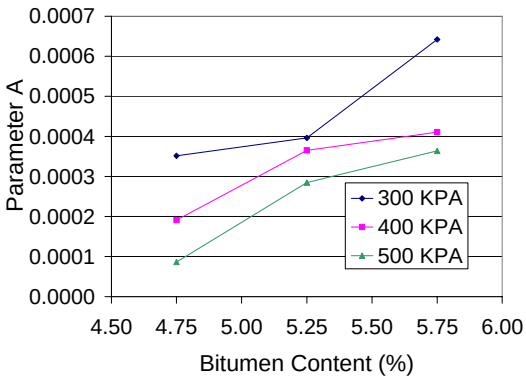

b) Under 0.8 sec pulse width and 1.8 sec pulse period

Figure D.13: Variation of model parameter A with applied load for specimens tested at 40°C

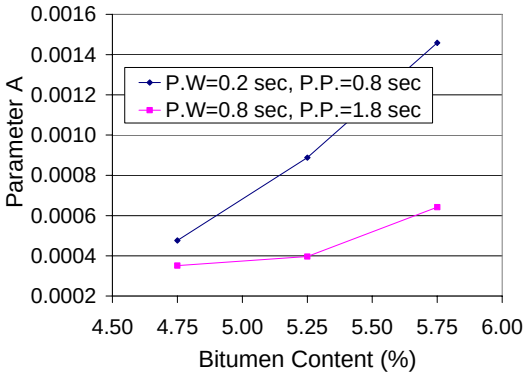

a) Under 300 Kpa stress

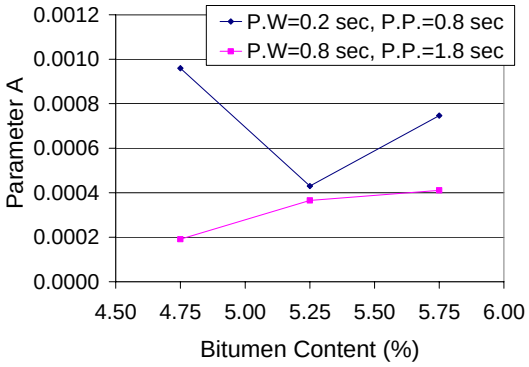

b) Under 400 Kpa stress

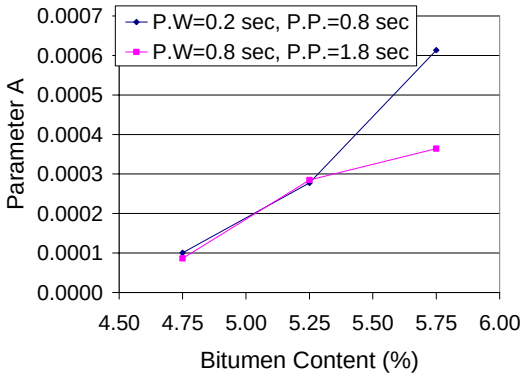

c) Under 500 Kpa Stress

Figure D.14: Variation of model parameter A with load frequency for specimens tested at 40°C

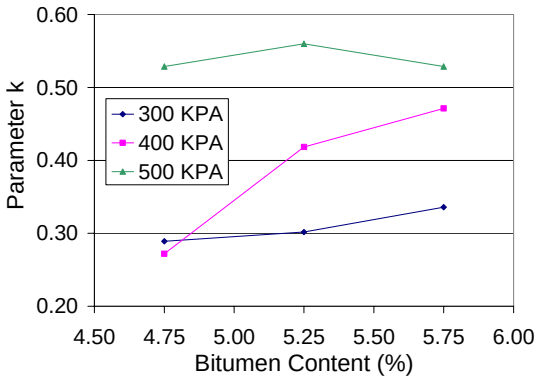

a) Under 0.2 sec pulse width and 0.8 sec pulse period

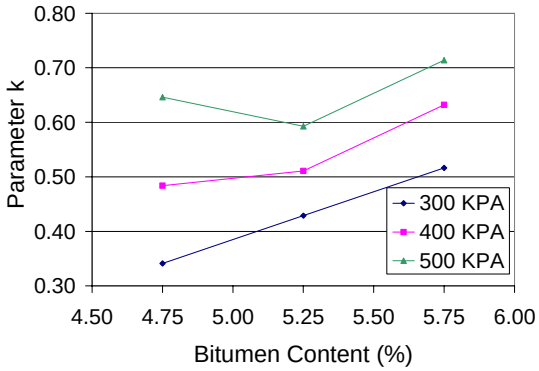

b) Under 0.8 sec pulse width and 1.8 sec pulse period

Figure D.15: Variation of model parameter k with applied load for specimens tested at 40°C

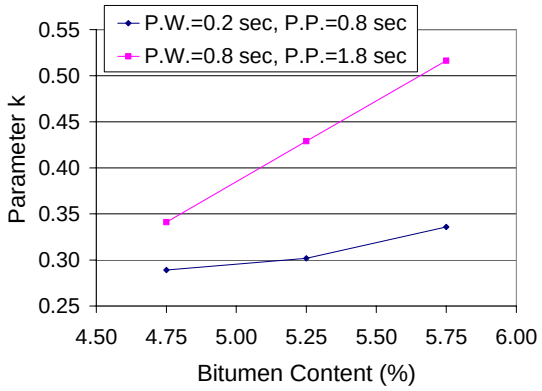

a) Under 300 Kpa stress

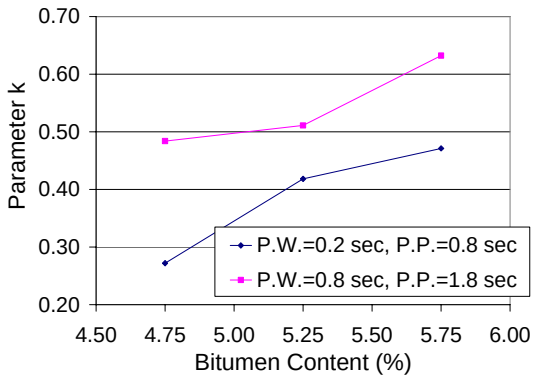

b) Under 400 Kpa stress

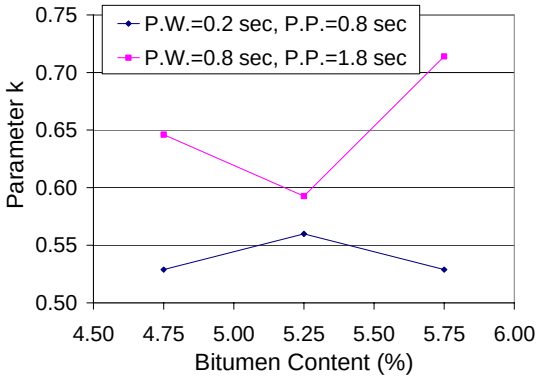

c) Under 500 Kpa Stress

Figure D.16: Variation of model parameter k with load frequency for specimens tested at 40°C

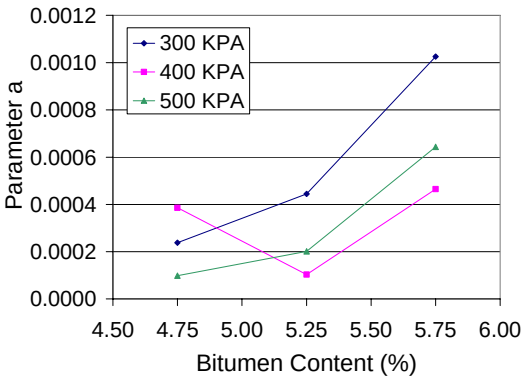

a) Under 0.2 sec pulse width and 0.8 sec pulse period

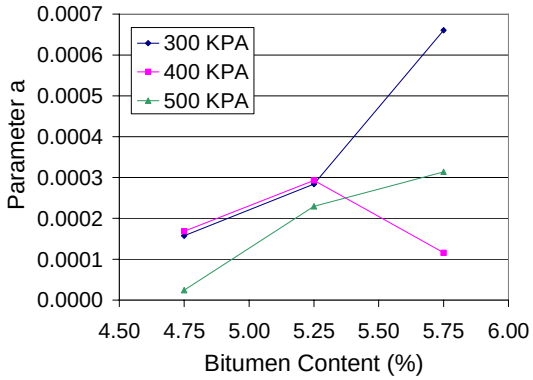

b) Under 0.8 sec pulse width and 1.8 sec pulse period

Figure D.17: Variation of model parameter a with applied load for specimens tested at 40°C

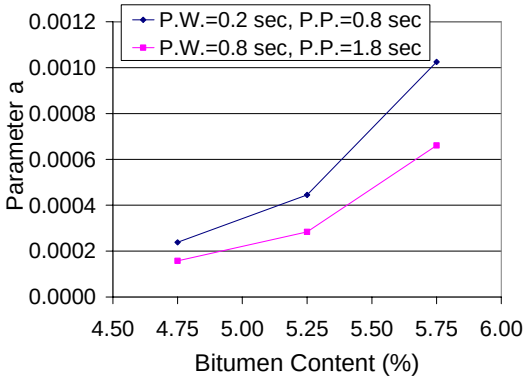

a) Under 300 Kpa stress

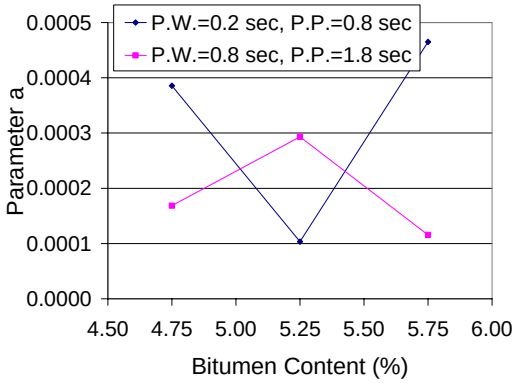

b) Under 400 Kpa stress

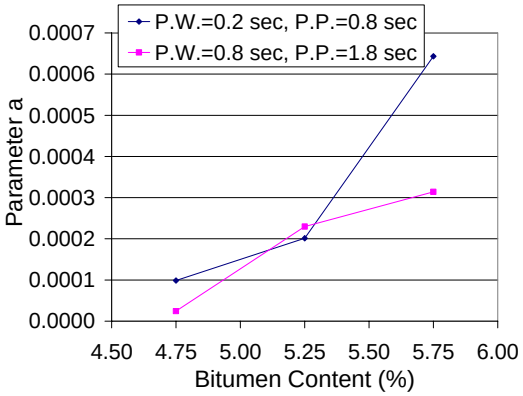

c) Under 500 Kpa Stress

Figure D.18: Variation of model parameter a with load frequency for specimens tested at 40°C

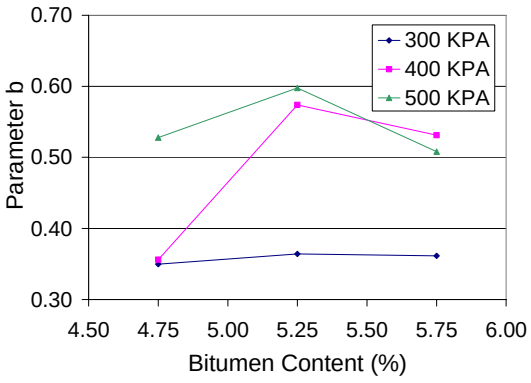

a) Under 0.2 sec pulse width and 0.8 sec pulse period

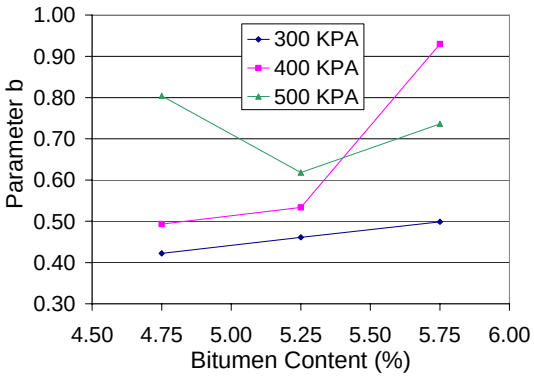

b) Under 0.8 sec pulse width and 1.8 sec pulse period

Figure D.19: Variation of model parameter b with applied load for specimens tested at 40°C

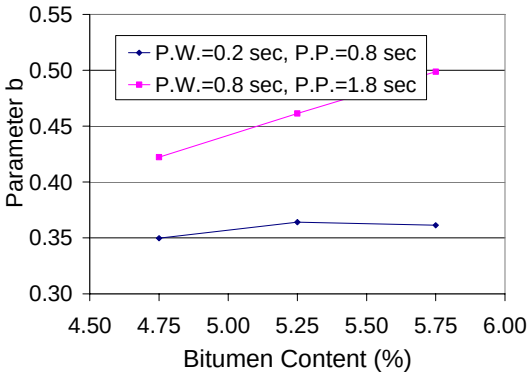

a) Under 300 Kpa stress

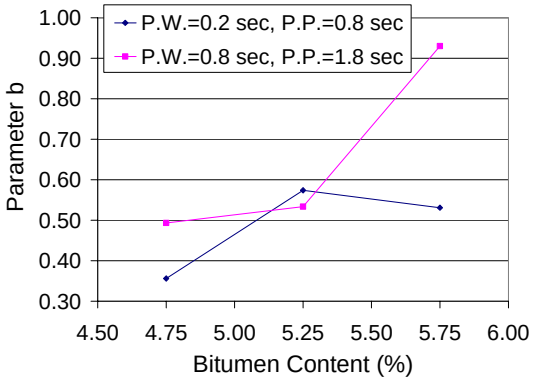

b) Under 400 Kpa stress

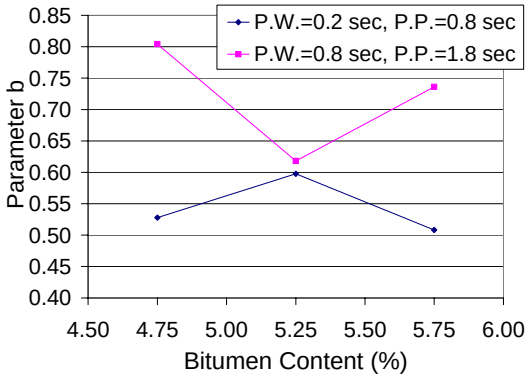

c) Under 500 Kpa Stress

Figure D.20: Variation of model parameter b with load frequency for specimens tested at 40°C